THE EFFECT OF SAD MOOD ON PAIN PERCEPTION: IMAGING FUNCTIONAL BRAIN NETWORKS

By

Lan Yang

A DISSERTATION

Submitted to
Michigan State University
In partial fulfillment of requirements
For the degree of

DOCTOR OF PHILOSOPHY

Neuroscience

2012

ABSTRACT

THE EFFECT OF SAD MOOD ON PAIN PERCEPTION: IMAGING FUNCTIONAL BRAIN NETWORKS

By

Lan Yang

People with chronic pain are often afflicted with psychiatric depressive disorders. Even the commonplace, everday experience of pain can be modified by ordinary emotion. However, the neural mechanisms underlying these phenomena are still unclear. Investigating the effects of sad mood on pain perception at the behavioral and the neural levels helps to understand the co-morbidity of depression and pain problems. This dissertation focuses on: (1) examining the effects of sad mood on perception of painful stimuli, and (2) identifying the functional brain networks that could provide the neural substrate for pain perception altered by sadness.

In Chapter 2, a task-evoked functional magnetic resonance imaging (fMRI) method has been used to investigate which brain areas are activated by painful and emotional stimuli. The hypotheses are that the subjective perception of pain intensity would be greater during sadness compared to neutral mood, and significantly increased neural activation would be observed in the primary cortical areas for pain perception. To test these hypotheses, the fMRI study has recruited sixteen healthy female subjects. The experimental trials include the delivery of painful electrical shocks concurrent with or without sad mood induced by the presentation of pictures from the International Affective Picture System (IAPS). The study identifies widely-distributed cortical and subcortical areas involved in the processing of pain and the altered pain perception by sadness. The cortical areas for pain processing are mainly located in the primary/secondary somatosensory, insular and cingulate cortices. Specifically, the posterior insular and the adjacent

secondary somatosensory cortices (pIn/SII) have significantly increased neural activation, when sadness intensifies subjective perception of pain.

In Chapter 3, using the resting-state fMRI and path analysis, it further examines the functional networks of pain processing and altered pain perception by sadness. The pain-relevant brain areas, such as primary somatosensory cortex, anterior cingulate cortex and thalamus, are intrinsically correlated with pIn/SII during rest. The path coefficients in the pain processing functional brain network increase during painful stimuli. The path analysis has also revealed a functional network in which the pIn/SII connects with emotion-relevant areas, such as the subgenual cingulate cortex, anterior insula and amygdala. These findings provided evidence of specific neural pathways that may be relevant to understanding the comorbidity of depression and pain problems.

DEDICATION

To Tao and Vesna

ACKNOWLEDGEMENTS

The writing of this dissertation has been one of the most significant academic challenges I have ever had to face. Without the help, support and guidance of the following people over years in Michigan State University, this study would not have been completed. It is to them that I owe my deepest gratitude.

First of all, I am extremely lucky to have Dr. Laura Symonds as my advisor, who committed years in training me to be a researcher, provided me an excellent atmosphere for doing research and financially supported my research. Her wisdom, knowledge and commitment to the highest standards inspired and motivated me. She offered valuable suggestions in guiding my research directions. She read and edited my manuscripts and dissertation drafts, as well as corrected my grammar errors without complaints. It is an honor to be her student and to work with her. I am also grateful for her influence on me to face challenges in school and in life confidently, persistently and optimistically. What I have learned from her would be my lifelong treasure carried with me after graduation.

I would like to thank Dr. David Zhu, a member of my Ph.D committee, for guiding me in designing experiments, collecting resting-state fMRI data, and patiently correcting my writing. I also appreciate the help from other members of my Ph.D committee: Dr. Gregory Fink and Dr. Sharleen Sakai. They gave the knowledge and insights in guiding my research and helping me to develop my research background in statistics, psychology, physiology and neuroanatomy. They patiently guided and encouraged me in the process of this dissertation.

I specially thank my lab manager, Lynn Mande, for everything. Without her support, I could not have accomplished anything. I would like to thank my fellow lab-mates, Ramin Rajaee and James Murphy, for many useful discussion, help and friendship.

I am grateful to the neuroscience program and the department of radiology of Michigan State University for financially supporting my doctoral training and providing experimental facility for my dissertation study. I thank the undergraduate students of the Michigan State University for participating in my experiments. I also thank all the professors at Michigan State University whom I have taken courses from and interacted with. I also thank all the friends I made in the neuroscience program. Thank you all for making my graduate-student life cheerful.

Last, I would like to thank my family. They are always supporting me spiritually, emotionally and psychologically. I would like to thank my husband, Tao Wu, for encouraging, supporting and loving me unconditionally during the past years. My parents, ShulinYang and Changfen Zheng, receive my deepest gratitude for their understanding and supporting during my undergraduate and graduate studies. I will never forget how difficult it was for them to accept my decision to leave China for my dream. I thank them for their faith in me and respecting every decision I made for my life. I also thank Tao's parents for unending encouragement and support.

I wish I could enumerate all the people I need to give thanks, but I am sure I missed many of them on this short acknowledgement. I am grateful for them and wish I could pass their kindness to other people in the future.

TABLE OF CONTENTS

LIST OF TABLES

LIST OF FIGURES

Chapter 1

Introduction

1.1 Pain and its Co-morbidity with Depression

In the United States, pain is one of the largest medical health problems and results in high societal costs. For example, low back pain alone anually costs $90 billion dollars in physician services, hospital costs and pharmacy expenditures, as well $7 billion dollars indirect costs in sick leave, early retirement, and lost household productivity (Dagenais et al., 2008).

Depression is frequently co-morbid with chronic pain. For example, patients with complaints of persistent pain are four times more likely to be diagnosed with an anxious or depressive disorder than those who are pain-free (Gureje et al., 2001). In primary care practice, up to 80% of depressed patients present with physical symptoms that include headache, abdominal pain and musculoskeletal pain (Stahl, 2002). Furtermore, there is evidence that both depression and chronic pain increase the risk for a subsequent first onset of the other. For example, in a cohort study examining the relationship between migraine and major depression during a 2-year period, researchers found that the risk of first-onset migraine in persons with pre-existing major depression was threefold higher than in persons with no history of major depression. In addition, the risk of first-onset major depression in persons with pre-existing migraine was more than fivefold higher than in persons with no history of headaches (Breslau et al., 2003).

The neural mechanisms underlying the co-morbidity of pain and depression remain unclear. Cognitive-behavioral training techniques and antidepressant medicine (e.g. selective serotonin reuptake inhibitors (SSRIs)) have been used to effectively treat individuals with either chronic pain or depression (Blanchard et al., 1985; Gallagher et al., 1999). Examples such as this suggest that pain and depression may share some common neural pathways.

1.2 The Phenomenon of Pain

Pain sensation, including pricking, burning, aching, stinging and soreness, is a sub-modality of somatic sensation and serves an important protective function to organisms by helping them to avoid injury and permanent damage. Unlike other somatic sensations, pain has a primitive quality intimately associated with emotional experiences. Moreover, the intensity of perceived pain can be influenced by emotional context so that the very same noxious stimulus may be perceived differently under different conditions and for different individuals. In this way, pain is a subjective perception. According to the International Association for the Study of Pain (IASP), pain is an "unpleasant sensory and emotional experience associated with actual or potential tissue damage, or described in terms of such damage" (Merskey and Bogduk 1994; p. 210). To better describe the necessary and sufficient associations among experiences of unpleasantness, sensation and tissue damage, a revised definition of pain was proposed by Price (1999) who suggested that pain is "a somatic perception containing (1) bodily sensation with qualities like those reported during tissue-damaging stimulation, (2) an experienced threat associated with this sensation, and (3) a feeling of unpleasantness or other negative emotion based on this experienced threat." In other words, a painful experience consists of both bodily sensation and negative feelings. Further, it is not necessary to objectively demonstrate actual or potential tissue damage: pain can occur without peripheral nociception. If a person describes his/her experience as pain, it is defined as pain regardless of actual tissue damage. This definition of pain highlights the importance of investigating the relationship between pain sensation and emotions.

1.2.1 Multi-dimensional Characteristics of Pain

In 1968, Melzack and Casey proposed a conceptual model of pain that explicitly formulated how the various dimensions of pain could be transmitted in the nervous system. Their model of

pain included sensory, affective and cognitive dimensions (Melzack and Casey, 1968). According to this model, the *sensory* dimension consists of a bottom-up sensory-discriminative system that provides information about the location, intensity and duration of painful stimuli, as well as the type of pain (e.g. burning or stinging). The *affective* dimension consists of a behavioral motivational system that is responsive to the aversive drive and affective characteristics of pain. This behavioral motivational system provides information about the unpleasantness of the painful sensation and drives the motivation to escape. The *cognitive* dimension consists of a cognitive control system that regulates the intensity of activation in the discriminative and motivational systems, shapes attitudes and beliefs towards pain, and drives decisions and strategies to modulate it. The interaction of sensory, affective and cognitive domains of pain thus determines our perception of a painful stimulus. The model is generally accepted in the field of pain research and its application will be described in the following sections, focusing on the sensory and affective dimensions of pain.

1.2.1.1 The Sensory Dimension of Pain

The sensory qualities of pain are diverse. When peripheral tissues are intensively stimulated, sensory receptors (nociceptors) are activated. The ensuing nociceptive sensations can be described according to their intensity, location and duration. For example, some types of pain are experienced as pressure, and described in such words as “pinching”, “cramping” or “pricking”. In terms of duration, pain can be acute or tonic. For example, if one touches a hot stove and immediately removes his or her hand, the pain is sharp and hot. If one’s hand is not removed immediately, resulting in deep tissue injury, persistent pain can arise from accompanying inflammation.

1.2.1.2 The Affective Dimension of Pain

Pain is an unpleasant sensory and emotional experience. Nociception only contributes part to the total pain experience, mainly because of the affective qualities of pain. For example, if a person suddenly receives an electrical shock, the unpleasant sensation can also be accompanied by visual attention to the electrical plug, autonomic responses, memories of past experiences, and emotions such as annoyance. All these responses result in the experience of, for instance, intense threat and subsequent fear. Importantly, it is possible to experience pain *without* nociceptive inputs. For example, we can experience another person's pain. This empathy for pain primarily involves the affective pain dimension (Singer et al., 2004).

1.3 The Neural Mechanisms of Pain Processing

In 1664, the reflex theory of Descartes proposed a direct-line pain pathway from pain receptors in the body to a pain center in the brain (see reviews in Deleo, 2006). This theory was the beginning of the modern doctrine of reflexes and the first documented attempt to understand pain transmission. Descartes's view of the human pain system directed pain treatment for more than 330 years. Studies during this same period investigated physiological mechanisms at every level of the direct pathway, from receptors to the cerebral cortex. The theory implied that the simple cutting of this pathway should alleviate pain. However, clinical evidence has shown that this manipulation does not always alleviate pain. Damage to nerves, instead of alleviating pain, can cause serious neuropathic pain at some point. Amputees often have the illusion that their missing limbs are still present and most experience phantom pain: a tingling or burning sensation in their missing limbs (Melzack, 1989). This phenomenon suggests that neural mechanisms of the pain experience are more complex than those described by the direct-line pain pathway.

A major reinterpretation of how pain is transmitted to the nervous system and how the neural architecture controls pain intensity came in 1965 with Melzack's and Wall's gate control theory

of pain (Melzack and Wall, 1965). The gate control theory postulates that the perception of pain is not simply the direct result of the activation of nociceptive receptors, but involves the interaction of different sets of neurons in the spinal cord. The idea is that pain results from the balance of activity of nociceptive and non-nociceptive afferents in the spinal cord. Neurons in lamina V and I receive convergent excitatory inputs from both nociceptive Aδ/C fibers and non-nociceptive Aβ fibers. It was proposed that Aβ fibers activated inhibitory interneurons in lamina II, which could then inhibit the firing of neurons in lamina V. In contrast, Aδ and C fibers inhibit interneurons in lamina II. In the spinal cord, a gate to the central transmission of noxious input is therefore "closed" by non-nociceptive afferents and is "opened" by nociceptive afferents. Neural gates in the spinal cord can be opened or closed by sensory stimuli ascending from the body.

1.3.1 Primary Ascending Pathways of Nociceptive Pain Transmission

To generate nociceptive pain sensation, information about tissue damage is transferred from the spinal cord to the brain through five major pathways: the spinothalamic, spinomesencephalic, spinoreticular, cervicothalamic, and spinohypothalamic pathways (Price, 1999). Within the brain, the destinations of the different pain-related ascending pathways have bearing on differential processing of separate pain components. The spinothalamic and spinamesencephalic pathways (Figure 1.1) are the major pathways important for sensory and affective dimensions of pain that are described in the following sections. The spinoreticular pathway originates from the spinal cord and terminates in both the reticular formation and the thalamus. This pathway is likely related to pain-related arousal and motor responses (Willis and Westlund, 1997). The cervicothalamic pathway arises from the lateral cervical nucleus and ascends to the ventroposterior lateral nuclei of the thalamus. Studies in both humans and rats demonstrate that this pathway signals pelvic visceral pain (Hirshberg et al., 1996). Finally, the spinohypothalamic

pathway projects directly to the hypothalamus and the supraspinal autonomic control centers, and is considered to contribute to autonomic and endocrine responses to painful stimuli (Bernard et al., 1996).

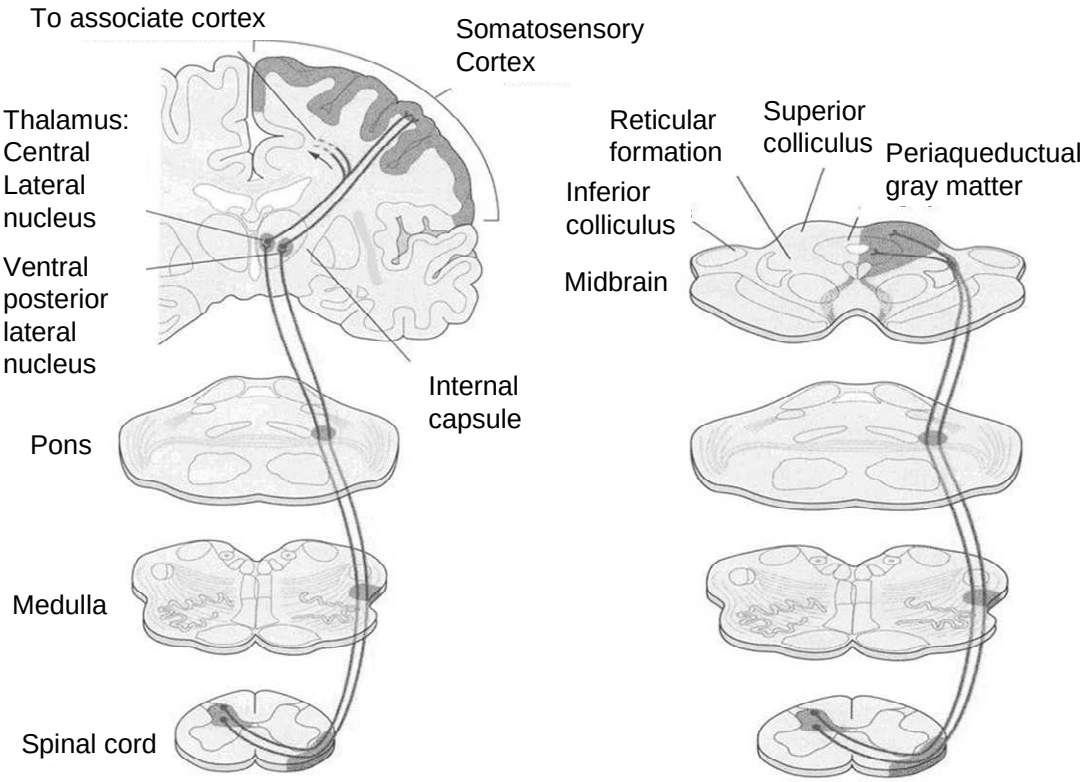

Figure 1.1 Two major ascending pathways for nociceptive processing: the spinothalamic pathway is shown on the left, and the spinomesencephalic pathway is shown on the right (Adapted from The perception of pain. In Kandel, Schwartz & Jessell (Ed.), Principles of Neural Science).

1.3.1.1 Spinothalamic and Spinomesencephalic Pathways

The ***spinothalamic pathway*** primarily carries nociceptive information about intensity, location and temperature, and is considered to be the major ascending central pathway for pain perception (Dennis and Melzack, 1977; Willis et al., 1985). Electrical stimulation of this tract at the level of the spinal cord or thalamus often evokes pain sensation in humans (Mayer et al.,

1975). The primary origin of the spinothalamocortical pathway is the dorsal horn of the spinal gray matter. Two types of neurons reside in laminae I and V-VII and receive information from peripheral nociceptive neurons. The first type, *nociceptive-specific* neurons, respond exclusively to stimuli that are potentially tissue-damaging. The second type, *wide-dynamic-range (WDR)* neurons, respond to weak mechanical stimuli such as light touch or movements of a single hair, and to noxious stimuli. Axons of both these types of neurons in the dorsal horn ascend in the dorsal column-medial lemniscal tract, where they synape on neurons in the dorsal column nuclei in the medulla before decussating and ascending in the anterolateral white matter, and terminating in the ventral posterior lateral and central lateral nuclei of the thalamus. From the thalamus, projections finally reach the somatosensory cortex. In addition, some nociceptive-specific and WDR neurons of the dorsal horn project to various ventrolateral and medial thalamic nuclei, as well as multiple levels of the brainstem and midbrain, including reticular formation nuclei, the superior colliculus, the periaqueductal gray, parabrachial nuclei and hypothalamus. These projections reflect the diverse functional consequences of the nociceptive input.

The ***spinomesencephalic pathway***, another major pain pathway, is thought to contribute primarily to the affective component of pain. This tract contains axons of neurons in laminae I and V of the spinal cord. In fact many of the same neurons that give rise to the spinothalamic tract are also the origin of the spinomesencephalic tract. Axons of these neurons in the dorsal horn cross to the contralateral side of the spinal cord, ascend in the dorsal column-medial lemniscal tract, where they synape on neurons in the dorsal column nuclei in the medulla before ascending in the anterolateral white matter and terminating in the mesencephalic reticular formation and periaqueductal gray matter of the midbrain. From there, some neurons continue as

the spinoparabrachial tract and project from the reticular formation to the parabrachial nucleus, and finally to the amygdala and hypothalamus. The destination of this tract suggests that it is likely to contribute to the affective dimension of pain. In addition, the tract may be related to the mechanism of autonomic responses and arousal that accompany pain experience.

1.3.1.2 Parallel Systems Associated with Sensory and Affective Dimensions of Pain

Projections from the thalamus to the cortex are commonly segregated into lateral and medial pain systems (Albe-Fessard et al., 1985). The *lateral pain system*, overlapping with parts of the spinothalamic tract, consists of projections from the ventral posterior lateral and central lateral nuclei of the thalamus to both primary and secondary somatosensory cortices (Vogt and Sikes, 2000). The *medial pain system* consists of projections from medial (midline and intralaminar) thalamic nuclei to the anterior cingulate cortex and amygdala; neurons from these latter areas project to nociception-regulating centers such as the periaqueductal gray (Vogt and Sikes, 2000; Sewards and Sewards, 2002).

The lateral pain system is considered to be intimately involved in processing the sensory-discriminative dimension of pain sensation. Evidence for this comes from single-unit electrophysiological studies of the physiological response characteristics of neurons in monkey primary somatosensory cortex (SI). Kenshalo and Isensee (1983) discovered different types of nocicepetive neurons in SI with similar receptive fields and physiological response characteristics to neurons in the spinothalamic pathway. The SI neurons, which receive excitatory input from thalamic nuclei including the ventral posterior lateral nucleus (VPLc), respond to graded nociceptive temperatures and provide precise information about nocicepetive intensity (Price et al., 1992). The secondary somatosensory cortex (SII) also contains nociceptive neurons and can encode the intensity of nociceptive heat stimulation (Dong et al., 1989). Human

studies have shed further light on the functional role of lateral pain system. For example, in one PET study, Hofbauer et al. (2001) demonstrated that hypnotic modulation of the perceived intensity of a noxious heat stimulus significantly changed pain-evoked activity within SI, suggesting that the sensory dimension of pain is encoded in SI.

In contrast to the lateral pain system, the medial pain system includes a number of interconnected areas within the limbic system. It is these limbic regions which are thare thought to process the affective dimension of the pain experience. It is known, for example, that ablations of anterior cingualte cortex (ACC) abolish affective responses of noxious stimuli, while sensory localization remains intact (Vogt and Sikes, 2000). Nociceptive neurons in ACC have large receptive fields that usually include the whole body and exhibit the capability to monitor the overall state of the body. Human neuroimaging studies have found that pain unpleasantness is mainly encoded in the posterior portion of ACC. For example, hypnotic modulation of the unpleasantness of experimental heat pain alters activation in ACC but not in SI (Rainville et al., 1997).

The lateral and medial pain systems, however, do not include all the brain regions that appear to be involved in the multi-dimensional processing of pain. Besides somatosensory and anterior cingulate cortical areas, there are insular, posterior parietal, medial and dorsal lateral prefrontal cortices also activated in neuroimaging studies of pain (Peyron et al., 2000; Symonds et al., 2006).

1.3.2 The Neuromatrix Theory of Pain

The gate control theory highlights the role of the spinal cord in pain transmission and its modulation. The neural signals in the dorsal horn that carry information about peripheral input can increase or decrease the flow of impulses to higher levels of pain processing centers.

However, pain is a multidimensional experience and to understand its neural basis, it needs to go beyond the level of the spinal cord and into the brain where supraspinal regions play very important roles in pain processing. Recent neuroimaging studies on empathy report that perceiving pain of others leads to personal distress and activates many brain regions known to be associated with processing nociceptive stimuli, such as anterior insula, anterior cingulate cortex and periaqueductal gray (Singer et al., 2004; Cheng et al., 2007). Such findings highlight the importance of supraspinal mechanisms in generating and modulating pain experience. In addition, the gate control theory cannot fully explain such phenomena as chronic pain, or phantom limb pain.

The *neuromatrix theory of pain* proposed by Melzak (1990) suggests that the multidimensional experience of pain is produced by characteristic "neurosignature" patterns of nerve impulses generated by a widely distributed and intrinsically interactive neural network in the brain. The conceptual model that has emerged from this theory includes four main precepts. First, the widely distributed neural network, the *neuromatrix*, includes the neural circuits between the thalamus and cortex as well as between the cortex and limbic system. Second, the spatial distribution and synaptic connections of the neuromatrix are initially determined genetically and are modified by sensory inputs. Third, the neural circuits in the neuromatrix allow parallel processing of cognitive, sensory and emotional components of pain. The outputs of parallel processing then converge in the neuromatrix. Parallel processing and synthesis of nerve impulses generates a characteristic pattern, the *neurosignature*, of the neuromatrix. Finally, the neurosignature projects to the brain areas, the *sentient neural hub*, which convert the flow of neurosignature into the continually-changed flow of awareness (e.g. pain perception), stress-

regulation programs (e.g. cortisol level and immune system activity) or the experience of movements.

The neuromatrix pain theory helps to account for pain as a multidimensional experience influenced by multiple stressors. The theory proposes that the neurosignature of pain experience is determined by the synaptic structure of the neuromatrix and is modulated by sensory inputs. Thus, the pain experience must be generated in the brain and influenced by the interaction of an array of neural circuits such as emotion-related brain areas and sensory signaling systems.

1.3.3 Brain Regions of Pain Processing

The neuromatrix pain theory predicts that there must be many different brain areas involved in pain experience. Because our pain experience includes sensory discriminations, arousal, cognitive evaluation, affect and motor responses, it makes sense that extensive networks of cortical and subcortical areas participates in pain processing.

With the development of neuroimaging techniques, it has become increasingly clear that widely-distributed and highly-interconnected brain regions in humans are invovled in generating the subjective pain experience. In a meta-analysis study reviewing functional imaging of brain responsive to pain, Peyron et al. (2000) described increased brain activity in a number of brain areas, including primary and secondary somatosensory (SI and SII), anterior cingulate (ACC), insular, posterior parietal and medial prefrontal cortices and thalamus. Several of the studies in the meta-analysis also observed increased activation in the cerebellum, striatum, and periaqueductal grey. Commonly, SII, insula, ACC, and thalamus are sufficient to generate the perception of pain to noxious stimuli (Peyron et al., 2000; Apkarian et al., 2005).

1.3.3.1 Brain Regions Associated with the Sensory Dimension of Pain

Cortical areas SI and SII contain nociceptive-specific neurons and wide-dynamic-range (WDR) neurons with similar physiological characteristics to the neurons in the thalamus and the dorsal horn of the spinal cord. Electrophysiological studies of SI cortical neurons in the anesthetized macaque monkey have characterized the responses to a series of noxious mechanical and thermal stimuli. Response characteristics of SI nociceptive neurons reveal that these neurons have either restricted contralateral receptive fields or very large receptive fields covering most of the body's surface (Kenshalo and Isensee, 1983). The restricted contralateral nociceptive neurons provide information about the localization, intensity and temporal attributes of a noxious stimulus. This is true in humans as well: PET studies have found that increases in regional cerebral blood flow (rCBF) in SI to painful heat stimuli are correlated with the intensity (temperature) of stimuli (Coghill et al., 1993). A broad region comprising the secondary somatosensory cortex (SII), neighboring area infraparietal 7b and the restroinsular cortex also contain nociceptive neurons that encode the intensity of nociceptive heat stimuli (Dong et al., 1989). The most consistant location of pain-related activity across PET and fMRI studies is located in this broad cortical region (Peyron et al., 2000). In a number of imaging studies, pain-related activations are reported as a focus of increased cortical blood flow (CBF), which overlaps on both posterior insular and SII cortices. In addition, the distribution of increased CBF in the posterior insular/SII cortices is bilateral during painful stimuli (Treede et al., 1999; Symonds et al., 2006).

1.3.3.2 Brain Regions Associated with the Affective Dimension of Pain

The anterior cingulate (ACC) and the anterior insular cortices are generally considered to encode the affective dimension of pain processing (Peyron et al., 2000). The ACC is part of the medial pain system and the nociceptive neurons in the ACC have large receptive fields covering

the whole body's surface. The characteristics of these neurons may reflect the general functions of the medial pain system in the cortex: to monitor the overall state of the body and to process the affective components of pain. The role of ACC in the affective dimension of pain is supported by imaging studies. For example, hypnotic modulation of pain unpleasantness (but not intensity) altered activation in ACC, but not in SI (Rainville et al., 1997). Tolle et al. (1999) extended the results of this PET study, using a regression analysis to analyze the relationship of noxious heat-related regional blood flow (rCBF) increases and experimental pain parameters, including detection of pain, encoding of pain intensity, and pain unpleasantness. They found that rCBF in the posterior portion of ACC was positively correlated with pain unpleasantness. A recent fMRI study showed that even without direct noxious stimulation, imaginary pain sensation can lead to ACC activation increases (Ogino et al., 2007). In this study, subjects were instructed to imagine pain in their own body while they were shown pictures of painful events, or were presented with pictures inducing emotions of fear. Comparing cerebral hemodynamic responses during the imagination of pain with those to emotions of fear, the researchers found that most pain-relevant brain areas were activated, including the ACC, right anterior insula, cerebellum, posterior parietal cortex, and secondary somatosensory cortex region. The ACC is activated during both imaginary pain and when viewing images evoking emotions of fear. This suggests that the ACC is likely engaged in both pain and emotional experiences.

The insular cortex receives direct projections from the medial thalamic nuclei and from the ventral and posterior medial thalamic nucleus. In addition, the anterior portion of the insular cortex is reciprocally connected with the amygdala (a region associated with emotions). Neurons in the insular cortex process information on the internal state of the body (Craig, 2003). Specificcaly, the anterior insular cortex responds to introspective awareness and subjective

feeling states (Critchley et al., 2004). Patients with lesions of anterior insular cortex do not display corresponding emotional responses to the pain, when perceiving noxious painful stimuli (Greenspan et al., 1999). This suggests that the involvement of the anterior insula in pain processing is related to the affective dimension of pain.

1.3.3.3 Supraspinal Modulation of Pain Transmission

Investigation of pain-modulation pathways began with the 1969 observation that direct stimulation of the periaquductal grey (PAG) in the rat could powerfully suppress pain perception (Reynolds, 1969). The brain regions to which the PAG connects, including the anterior cingualte cortex (ACC), insula, amygdala, and rostral ventromedial medulla (RVM), form the descending pain modulation pathways. The RVM receives information from the PAG and serves as an integral relay in descending modulation of nociception, projecting to the origin of ascending pain pathways in the dorsal horn of the spinal cord. The RVM has two classes of pain-modulating neurons: on-cells and off-cells. On-cells are directly inhibited by endogenous opioids and they facilitate pain transmission. In contrast, off-cells are inhibited by on-cells and they inhibit pain transmission (Porreca et al., 2002). The existence of on- and off-cells within the RVM raises the possibility that pain can be modulated by various psychological conditions. For example, descending pathways from cortical areas could either facilitate or inhibit nociception transmitted from the spinal cord. Recent fMRI studies do, in fact, indicate that cingulate and frontal cortices have an effect on the PAG and possibly modulate pain during distraction (Valet et al., 2004). A particularly compelling fMRI study in which subjects were given in real-time biofeedback data based on fMRI signal changes showed that both healthy individuals and chronic pain patients can be trained to control their own activity in the rostral ACC and to modulate their pain experience

(deCharms et al., 2005). These studies clearly recognize the role of the cortical regions and PAG in modulating pain perception.

1.4 The Neural Mechanisms of Emotions

Charles Darwin's view that many of the different emotions were similar across species laid the groundwork for the modern field of affective neuroscience. He compared countless sketches of animals and people in different emotional states and proposed that emotional expressions in humans are "patterns of action" and that there are a limited set of basic emotions across species and cultures. These ideas prompted the use of animals in research on human emotions. Later, in 1884 the James-Lange theory proposed that emotions are the experiences of sets of body changes that occur in response to emotive stimuli, and that different patterns of body changes determine different emotions (see reviews in Dalgleish, 2004). The most obvious sign of emotional arousal in animals, including humans, is activity in the autonomic system; e.g. increased or decreased heart rate, cutaneous transduction and gastrointestinal motility. The James-Lange theory is still influential in contemporary affective neuroscience, especially in arguments that bodily feedback modulates emotional experience and that emotional responses can be at least partly distinguished on the basis of autonomic activity.

1.4.1 Neuroanatomical Theories of Emotions

The first substantive theory of the brain mechanisms of emotions was proposed by Cannon and Bard in 1931. They investigated the effect of brain lesions on the emotional behavior of cats and found that removal of the neocortex caused cats to make sudden and ill-directed anger attacks (Bard, 1937). They argued that the hypothalamus is involved in the emotional responses and that removal of the neocortex breaks the hypothalamic circuit from top-down control. Their work suggested that the hypothalamus is a critical center for coordinating emotional behaviors.

Around the same time, James Papez (1937) proposed that the central neural circuits, now known as the 'Papez circuit', were responsible for emotional behaviors. He included both the hypothalamus and cingulate cortex in his proposed emotional circuits, and demonstrated that the hypothalamus and cingulate cortex were interconnected via projections from the anterior thalamus and the hippocampus. Papez proposed that emotional information arrived at the thalamus and diverged into two streams, one of them directed to the cortex (upstream), and the other directed to the hypothalamus (downstream). The upstream pathway transmitted information to the sensory cortices, especially to the cingulate region. Through this pathway, emotional information was converted into perceptions, thoughts and memories. The pathway extended from the cingulate cortex to the hippocampus and, via the fornix, to the mammillary bodies of the hypothalamus. The downstream pathway projected from the thalamus directly to the mammillary bodies of the hypothalamus, completing the circuit and integrating the work of Bard (1937). The 'Papez circuit' accounted both for generation of emotions and the top-down control of emotional responses.

Over time, the neural circuits for the regulation of emotional responses have come to include more brain regions. Kluver and Bucy (1939) showed that bilateral lesions of the medial temporal lobe in rhesus monkeys led to a set of abnormal emotional behaviors (Kluver-Bucy syndrome), including bizarre oral behaviors, hyperactivity and hypersexuality. It was later shown by Weiskrantz (1956) that bilateral lesions of the amygdala were sufficient to induce the emotional disturbance of Kluver-Bucy syndrome. A decade later, MacLean proposed the limbic system model based on Papez's and Bard's ideas and integrated them with the findings from the work of Kluver and Bucy (MacLean, 1949). This model included many of the components of the 'Papez circuit', such as the thalamus, hypothalamus, hippocampus and cingulate cortex, as well as other

important structures such as orbital and medial prefrontal cortex and amygdala. McLean separated the emotional brain into two parts: (1) the ancient reptilian brain (striatal complex and basal ganglia), which he proposed is the basis of primitive emotions such as fear and aggression; and (2) the old mammalian brain (limbic system), which in his view enhances primitive emotional responses and elaborates social emotions. Finally, in McLean's model, the new mammalian brain (neocortex) allows for emotions to interface with cognition and in addition exerts top-down regulation of emotional responses.

1.4.2 Brain Regions Associated with Emotions

In the past ten years, assumptions regarding the neuroanatomical structures involved in emotions have been tested using neuroimaging techniques in humans. PET and fMRI studies have begun to describe the key emotion-related brain regions, such as the anterior cingulate, insular and medial prefrontal cortices, and the amygdala (Phan et al., 2002; 2004).

The anterior cingulate cortex (ACC) is important for integrating attention and emotional information, and for regulating emotional behaviors. In particular, the ACC may mediate arousal responses accompanying emotional behaviors. There is evidence that rostral ACC projects to autonomic areas such as hypothalamus and brain stem, and with orbitofrontal, insular and medial temporal regions that also project to these homeostatic centers (Barbas et al., 2003). Direct stimulation of rostral ACC in animals and humans evokes autonomic responses. PET and fMRI studies have reported abnormalities in ACC activation in psychiatric patients with obsessive-compulsive disorders, post-traumatic stress, and depression, compared to healthy individuals (Devinsky et al., 1995; Rauch et al., 1994; Semple et al., 2000; Drevets, 2001). The subgenual cingulate cortex (sACC) appears to be associated with sadness. Approximately 46% of studies that induced sadness in the experimental protocol reported that sACC is activated (Phan et al.,

2002), and it appears that this region is active whether sadness is induced using either recall-generated sadness or autobiographical scripts (Reiman et al., 1997; Lane et al., 1997; Liotti et al., 2000). In PET imaging studies, Mayberg et al. (1999) addressed the potential mechanism mediating top-down regulation of mood disorders and found that sadness was not only accompanied with increased activation in sACC and the anterior insula, but also with decreased activation in the right dorsolateral prefrontal and inferior parietal cortices. These same investigators also discovered that recovery from depression involved the same regions in a reversed activation pattern, with decreased limbic metabolism and increased cortical metabolism.

The insular cortex projects to brain regions such as the amygdala and hypothalamus that play critical roles in regulating autonomic activity (Augustine, 1996). Activation in the insular cortex has been reported in many neuroimaging studies in which emotions have been manipulated, including when emotional recall is used and when emotions are induced by viewing pictures (Phan et al., 2002; Lane et al., 1997). There is also empirical evidence that right anterior insula activity reflects introspective representation of bodily responses which is crucial to subjective emotional states arising from autonomic visceral responses (Critchely et al., 2004).

The amygdala also appears to be critical for processing emotions. Neuroimaging studies have shown that the amygdala responds to fearful faces (Young et al., 1995; Morris et al., 1996; Philips et al., 1997) and is important for recognizing fearful facial expressions. In addition, recordings of neurons in the amygdala of the monkey reveal that a population of neurons located in the basal accessory nucleus of the amygdala responds to human or monkey faces (Leonard et al., 1985). It has been suggested that the damage of these neurons would cause the deficits in emotional response (Leonard et al., 1985). Activity in the amygdala is susceptible to the top-down control. For example, it has been shown that attention can modulate amygdala activity

(Pessoa et al., 2005). Amygdala activation has been found in response to stimuli other than fearful faces, including aversive pictures (Taylor et al., 1998), sad faces (Blair et al., 1999), and even recall of pleasant pictures (Hamann et al., 1999). Thus, it is possible that the amygdala may respond to general emotional stimulus salience, regardless of emotional valence.

The relationship between the frontal lobe and emotions is perhaps best illustrated by the classic case of Phineas Gage. In 1848, Gage, a railroad worker, survived an explosion which caused a large iron rod to be completely propelled through his head, destroying large regions of his frontal lobes. The injury dramatically affected his personality and behavior. It is now known that the prefrontal cortex, especially medial prefrontal cortex (mPFC), has an important role in emotional processing (Phan et al., 2002). The activation of mPFC is engaged in processing emotions induced by emotional films, pictures and recall (Lane et al., 1997; Reiman et al., 1997). Positive and negative emotions, such as happiness, sadness and disgust, and the mixture of emotions all can activate the mPFC.

1.5 The Interaction of Pain and Emotions

1.5.1 Emotions Influence the Perception of Pain

Numerous behavioral experiments have reported that pain experiences are altered by emotional states. In general, negative emotions increase the perception of pain intensity and decrease tolerance to pain, while positive emotions attenuate pain intensity, raise pain thresholds, and increase tolerance. For example, a positive mood induced by humorous film clips increased cold-pressor pain tolerance, while a negative mood induced by film clips of the holocaust decreased it (Weisenberg et al., 1998). Meagher et al. (2001) found that male subjects who viewed slides that provoked feelings of fear or disgust were more sensitive to cold pain, but less

sensitive to pain when they watched erotic slides. It has also been reported that perceived pain intensity is enhanced by pain-relevant anxiety (Ploghaus et al., 2001).

1.5.2 Neural Substrate Correlated with the Interaction between Pain and Emotions

Both emotion and pain are multidimensional contrusts that contain motor, valence, sensory and physiological components. They are considered to be parts of a large motivational system that promotes survival (Mollet and Harrison, 2006). In the motivational system, there are appetitive and defensive sub-systems guiding individuals toward survival-needed stimuli (e.g. food and water) and warning individuals away from harmful stimuli (e.g. injuries). Emotions are often described in terms of their place on a range of two main components: valence (from negative to positive) and arousal (from calm to excited). Positive emotions can be thought of as the result of appetitive system activity, and negative emotions as a result of defensive system activity. The level of arousal can be thought of as the degree of activity of the motivational system. Because pain comprises emotional, sensory and cognitive components, emotion is inherently part of pain. Pain sensation can be considered to be generated in the defensive system which motivates organisms to avoid noxious stimuli. The integration of pain and emotion may account for a wide range of behavioral and physiological changes. It would therefore not be surprising if a wide range of brain regions were involved in the interaction between pain and emotion. Further, there should be either some overlap in the neurocircuits of these two states, or a close association between them. Several limbic structures are potentially associated with the interaction between pain and emotion.

The cingulate cortex: The medial pain system includes projections from the midline and intralaminar thalamic nuclei to the anterior cingulate cortex (Vogt and Sikes, 1999). Recently, Vogt reviewed the linkages between pain and emotion in the cingulate cortex by analyzing the

results of 40 human imaging studies in which noxious stimuli were presented, and results of 23 studies in which simple emotions were experienced (Vogt, 2005). His findings include the following: (1) both noxious thermal stimulation of the skin and fear induced by events, objects or memories with negative valence activate the anterior mid-cingulate cortex (mACC/BA24); (2) both happiness and pain induced by balloon distention of the distal esophagus activate a region within the posterior anterior cingulate cortex (pACC); (3) hypnotic amplification of unpleasantness during noxious stimulation enhances activity in the caudal part of pACC. These findings suggest that during some painful states in which both pain and emotion are experienced, a portion of the cingulate cortex including the pACC and the mACC may be involved in their integration. Mu-opioid receptors are found in a number of regions in the brain, including both the ACC and the amygdala, which are shown to release endogenous opioids that bind to μ-opioid receptors under sustained pain stimuli (Zubieta et al., 2001).

The Insular cortex: Insular cortex plays a role in diverse functions such as emotions, homeostasis, and self-awareness (Craig, 2002; Critchley et al., 2004). Both pain and emotion represent important changes in the internal states of an organism. Therefore, it is possible that the link between emotion and pain may be associated with the activity in the insular cortex. Damasio et al. (2000) reported in a PET study that processing emotion activated regions of the insular cortex. In their experiments, 41 normal subjects recalled and re-experienced personal life episodes marked by sadness, happiness, anger or fear. The results indicated bilateral, but asymmetric, activations in anterior/middle insular cortex during either sadness or anger, as well as positive activations in right anterior/middle insular cortex during either happiness or fear. In another study, the activity in the bilateral anterior insular cortex of a neuropathic pain patient was increased by unpleasant odors (Villemure et al., 2006). This identified activation pattern in

anterior insula was close to the activation pattern of sadness found in the experiment of Damasio et al. (2000). Evidence from these studies suggests that the insular cortex may be an important region involved in both emotional and painful experience.

The amygdala: The amygdala may also integrate neural activity associated with negative emotions and pain. In a PET study, Zubieta and colleagues (2001) examined the function of the opioid system in healthy human subjects undergoing sustained muscle pain. Significant activation of the μ-opioid receptor system was detected in selected volumes of interest in the amygdala ipsilateral to the painful stimulus, indicating a regional release of endogenous opioids during sustained pain. In another PET study, Zubieta et al. (2003) reported that sustained sadness was associated with significant deactivation of μ-opioid neurotransmission in the amygdala. These lines of evidence suggest that in addition to the amygdala's well-documented role in affective processing, it is involved in the μ-opioid-mediated sensory responses.

The frontal lobe: The medial prefrontal cortex (mPFC) also may be associated with the interaction between emotion and pain. An fMRI study in rheumatoid arthritis patients found that applying pressure to arthritic joints provoked joint pain and led to increased activation in the bilateral MPFC (Schweinhardt et al., 2008). Moreover, the increased activation in the MPFC was significantly positively correlated with the patients' Beck Depressive Inventory (BDI) scores. The right ventrolateral prefrontal cortex (VLPFC) may be involved in emotional regulation of pain by driving top-down pain inhibitory pathways. This region, for example, was identified in an fMRI study in which religious beliefs decreased pain perception. Among practicing Catholics, an image of the Virgin Mary induced context-dependent analgesia during acute electrical pain stimuli, concurrent with increased activation in the right VLPFC (Wiech et al., 2008).

1.6 Background to the Methodology

Until twenty year ago, pain was investigated primarily at the peripheral and spinal cord levels. Studies mainly relied on animal models, in which ablation methods, pharmacological manipulation and electrophysiological methods were employed. Functional neuroimaging has fundamentally changed our knowledge about pain sensation and led to the identification of brain regions linked to pain sensation in humans. Because pain is a subjective experience and can change under different circumstances, non-invasive techniques such as functional magnetic resonance imaging (fMRI) allow us to investigate the brain activity of conscious subjects and to record functional activity across the entire brain simultaneously. The experiments in the dissertation employ fMRI methods to investigate functional networks for altered pain experience by sad mood. First, task-driven fMRI methods are used to identify brain activation patterns when pain is affected by sadness. Second, resting-state fMRI methods are used to investigate the intrinsic connectivity within brain networks for pain and emotion. Third, path analysis is applied to the fMRI datasets to investigate the functional connectivity of brain networks that underlie altered pain perception during sadness.

1.6.1 Task-driven fMRI and Data Analysis

Most fMRI experiments examine brain activity by measuring the blood-oxygenation-level dependent (BOLD) signal, which relies on the different magnetic properties of oxygenated and deoxygenated hemoglobin (Ogawa et al., 1990). The BOLD signal is correlated with neuronal activity, as local neuronal activity increases metabolic requirements. Logothetis et al. (2001) presented empirical evidence that local field potentials in the visual cortex of monkeys were significantly correlated with the BOLD hemodynamic response. In that landmark study, intracortical electrophysiological recordings were made while simultaneously recording the BOLD signals with fMRI.

Task-driven fMRI experiments detect regional changes in the BOLD signal as neurons in specific brain areas respond to the designed tasks. For example, in this dissertation study, a task-driven fMRI study was designed to deliver pain, either alone, or accompanied with visual stimuli to investigate how sadness influences pain perception. Good experimental design is necessary in functional MRI studies and several issues need to be considered including: (1) the specific dependent variables to be measured (e.g. brain activation under different tasks); (2) whether a between-subject or within-subject design is more appropriate; (3) the implementation of adequate control conditions; (4) control of confounding factors (e.g. induced emotions other than sadness); and (5) the signal-to-noise ratio necessary to statistically detect the BOLD signal. Task-driven fMRI studies do not "draw pictures" of absolute BOLD signals, but analyze the percent change in the signal by comparing task periods to an arbitrary baseline of non-task periods. Brain regions that are active and that potentially participate in performing the task are identified on the basis of a statistically-significant difference in fMRI signal intensity during the task compared to the baseline. In this dissertation study, there are three different tasks: (1) painful electrical shocks; (2) mood induction with emotionally-evocative pictures; (3) painful electrical shock accompanied by emotional pictures. Non-emotional pictures are used during the baseline periods to control for activation associated with merely watching and paying attention to colorful pictures. To evaluate brain activation in a task condition compared to a baseline condition, most fMRI experiments use either an event-related design or a block design, or a mixture of the two. Block designs are most useful for discovering the magnitude of neural activity in one condition versus another, especially if the response to the task is slow, as in responses to electrical shocks and presentation of affective pictures. Block designs are powerful for detecting significant fMRI

activity, and minimizing low-frequency noise, and the design and analysis are relatively straightforward.

The procedure of a task-drive fMRI experiment is shown in the following chart (Figure 1.2). Functional brain imaging data is collected on individual participants. The experimental design is based on the number of experimental trials, the number of blocks in each run, the length of each block and the number/duration of stimuli during each block. Once the experimental design is finalized, participants are recruited to collect functional and anatomical datasets in MRI. The functional datasets of each individual are preprocessed to convert 2D images into 3D datasets, align separate slices to the same temporal origin, correct head movements, and eliminate outliers. Assuming the hemodynamic response function (HRF) has a fixed shape in any active brain region regardless of stimulus type, we can focus on the differences of the magnitude of the HRF in active brain regions. Regression analysis is applied to an individual subject's dataset to identify the significant brain activation during different tasks. Group analysis such as ANOVA can then be used to identify significantly activated brain regions across subjects. Finally, regions of interest analysis or connectivity analysis can be used in post-processing.

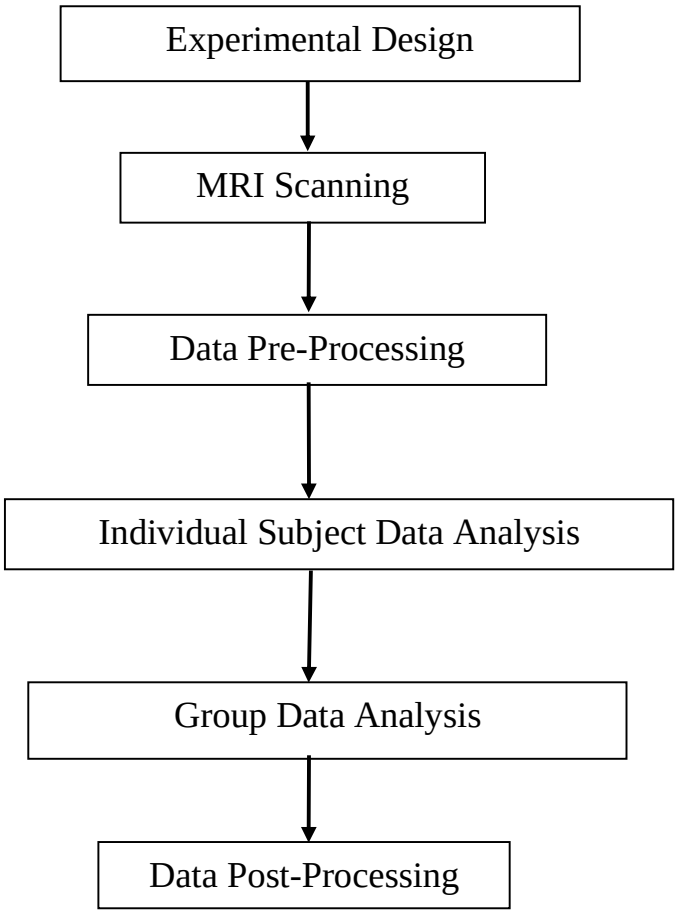

Figure 1.2 Flow charts of a task-driven fMRI experimental procedure.

1.6.2 Resting-State fMRI and Data Analysis

Traditional task-driven fMRI studies detect increased brain activity in response to specific experimental tasks. The signal that is analyzed in task-driven fMRI studies only accounts for a small amount of body metabolism, approximately 5% or less. The resting brain consumes 20% of the body's energy. This raises the question of why the brain consumes so much energy in the resting state. One explanation comes from the observation that most of the energy is used to support ongoing neuronal signaling (Fox et al., 2005). Thus, the spontaneous BOLD signals, which indirectly measure neuronal activity based on the brain metabolism, in the resting human brain could be meaningful. It has been found that spontaneous BOLD activity in the left

somatomotor cortex is specifically correlated with spontaneous fluctuations in the right somatomotor cortex and with medial motor areas in the absence of motor behavior (Fox et al., 2005). This empirical observation suggests that the spontaneous BOLD activity is not random noise, but reflects the functionality of the resting brain. Detecting brain activation patterns during resting states could provide insights into the intrinsic functions of the brain.

Based on the assumption that the components of a neural network are functionally connected, the BOLD signal fluctuations of these components can be reasonably assumed to be correlated in the resting state. This assumption is the basis of resting-state fMRI. Functional imaging studies of the resting brain have been conducted for many brain systems, including somatomotor, visual, auditory, episode memory and attention systems (see reviews in Fox and Raichle, 2007). These studies have shown that brain regions with similar functionality tend to have correlated spontaneous BOLD activity. Many resting-state fMRI studies have found that a particular set of brains regions is typically more excited at rest than during cognitive task performance (Raichle et al., 2001; Greicius et al., 2003). This pattern of activity is called the "default mode" brain network, and includes both positive and negative correlations of activity among separate brain regions. The task-negative regions are distributed in the medial prefrontal, lateral parietal, and posterior cingulate/precuneus cortices. Task-positive regions are distributed in the intraparietal sulcus, the frontal eye field region and the middle temporal region.

Resting state fMRI methods have been used to investigate the neural mechanisms that underlie pain. Baliki and colleagues (2008) investigated how chronic back pain disrupts the default mode network during the resting state. Using the brain regions of the default mode network as the seed regions in a correlation analysis, they found that correlation maps of healthy controls were very close to the default mode network described by Raichle et al. (2001) and

Greicius et al. (2003). However, chronic pain patients showed much smaller cortical areas with negative correlations and larger areas with positive correlations than healthy controls. The reduction in the total brain area exhibiting anticorrelation suggests a disruption of the balance of the positive and negative correlations in the default mode network and impairment of cortical functional connectivity in chronic pain patients. The disruption of the default mode network in the chronic pain patients may underlie the cognitive and behavioral impairments that accompany chronic pain. In another study, Cauda and colleagues (2009) explored the thalamocortical connectivity in a group of patients suffering from peripheral neuropathic pain by using a resting state fMRI paradigm and predefined regions of interest (i.e., primary somatosensory cortex, ventral posterior lateral thalamic nucleus, and medial dorsal thalamic nucleus). Compared with a group of healthy subjects, the patients showed decreased temporal correlations between predefined regions of interest, indicating a decreased resting state functional connectivity between the thalamus and the cortex. These data support the authors' interpretation that chronic pain can disrupt thalamic feedback during the resting state.

Both the scanning protocol and pre-processing methods used in resting fMRI studies are similar to those in task-driven fMRI studies. Common techniques used to identify spatial patterns of spontaneous BOLD activity include simple correlation analysis and independent component analysis (ICA). Simple correlation analysis is to extract the BOLD signal from a defined seed region and determine the temporal correlation between the extracted signal and signals from other brain regions. This technique is straightforward and the results are easy to interpret. In contrast, ICA does not require defining a seed region. The algorithm of ICA decomposes the entire BOLD dataset into independent components which are maximally independent statistically. Each component represents either a meaningful spatial pattern of spontaneous brain activation or

noise. Noise components are automatically separated, but researchers must determine which components reflect noise and which reflect functional anatomical networks.

1.6.3 Functional Connectivity of the Pain Network

1.6.3.1 Path Analysis

Interregional Pearson product-moment correlation coefficients historically have been used to determine which brain regions are functionally correlated during a specific experimental task. However, interpretations based on pair-wise correlations are complicated when multiple neuroanatomical systems are involved. Path analysis was therefore proposed as a method to quantify the interaction among many brain regions (McIntosh et al., 1992). Path analysis uses information about the anatomical connections and correlation coefficients among brain regions to determine the functional connectivity in a given experiment. It attempts to find causal relationships among brain regions. The application of path analysis to fMRI datasets is based on the assumption that correlation patterns between two brain regions are due to either common influence on both regions or to direct anatomical connections between them. If two regions are functionally linked in a specific task, the correlation coefficient of their activity will be large. The correlation between two brain regions is expressed as the sum of the compound paths connecting the two regions. Mathematically, the goal of path analysis is to obtain a set of path equations to minimize the difference between the observed covariances and those implied in the solution of equations. The analysis uses a series of successive “guesses” to find the best-fitting model of the observed fMRI dataset. Increased path coefficients from region A to region B under different experimental conditions will indicate increased strength of functional connectivity between those regions. In other words, activation in region A would predict more increased activation in region B while holding all other relevant regional connections constant.

1.6.3.2 Anatomical Connections of Brain Networks for Pain and Emotion

To apply functional connectivity techniques, it is necessary to construct hypothetical models of functional connectivity based on what is known about the anatomical connections among target brain regions. Fortunately, the ascending spinothalamocortical pathway has been extensively investigated in both animal lesion studies, and electrophysiological and neural imaging studies for humans (see reviews in Price, 1999). In this dissertation, we proposed a hypothetical model for pain processing based on known connections in the pain network (Figure 1.3). Projections originating from the dorsal horn of the spinal cord reach the central targets in brain stem sites, including the periaqueductal gray (PAG), continue to the ventrocaudal part of the medial dorsal nucleus (MDvc) and the ventroposterior lateral (VPL) nucleus of thalamus, and finally terminate in the cortical somatosensory areas (i.e., SI and SII). SI and SII are reciprocally connected, and projections from these two areas continue to the cortical limbic structures including insular and cingulate cortices (Manzoni et al., 1986; Conti et al., 1988). Anatomical evidence from monkey studies suggests that reciprocal connections exist between SII and the parietal lobe/ BA7b (PPC), and that there are projections from the parietal lobe to the cingulate gyrus/BA 23 (PCC) as well as the insular cortex (Neal et al., 1987). The insula also receives direct afferents from SII (Mesulam and Mufson, 1982). Within the cingulate cortex, the posterior subdivision/BA23 (PCC) has reciprocal connections with the anterior subdivision/BA 24 (ACC), and both subdivisions have widespread connections within the cortex including the insular region (Pandya et al., 1981). In addition, the anterior cingulate and the anterior insular cortices receive direct projections from the ventromedial part of the posterior nuclear complex (VMpo) and ventrocaudal part of the medial dorsal nucleus (MDvs) of the thalamus (Zhang and Craig, 1997).

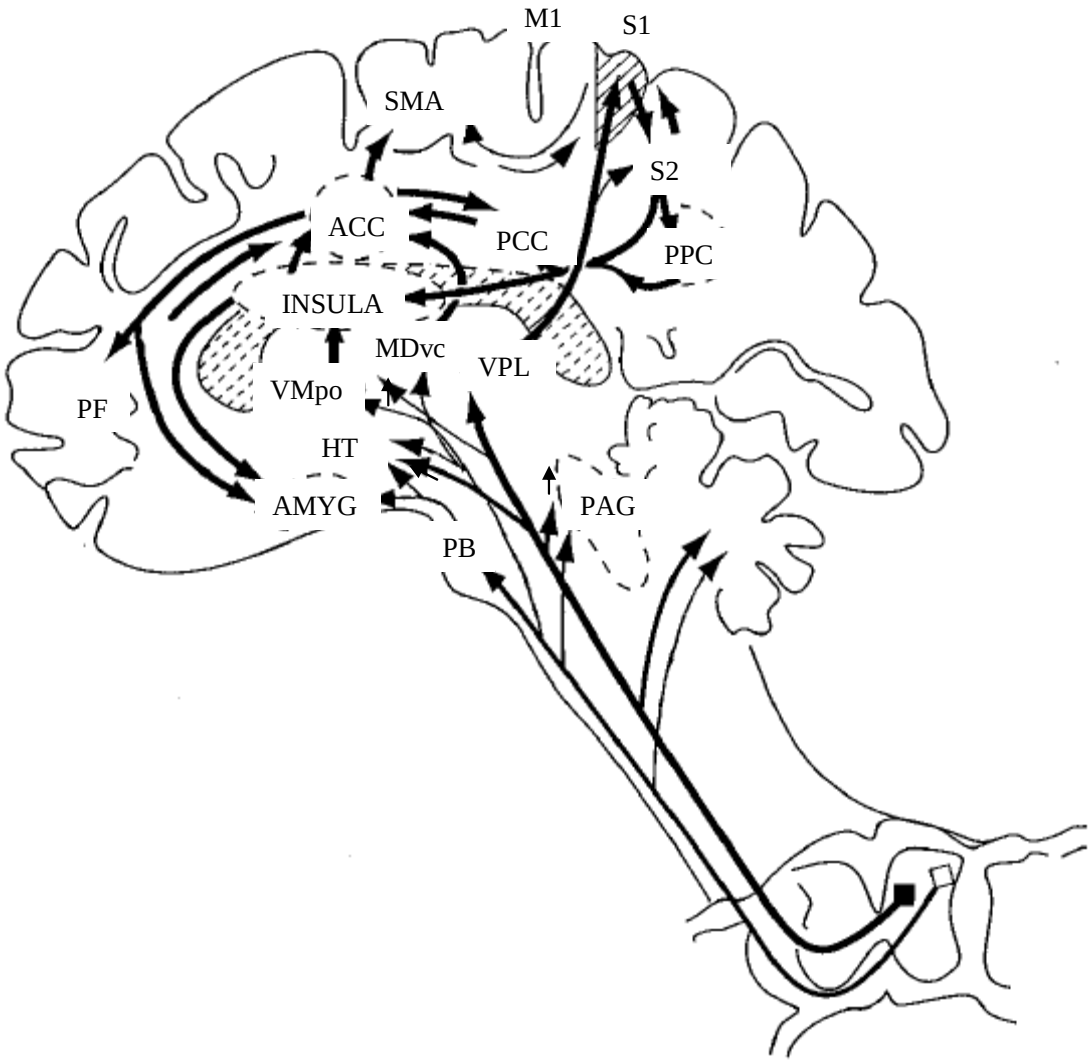

Figure 1.3 Cerebral cortical pathways involved in the pain processing (Price, 2000).

To construct a functional connectivity model of the interaction between pain and emotion, connections of the pain network mentioned in the previous paragraph are included. In addition, several other areas and their connections that are part of the brain's emotional circuitry are included in the model. Subgenual cingulate cortex (sACC/BA25) is one of the important nodes for processing sadness; this area has reciprocal connections with other subdivisions of the cingulate cortex, including anterior cingulate cortex (ACC/BA24) and posterior cingulate cortex (PCC/BA23) (Pandaya et al., 1981; Cavada and Goldman-Rakic, 1989). Therefore, reciprocal

connections between ACC/BA 24 and PCC/BA23, as well as reciprocal connections between ACC/BA24 and sACC/BA25 are included in the hypothetical model to analyze functional connectivity of pain and emotion networks. The amygdala/hippocampal complex is another important node involved in emotional experience and has widespread reciprocal projections with the cingulate cortex and the periaqueductal gray (PAG). The direct projection from the amygdala to the PAG has an important role in opioid analgesia (Finnegan et al., 2004). It is therefore necessary to include the reciprocal connections between amygdala and PAG, as well as connections between amygdala and cingulate cortex in the same model. The insular cortex is another important brain region involved in processing emotions and homeostasis. The insular cortex has reciprocal connections with the amygdala (Mufson et al., 1981). It also has connections with wide-spread brain regions such as the secondary somatosensory, prefrontal, temporal, and parietal cortices as well as the PAG (Augustine, 1996). Finally, the medial prefrontal cortex projects to the anterior cingulate cortex and from there to posterior cortical regions, as well as to subcortical regions and the amygdala (Price, 2000; Miller and Cohen, 2001). This projection originating in the prefrontal cortex may be involved in top-down modulation of pain sensation.

1.7 Research Questions of This Dissertation

Pain research has dramatically advanced in the past 40 years. In the 1970s, we knew almost nothing about the cortical representation of pain; currently, we know that widely-distributed cortical regions are involved in pain processing. The integration of pain and emotions has been addressed in several brain regions including the anterior cingulate, the amygdala and the insular cortex. However, to our knowledge, few studies explore the effect of negative emotions on pain perception in a functional brain network. This dissertation focuses on the interaction between

pain perception and sadness at the cortical and subcortical level in humans. The first research aim explores how sadness affects subjective pain in the brain. The second research aim identifies the functional network in which pain-relevant and emotion-relevant brain regions interconnect when pain experience is altered by sad mood. Knowledge of these funcitonal networks will help to understand the mechanisms underlying subjective pain experiences and identify neural circuits that may be important to understanding the comorbidity of pain and emotional disorders.

Chapter 2

An fMRI Study of Pain Perception Modulated by Sad Mood

2.1 Introduction

Pain is both an objective sensory experience that mirrors the intensity of noxious stimuli, and a subjective one that can range from mildly unpleasant to excruciatingly noxious. Emotional state can profoundly influence pain perception. Laboratory studies have shown that emotions induced by self-reflective statements, music, pictures or film-clips with emotional content can alter pain experience (Willoughby et al., 2002; Tang et al., 2008; Meagher et al., 2001; Weisenberg et al., 1998). For example, inducing a depressed mood using self-reflective statements can significantly shorten the time an individual can tolerate keeping a hand submerged in ice-cold water (Willoughby et al., 2002). Among chronic back pain patients, experimentally induced depressed mood increases self-reported pain and decreases tolerance of pain elicited by holding a heavy bag (Tang et al., 2008).

Neuroimaging techniques such as positron emission tomography (PET) and functional magnetic resonance imaging (fMRI) are increasingly being used to study brain activation in humans using experimental protocols in which painful stimuli are delivered to participants who can simultaneously report their subjective pain experience. In such experiments, neural activation during painful stimulation is distributed widely throughout cortical and subcortical regions of the brain, including somatosensory, prefrontal, insular and anterior cingulate cortices, areas that are included in the so-called “pain matrix” (Peyron et al., 2000; Melzack, 1990). There is now evidence that some of these brain regions spatially overlap those associated with emotion (Vogt, 2005). For example, regions in cingulate and insular cortices that process pain sensation are also likely to be involved in both mood disorders and ordinary emotion (Apkarian, 2005;

Ressler and Mayberg, 2007; Damasio et al., 2000). Furthermore, neuroimaging data from patients with either depressive or chronic pain conditions suggest that the neural substrates of pain and depression are at least partially overlapping. For example, when painful thermal stimuli are administered to the right arm, prefrontal and insular cortices show hyper-activation in patients with major depression, compared with healthy subjects (Bär et al., 2007). When pressure is applied to a painful joint of rheumatoid arthritis patients, the neural activity in an area of the medial prefrontal cortex that is often active during the experience of pain is significantly correlated with their scores on the Beck Depression Inventory (Schweinhardt et al., 2008). Studies such as these suggest that brain regions relevant to pain and to depression may be functionally associated with one another. At this point we do not know how neural activity related to an emotional state could affect activity in brain regions responsive to pain, or whether such a relationship helps to explain why chronic pain and depression are so often co-morbid.

In this study, we used emotionally evocative pictures to induce a sad mood in healthy female subjects and compared neural activity in response to painful electric shocks in both emotional and non-emotional conditions. Our hypotheses were that: (1) subjective perception of pain intensity would increase during sadness; and, (2) increased pain perception would be accompanied by significantly altered neural activation in some regions of the pain matrix, particularly the somatosensory and insular cortices.

2.2 Methods

2.2.1 Subjects

Sixteen right-handed, healthy women (ages 19-22) were recruited from the Department of Psychology Human Subject Pool at Michigan State University. None of the participants had a history of chronic pain, substance abuse, hospitalization for psychiatric disorders or brain injury.

Handedness was evaluated using the Edinburgh Handedness Inventory (Oldfield, 1971) and an MRI safety questionnaire was administrated to ensure that participants met inclusion criteria for imaging. Participants provided written informed consent, and they were free to withdraw from the experiment at any time. All procedures were approved by Michigan State University's institutional review board.

Upon arrival, participants completed two self-report questionnaires to screen for symptoms of psychiatric disturbance or medical disorders that could affect pain perception: the Beck Depression Inventory (BDI) (Beck et al., 1996) and the Brief Symptom Index (BSI) (Derogatis, 1992). Cutoff scores for excluding participants were greater than 19 for the BDI and greater than 63 for the BSI. In addition, participants were administered the Affective Intensity Measure (AIM) (Larsen, 1984) to ensure that they were likely to respond emotionally to the picture stimuli. Cutoff scores for excluding participants was less than 80 for the AIM.

2.2.2 Experimental Procedure

Painful Stimuli: Acutely painful stimuli were delivered through gold-plated electrodes applied to the lateral surfaces of the second phalange of the right index finger using a 9-V battery-powered Neurometer® adapted for the MRI environment (Neurotron, Baltimore, MD). To maximally stimulate small-diameter C fibers, the AC current was set at 5 Hz (Katims et al., 1997; Symonds et al., 2006).

Pain thresholds and current intensity settings were individualized for each participant using a standard procedure developed in the laboratory (Symonds et al., 2006). Briefly, the procedure was as follows. For each participant we first obtained the *Current Perception Threshold* (CPT) and *Nociceptive Threshold* (N-CPT) following the standard procedure described in the manual for the Neurometer. Pain ratings (5 to 100) of 3-sec pulses delivered at 0.05 mA increments were

then collected from each subject. These pain ratings for multiple stimulus intensities were used to establish a linear stimulus-response function. To equalize subjective pain intensity across participants, the current intensity corresponding to a numerical rating of 35 was selected for painful stimulation during imaging. All participants were informed that the painful stimulus during imaging would be at an intensity somewhere between their ratings of 5 and 60. In reality, it remained constant throughout all experimental conditions, set for each participant at the intensity that had been given a rating of 35. Several pulses of painful stimuli of varying intensity were tested briefly when participants were placed into the scanner to familiarize them with the experimental environment and to reduce anxiety.

Mood Induction and Ratings: Pictures selected from the International Affective Picture System (IAPS) (Lang et al., 1993) were presented on an LCD screen in the scanning room. Thirty pictures with negative valence were specifically used to induce sadness. All pictures had low-to-moderate arousal ratings (< 6.5). Previous studies in our laboratory have established that these pictures specifically induce sadness and do not induce other negative emotions such as fear, disgust or anxiety, which have been reported to influence pain perception (Sudheimer et al., 2001). Thirty non-emotional neutral pictures (mean valence = 4.85; mean arousal = 3.26) were used during the control condition. Participants rated both their level of pain perception and their emotional states on a numerical scale (0 = ‘no pain at all’/ ‘least possible’; 100 = ‘worst pain imaginable’/ ‘most possible’). Ratings for intensity of both pain and emotions were obtained before and after each imaging trial to obtain baseline and post-trial measurements.

Imaging Protocol: Participants were placed in the scanner, and a strip of tape was secured across the forehead to minimize head movement. To familiarize subjects with the fMRI environment, a 2.5-min practice imaging trial was run. After the practice run, three separate 4.5-

min trials were run for each participant (see Figure 2.1). Each trial was divided into alternating 30-sec periods of rest and task. Rest periods for all three trials consisted of presenting a sequence of five non-emotional (neutral) IAPS pictures (6 sec/each). Stimuli for task periods for each of the three trials were as follows: Trial 1 (*Pain Only*) six electrical shocks (3-sec on, 2-sec off); Trial 2 (*Sad Only*) five sad pictures presented sequentially, each for 6 seconds; Trial 3 (*Sad and Pain*), electrical shocks as in Trial 1 and sad pictures as in Trial 2 administrated simultaneously.

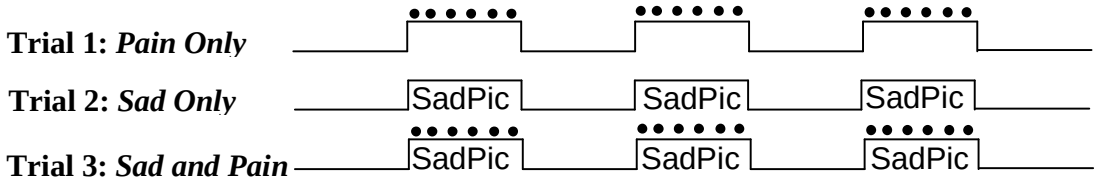

Figure 2.1 Block design of fMRI trials: *Pain Only*, *Sad Only*, and *Sad and Pain*. Dotted black line in Trial 1 and Trial 3 indicates delivery of 6 pulses of electrical shock, each presented for 3 seconds with 2 seconds between pulses.

2.2.3 Image Acquisition

Imaging was performed on a GE 3.0 Tesla scanner equipped with an eight-channel head coil, allowing for whole brain imaging. Each functional scan continually collected $T2^*$-weighted images of 74 whole brain volumes (matrix size = 64 × 64). The first 4 volumes were excluded to allow the scanner to reach a steady state. Functional images were acquired using gradient echo-planar pulse sequences (TE = 25 ms; TR = 3000 ms; flip angle = 90^o; FOV = 240 mm; voxel size = 3.75 × 3.75 × 4 mm). The whole brain volume was covered by 38 contiguous 4 mm thick axial slices. An anatomical scan following functional imaging collected 128 T1-weighted axial images (TE = 5ms; TR = 24 ms; flip angle = 90^o; FOV = 240 mm; matrix size = 256 × 256;

voxel size = 0.938 × 0.938 ×1.5 mm). These high-resolution Spoiled Gradient-recalled Echo (SPGR) images were used as an underlay for functional activity maps.

2.2.4 Image Analysis

All images were analyzed using the Analysis of Functional NeuroImages (AFNI) software package (Cox, 1996). Analysis of fMRI data followed conventional procedures for processing single subject data, conversion to standard stereotaxic coordinates (Talairach and Tournoux, 1988), group analysis, and region of interest (ROI) analysis. These procedures are briefly described below.

For each subject, raw functional and anatomical image files (two-dimensional slices) were converted to three-dimensional AFNI datasets. For functional images, Echo Planar Imaging (EPI) time series were corrected for inter-slice time shift and in-plane motion artifact. EPI time series were then processed using spatial smoothing with an 8 mm FWHM Gaussion filter to reduce random low-frequency noise. EPI time series were normalized as percent signal changes, relative to the mean BOLD signal in each voxel. A reference function was selected as an ideal predictor of the hemodynamic response function (HRF) based on the timing of the experimental protocol's block design (Figure 2.1). In a multiple regression analyses, the amplitude of the normalized Blood-Oxygen-Level-Dependent (BOLD) signal was then predicted on a voxel-by-voxel basis with multiple predictors, including the gamma waveform that best predicted the HRF, a constant to represent the baseline, the degree of the polynomial in the baseline model, and the motion correction parameters. General linear tests were also applied to each voxel to generate F-statistic and t-statistic maps representing changes in BOLD contrast, and pair-wise comparisons for all experimental conditions were performed. Images for both anatomical and functional time-series were linearly interpolated to volumes with 1-mm^3 voxels, then co-registered and converted to

standard stereotaxic coordinates to allow averaging across subjects. The percent signal changes of each dataset (i.e., participant) were used as input for group analysis, a voxel-by-voxel analysis of variance (ANOVA).

For whole brain group analysis, ANOVA was used to investigate significant activation in brain regions during the three trials (*Pain Only*, *Sad Only*, and *Sad and Pain*) with a mixed-effect two-factor model. Experimental trial (3 levels) was the first factor (fixed effect) and subject (15 levels) was the second factor (random effect). One dataset from the 16 subjects was discarded from the imaging dataset, because she did not show a difference in pain perception ratings during the experimental *Sad and Pain* trial compared with the *Pain Only* trial. Monte Carlo simulations were applied to obtain the corrected type I error (i.e., alpha level) and cluster size for the group analysis of the whole brain. For example, based on the Monte Carlo Simulations at an individual voxel-detection probability of $p \leq 2 \times 10^{-5}$, the corrected alpha level for the whole brain was determined to be 0.001, and the clusters considered to be active would have to be at least 125 mm^3. Cluster volumes had to be at least 55 mm^3 at a more relaxed alpha value of 0.005. In this study, alpha value less conservative than 0.005 is not used, so that it is possible to separate adjacent clusters (e.g. amygdala/hippocampus and occipital/fusiform gyri). A mask was created using a corrected alpha level threshold and a set of clusters was obtained to use as regions of interest (ROIs). Average z-scores across fifteen subjects for each experimental condition or contrast condition were then obtained for each of the ROIs. In addition, the contrast analysis of (*Sad and Pain – Pain Only – Sad Only*) was performed to detect significantly increased brain activation for the condition in which painful and sad stimuli were presented simultaneously compared to conditions in which they were presented alone. In this contrast analysis, many potentially meaningful ROIs (e.g., subgenual cingulate cortex, periaqueductal grey, and right

amygdala/hippocampal complex) did not survive at an alpha level of 0.001, so a more liberal alpha level of 0.005 was applied in order to explore these potentially relevant regions.

2.3 Results

2.3.1 Behavioral Data

All sixteen participants completed the experimental protocol and were included in the initial analysis of behavioral data. Beck Depression Intensity scores and Brief Symptom Index scores, which were all below the exclusion cutoff, were 3.8 ± 3.4 SD and 23.5 ± 17.5 SD respectively. Affect Intensity Measure scores were all higher than the cutoff (mean of AIM: 136.4 ± 15.1 SD). The sad emotion induction protocol successfully induced sadness in the group of sixteen participants: mean numerical ratings of sadness for the *Sad Only* trial were 7.0 ± 3.2 before and 47.4 ± 7.1 after (paired t (15) = 5.98, P < 0.0001). These ratings were not significantly different from those during the *Sad and Pain* condition (paired t (15) = 1.07, P = 0.2, see Figure 2.2).

In further analyses, data from one participant was excluded because she did not show increased pain perception in the *Sad and Pain* trial. For the remaining 15 participants, the mean rating of perceived pain intensity during the *Pain Only* trial was 37.9 ± 5.6. As expected, during both the *Pain Only* and the *Sad and Pain* trials, pain intensity was rated significantly higher for the task periods (pain stimulation) compared to baseline (paired t (14) = 5.8, P < 0.001; paired t (14) = 6.5, P < 0.001, respectively). Finally, pain was rated as more intense when painful stimuli were administered while participants were viewing sad pictures and experiencing a sad mood than when they were viewing neutral pictures, even though the intensity of the painful stimululation was identical in both conditions (mean pain rating for *Sad and Pain* was 51.41±6.67 and mean rating for *Pain Only* was 37.89 ± 5.63; paired t (14) = 2.6, P = 0.02, see Figure 2.3).

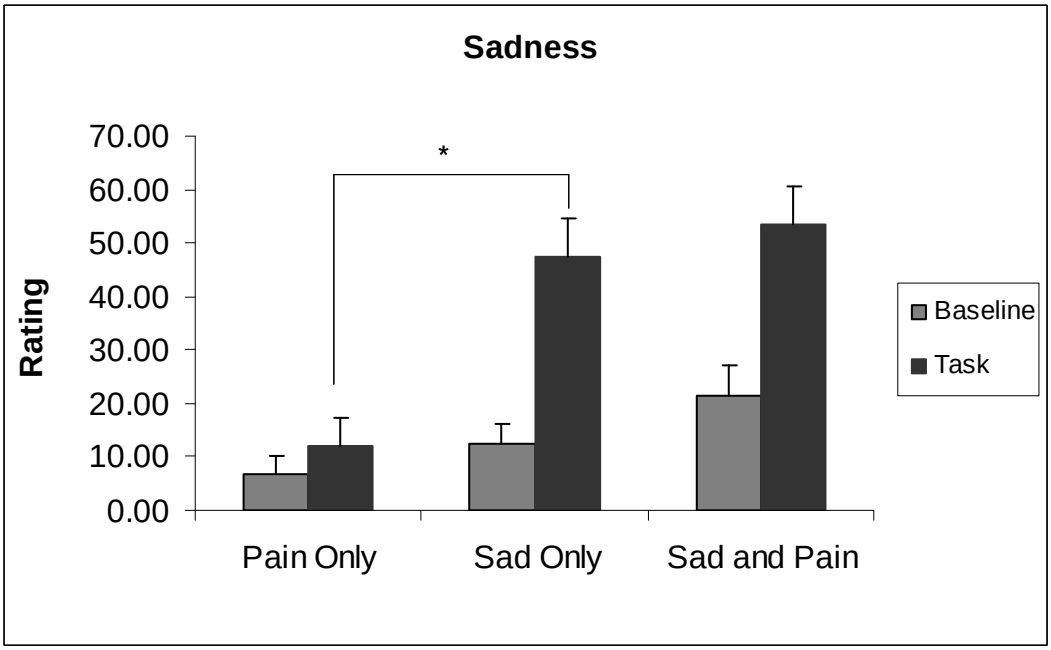

Figure 2.2 Mean ratings of sadness before and after each experimental task. The '*' indicates significant difference in the paired t-test ($P < 0.0001$)

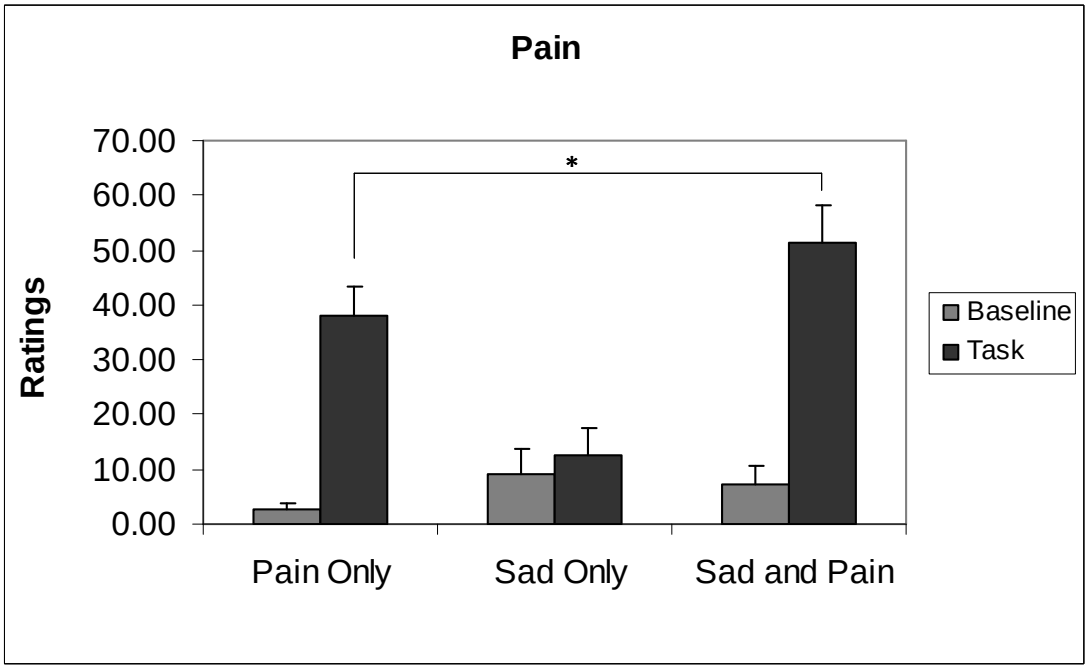

Figure 2.3 Mean ratings of pain intensity before and after each experimental trial. The '*' indicates that pain was rated significantly more intense for the *Sad and Pain* trial than *Pain Only* in the paired t-test ($p < 0.001$).

2.3.2 Neuroimaging Data

2.3.2.1 Brain Regions Activated During Experimental Tasks

Location of brain activation in response to acute painful shocks was consistent with previous findings from both our own lab (Symonds et al., 2006) and other groups (see reviews in Peyron et al., 2000). During the *Pain Only* condition, significant brain activation was observed in the contralateral (left) primary somatosensory (SI), bilateral posterior insular/secondary somatosensory (pIn/SII) and contralateral (left) anterior cingulate (BA 32) cortices (Figure 2.4; see Table 2.1 for coordinates, volumes of clusters, and mean z scores). These three brain regions are main components of the brain network activated during acute pain conditions, as summarized in the meta-analysis of Apkarian (2005). During the *Sad Only* condition, significantly active regions were bilateral medial prefrontal cortex (BA9), ipsilateral (right) inferior frontal cortex (BA 45, 44), bilateral amygdala/hippocampal complex, and bilateral occipital/fusiform gyri (Figure 2.5 and Table 2.1). Finally, during the *Sad and Pain* condition significant activation was located in bilateral pIn/SII and contralateral (left) anterior cingulate (BA 32) cortices. These two regions of activation were also observed during *Pain Only*. Significant activation during *Sad and Pain* was also observed in the ipsilateral (right) medial prefrontal cortex, bilateral amygdala/hippocampal complex, bilateral occipital/fusiform gyri and ipsilateral (right) anterior insular cortex. Except for the insular cortex, these regions also contained significant activation during *Sad Only*. Subcortically, during *Sad and Pain,* significant activation was observed in the contralateral (left) thalamus and contralateral (left) periaqueductal grey (Figure 2.6, Figure 2.7 and Table 2.1).

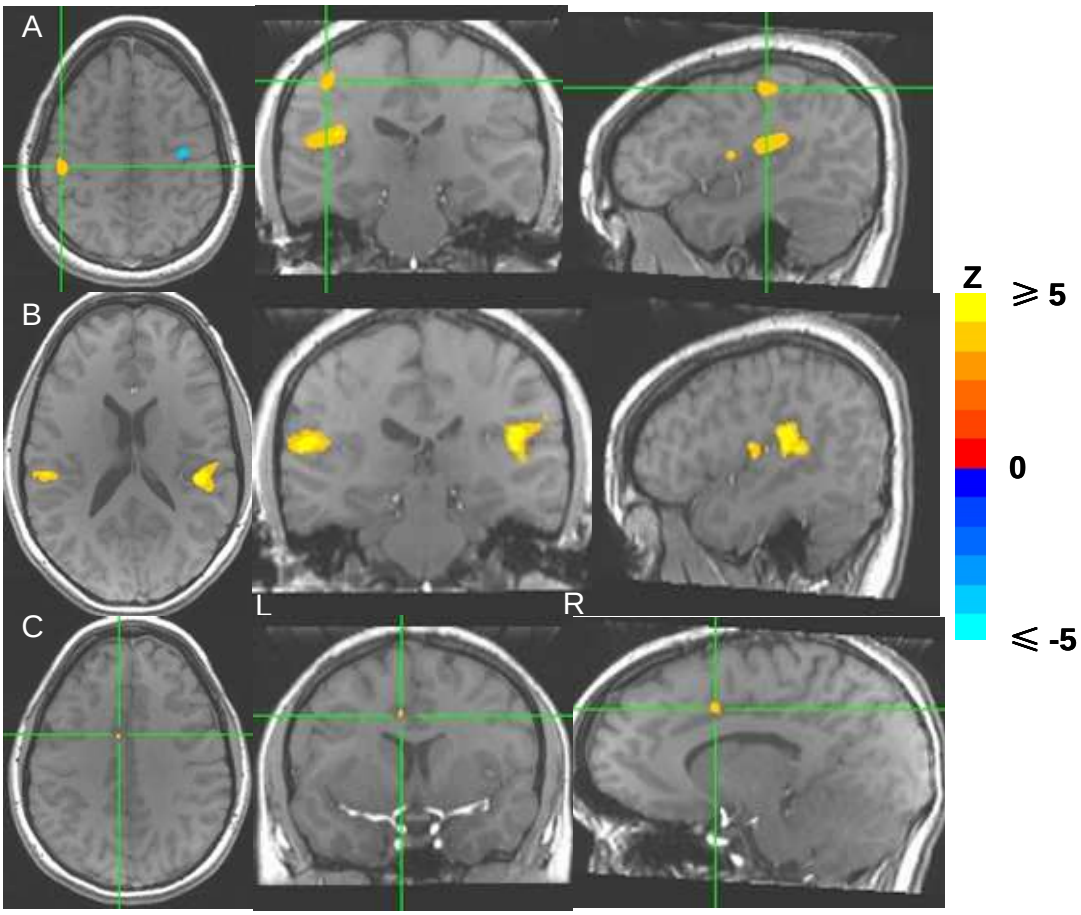

Figure 2.4 Brain activation during the *Pain Only* condition. Images in all three rows left to right: axial, coronal and parasagittal. Left hemisphere shown on left in axial and coronal views. Green crosshairs centered on region of interest. Row A: left primary somatosensory cortex (SI); Row B: bilateral posterior insular/secondary somatosensory cortices (pIn/SII); Row C: left anterior cingulate gyrus (BA 32). Alpha value, corrected for whole brain, is 0.001. (For interpretation of the references to color in this and all other figures, the reader is referred to the electronic version of this dissertation.)

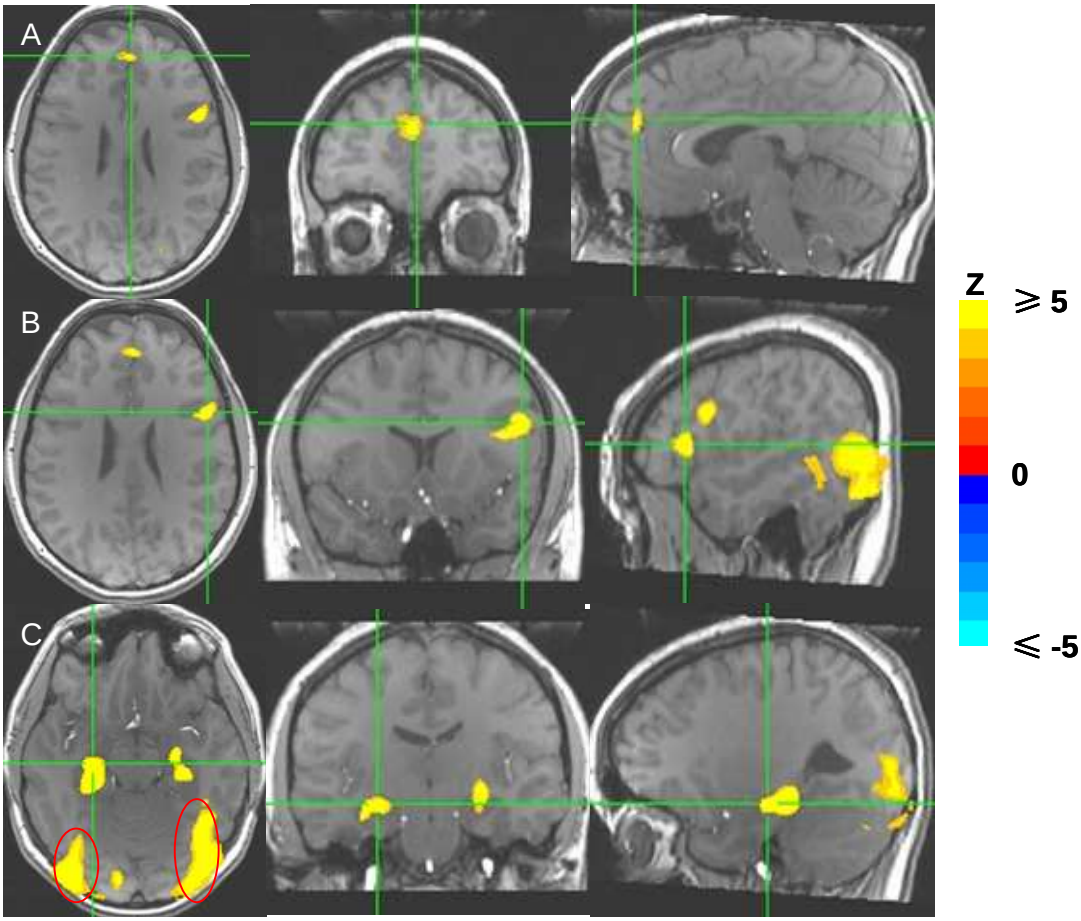

Figure 2.5 Brain activation during the *Sad Only* condition. Images in all three rows left to right: axial, coronal and parasagittal. Left hemisphere shown on left in axial and coronal views. Green crosshairs centered on region of interest. Row A: bilateral medial prefrontal gyrus (BA 9); Row B: right inferior frontal gyrus (BA 45/44); Row C: bilateral amygdala/hippocampal complex. Circles in the axial image indicate bilateral occipital/fusiform gyri. Alpha value, corrected for the whole brain, is 0.001.

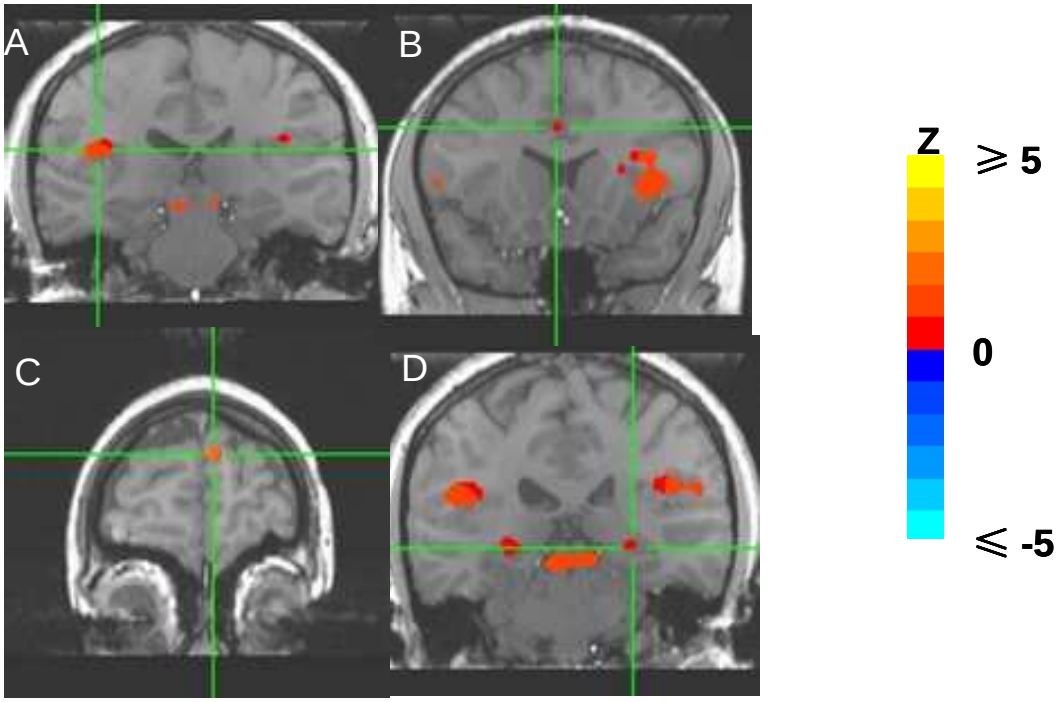

Figure 2.6 Brain activation during the *Sad and Pain* condition. All images are in the coronal plane. Green crosshairs centered on region of interest. Left hemisphere shown on left. A: bilateral posterior insular/secondary somatosensory cortices (pIn/SII); B: left anterior cingulate gyrus (BA 32). C: right medial prefrontal cortex; D: bilateral amygdala/hippocampal complex. Alpha value, corrected for the whole brain, is 0.001.

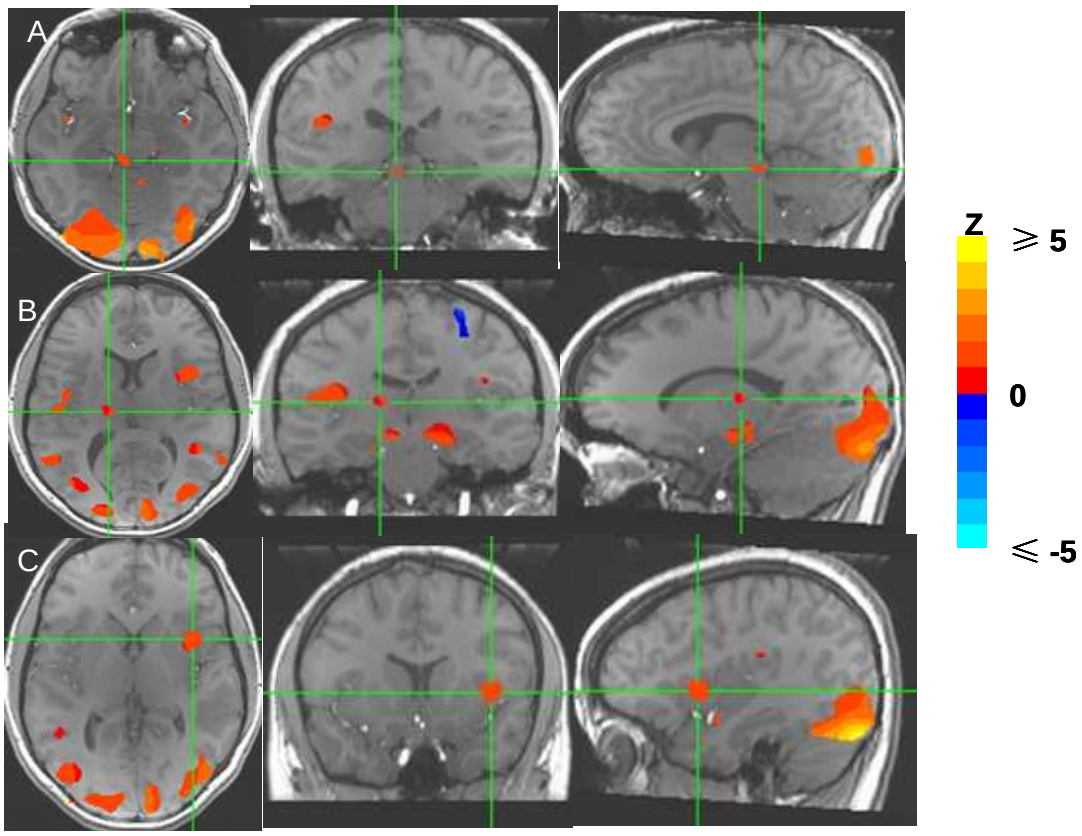

Figure 2.7 Brain activation during the *Sad and Pain* condition. Images in all three rows left to right: axial, coronal and parasagittal. Left hemisphere shown on left in axial and coronal views. Green crosshairs centered on region of interest. Row A: left periaqueductal grey (PAG); Row B: left thalamus; Row C: right anterior insular cortex. Alpha value, corrected for the whole brain, is 0.001.

Condition	Cluster location	Active volume (mm^3)	Mean z value	Max z value	Center location (x,y,z)
Pain Only ($P \leq 0.001$)	Left SI	479	3.44 ± 0.01	3.72	(-44, -25, 47)
	Left posterior insula/SII	2516	3.59 ± 0.01	4.33	(-44, -25, 17)
	Right posterior insula/SII	2164	3.47 ± 0.01	3.86	(47, -29, 20)
	Left anterior cingulate (BA 32)	162	3.3 ± 0.01	3.44	(-10, 7, 39)
Sad Only ($P\leq 0.001$)	Bilateral medial prefrontal (BA 9)	550	4.05 ± 0.01	4.39	(0, 48, 26)
	Right inferior frontal (BA 44/45)	1979	4.22 ± 0.01	4.92	(46, 15, 19)
	Left amygdala/hippocampus	2555	4.40 ± 0.01	5.46	(-26, -24, -10)
	Right amygdala/hippocampus	2033	4.23 ± 0.01	5.95	(26, -18, -7)
	Left occipital /fusiform gyri	22191	4.32 ± 0.00	6.10	(-35, -79, -4)
	Right occipital gyri/fusiform gyri	22916	4.48± 0.00	5.35	(41, -70, -3)
Sad and Pain ($P<0.001$)	Left posterior insula/SII	3155	3.89± 0.01	5.23	(-42,-28,18)
	Right posterior insula/SII	2871	3.42± 0.00	3.83	(52, -25,23)
	Left anterior cingulate (BA 32)	157	3.15±0.00	3.29	(-6, 4, 39)
	Right medial prefrontal (BA9)	308	3.43±0.01	3.84	(5, 45, 30)
	Left amygdala/hippocampus	1349	4.07±0.01	4.73	(-18, -29, -2)
	Right amygdala/hippocampus	901	3.98±0.00	4.28	(15, -29, -3)
	Left occipital/fusiform gyri	26964	4.89 ± 0.00	6.50	(-41, -70, -10)
	Right occipital/fusiform gyri	20382	4.23± 0.00	5.29	(41, -69, -7)
	Right anterior insula	1948	3.38 ± 0.00	3.57	(34, 21, 14)
	Left thalamus	149	3.43± 0.08	3.43	(-17, -18,8)
	Left PAG	171	4.00 ± 0.01	4.19	(-5, -28, -8)

Table 2.1 Brain regions activated during three experimental trials.

2.3.2.2. The Interaction of Sadness and Pain

Brain regions associated with the interaction of sadness and pain were revealed by a group-wise whole brain t-test contrast analysis (*Sad and Pain – Sad Only – Pain Only*). Positive values in the active clusters revealed by this contrast analysis indicated significantly greater brain activation in response to painful stimuli presented with sad pictures than to either painful stimuli or sad pictures presented alone. At an alpha level of 0.005, corrected for the whole brain, significant activation was observed in bilateral subgenual cingulate cortex (sACC), contralateral (left) posterior insula/secondary somatosensory cortex (pIn/SII), contralateral (left) periaqueductal grey (PAG), bilateral amygdala/hippocampal complex and bilateral occipital/fusiform gyri (Figure 2.8 and Table 2.2). The contrast analysis (*Sad and Pain – Sad Only*) revealed that, as in the *Pain Only* condition, bilateral pIn/SII and contralateral (left) ACC were preferentially active during acute painful stimuli (Figure 2.9 and Table 2.2).

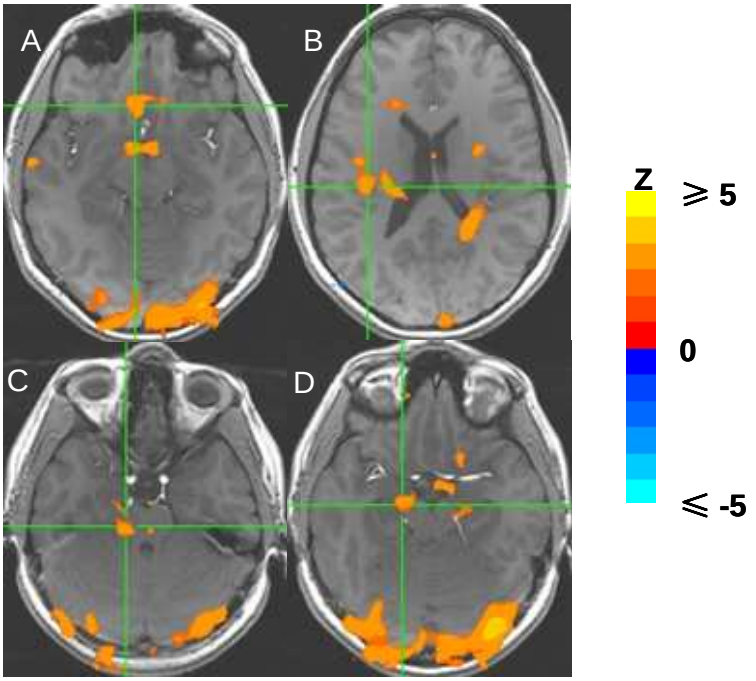

Figure 2.8 Brain activation as a result of the contrast analysis (*Sad and Pain – Sad Only – Pain Only*). All images are in the axial plane. Green crosshairs centered on region of interest. Left hemisphere shown on left. A: bilateral subgenual anterior cingulate cortex; B: left posterior insular/secondary somatosensory cortices (pIn/SII); C: left periaqueductal grey (PAG); D: bilateral amygdala/hippocampal complex. Alpha value, corrected for the whole brain, is 0.005.

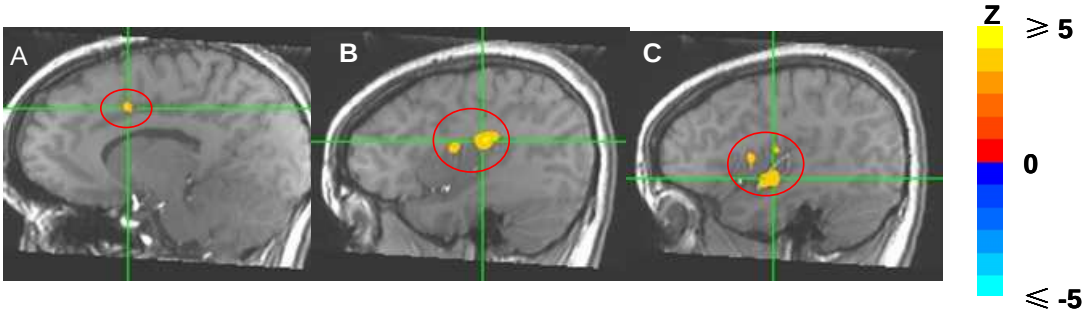

Figure 2.9 Brain activation as a result of the contrast analysis of (*Sad and Pain – Sad Only*). Images are in the parasaggital plane. Green crosshairs centered on region of interest. A: left anterior cingulate cortex (BA 32); B: left posterior insular/secondary somatosensory cortices (pIn/SII); C: right pIn/SII. Alpha value, corrected for the whole brain, is 0.001.

Condition	Cluster location	Active volume (mm^3)	Mean z value	Max z value	Center location (x,y,z)
Sad and Pain – Sad Only – Pain Only ($P \leq 0.005$)	Left posterior insula/SII	666	3.52 ± 0.01	3.97	(-38, -22, 19)
	Left/Right subgenual anterior cingulate cortex	94	2.94 ± 0.01	3.14	(-6, 25, -8)
	Left amygdala/ hippocampal complex	106	3.37 ± 0.01	3.52	(-19, -12, -14)
	Right amygdala/ hippocampal complex	476	3.41 ± 0.01	3.64	(19, -17, -11)
	Left periaqueductal grey	414	3.03 ± 0.01	3.49	(-6, -30, -11)
	Left occipital/fusiform gyri	13191	3.62 ± 0.01	4.10	(-40, -71, -4)
	Right occipital/ fusiform gyri	13916	3.48± 0.00	3.85	(41, -70, -3)
Sad and Pain – Sad Only ($P \leq 0.001$)	Left posterior insula/SII	2516	3.6 ± 0.005	4.34	(-40, -23, 18)
	Right posterior insula/SII	835	3.5 ± 0.006	3.87	(38, -15, 13)
	Left anterior cingulate cortex	162	3.35 ± 0.005	3.44	(-11, 2, 39)

Table 2.2 Brain activation as results of contrast analyses of (*Sad and Pain – Sad Only – Pain Only*) and (*Sad and Pain – Sad Only*).

2.4 Discussion

Previous behavioral studies have reported that emotional states can alter the perception of pain, but the neural mechanisms that account for this phenomenon have not yet been elucidated. In this study, we replicated this finding, observing that a sad state induced by showing emotionally evocative pictures significantly increases subjective pain intensity. Further, we found that neural activation associated with increased pain perception is significantly increased in a region of the contralateral parietal operculum that includes posterior insular/secondary somatosensory cortex (pIn/SII). This region is known to be an important area in the complex of brain regions commonly found to be activated during the experience of pain, often referred to as

the “pain matrix” (Peyron et al., 2000; Apkarian et al., 2005). In addition to pIn/SII, three other brain areas showed significant activation associated with increased pain perception during sadness: the subgenual anterior cingulate cortex, amygdala/hippocampal complex, the occipital gyri. These cortical areas are likely to be associated with emotional processing of sad pictures, and it is possible that activation in these brain regions reflects increased sadness during the presentation of sad pictures and pain stimulation. However, the behavioral data do not show significant differences in the ratings of sadness during *Sad Only* and *Sad and Pain* conditions. We therefore suggest that the activation in subgenual anterior cingulate cortex and amygdala/hippocampal complex, together with that in the midbrain periaqueductal grey (PAG), may be involved in the modulation of pain perception through the descending pain transmission pathway.

2.4.1 Increased Activation in Posterior Insular and Somatosensory Cortices

The secondary somatosensory cortex occupies a large area in the parietal operculum. The exact anatomical border between the granular cortex of the inner part of the operculum and that of the posterior insular cortex cannot be delineated using MRI, and the majority of pain neuroimaging studies do not differentiate the secondary somatosensory area from the anatomically contiguous posterior insular cortex (Peyron et al., 2000; Apkarian et al., 2005). Thus, as in other fMRI reports, to describe the activation evoked in this cortical region by acute painful stimuli, this study uses a term that includes both regions, here called the “posterior insular/secondary somatosensory cortex” (pIn/SII).

The pIn/SII is thought to be important for processing the sensory-discriminative dimension of pain (Treede et al., 1999). Evidence for this is based primarily on PET studies in which perceived pain intensity is correlated with regional cerebral blood flow in the pIn/SII (Coghill et

al., 1999), and fMRI studies in which participants' ratings of the sensory-discriminative dimension of mechanical pain are correlated with BOLD signal in this region (Maihöfner et al., 2006). In the present study, we found bilateral activation in pIn/SII when painful shocks were administered to the right index finger. In addition, activation in the left pIn/SII, contralateral to the stimulation site, was significantly greater in both BOLD signal intensity and area of activation when painful shocks were administered concurrent with sad stimuli compared to when painful shocks were administered alone, even though the intensity of pain stimuli was identical in the two conditions. We suggest that the increased activation in the left pIn/SII reflected the increased behavioral ratings of subjective pain intensity. Further, based on what is known about the anatomical circuitry of this region, we believe it is likely that the increased activation is primarily due to the posterior insular cortex. In the Old World macaque monkey, axons of neurons in nociceptive specific lamina I of the spinal cord project to the posterior part of the ventral medial thalamic nucleus which in turn projects to the dorsal margin of posterior insular cortex (Craig, 1995). In this study painful stimuli were applied to the right side of the body, and it is therefore not possible to separate the potentially unique roles of contralateral and ipsilateral pIn/SII. It may be that left pIn/SII is involved in altered pain perception regardless of whether it is ispilateral or contralateral to the stimulation site.

2.4.2 Role of Anterior Cingulate Cortex

The anterior cingulate cortex (ACC) is an important brain region for processing the affective component of pain (Rainville et al., 1997; Hsieh et al., 1999; Tölle et al., 1999). A 1997 PET study in which hypnotic suggestions were used to alter the unpleasantness of noxious heat stimuli without changing the perceived intensity demonstrated that regional cerebral blood flow changes within the ACC were positively correlated with ratings of pain unpleasantness (Rainville

et al., 1997). Further evidence for the role of the ACC in processing the affective dimension of pain is seen is a recent fMRI study examining BOLD responses to electrical pain-inducing stimuli while participants viewed randomly presented pictures of sad, happy or neutral faces. Although neither pain nor emotional ratings were collected until after the scanning session, the researchers reported that postscan pain ratings were higher during presentation of sad faces than during happy or neutral faces. Analysis of the imaging data in that study found that activation of ACC was significantly greater during presentation of sad faces (Yoshino et al., 2010). Consistent with other fMRI studies of pain processing (see reviews in Peyron et al., 2000; Apkarian et al., 2005), the present study observed activation in ACC contralateral to the body site of painful stimulation. However, we did not find that activation of ACC during the concurrent administration of painful stimuli and sad pictures was significantly increased compared to administration of painful stimuli alone. This difference in results between our study and that of Yoshino et al. is perhaps best explained by a difference in experimental design. Unlike Yoshino et al., we did not use emotional facial expression to induce sadness, but instead chose stimuli that were more general and had been shown in pilot studies to reliably induce a sad feeling state. Several fMRI studies have demonstrated that empathy for pain involves affective components of pain and is correlated with activation of ACC (Singer et al., 2004; Jackson et al., 2006). Perhaps presentation of sad faces in the Yoshino et al. study induced empathy in the participants, thereby tapping into the affective dimension of pain and causing increased activation of ACC. The activation pattern in the current study most likely directly influenced the sensory dimension of pain processing and increased activation in the pIn/SII without exacerbating the affective dimension or activation in the ACC. This neural activation pattern is consistent with our

behavioral findings that the ratings of sadness during the presentation of sad pictures were not significantly different between conditions with and without painful stimuli.

2.4.3 Sadness and the Descending Pain Pathway

In addition to pIn/SII, brain areas located in subgenual anterior cingulate cortex, amygdala, and the occipital gyri showed significant activation in the contrast analysis using the equation of *Sad and Pain – Sad Only – Pain Only*, indicating more activity during the *Sad and Pain* condition compared to either the *Sad Only* or the *Pain Only* conditions. Each of these three areas has been reported to be associated with emotional processing. In a meta-analysis of 55 PET and fMRI studies on emotional activation, 46% of sad induction studies consistently reported activation of the subgenual anterior cingulate cortex (sACC) (Phan et al., 2002). Although Reiman and colleagues (1997) found sACC activity to recall-generated but not film-induced sadness, Phan et al. (2002) found that sadness induced by recall or auditory or visual stimuli was associated with the activation of sACC. Activation of sACC may not always be observed when the targeted emotional state (i.e., sadness) does not achieve a desired intensity. This can happen, for example, when mood induction is acoompanied by additional cognitive tasks. Interestingly, in resting state studies, hypometabolism has been found in the sACC of patients with clinical depression, and activation of sACC increases when patients respond to pharmacologic treatment (Mayberg et al., 1999; Mayberg et al., 2000). Further evidence of an association between sACC activation and sadness is supplied by Liotti et al. (2000) who note increased sACC activation if subjects are scanned after achieving a predetermined level of emotion intensity.

Many studies have found an association between amygdala activation and fear-related emotions, including 30 of the 55 neuroimaging studies analyzed by Phan et al. (2002). In addition, PET studies have found enhanced activation in amygdala with increasing intensity of

sad facial expression (Blair et al., 1999), and in response to viewing both pleasant and aversive pictures (Hamann et al., 1999). Thus, the human amygdala may play a general role in processing salient emotional stimuli, regardless of the valence.

Finally, the occipital cortex is commonly activated by a wide range of visual emotion tasks, including viewing emotionally-evocative pictures and films, and faces with emotional expressions (Lang et al., 1998; Lane et al., 1999; Morris et al., 1996; Beauregard et al., 1998). Although it is possible that increased activation in the occipital cortex as well as in the sACC and amygdala reflects increased sadness when pain stimuli are delivered to participants in a sad emotional state, the behavioral data do not show increased ratings of sadness during the *Sad and Pain* condition compared to the *Sad Only* condition. Instead, we suggest that, at least in the sACC and amygdala, increased activation may indicate modulation of pain perception through known pain transmission pathways. The medial (midline and intralaminar) thalamic nuclei project directly to both the anterior cingulate cortex and amygdala, which in turn each project to the nociception-regulating center of periaqueductal gray (PAG) (Vogt and Sikes, 2000; Sewards and Sewards, 2002). Thus, the projections from the PAG to the thalamus, and from the PAG to the insular/somatosensory cortices, provide pathways to integrate sad and painful information within the brain regions of the "pain matrix".

In this study, the PAG, like the sACC and amygdala, was significantly more active during the *Sad and Pain* condition compared to either the *Sad Only* or *Pain Only* condition. The PAG can either inhibit or facilitate pain processing (Porreca et al., 2002). In the present study, the PAG was likely involved in the facilitation of pain processing, since increased BOLD signal in the PAG occurred during conditions in which participants rated painful shocks accompanied with sadness as more intense than painful stimuli delivered alone. Top-down pain facilitation has been

examined in numerous animal studies. For example, chemical or electrical stimuli, applied to the rat anterior cingulate cortex (ACC) (which sends projections to the PAG), enhances the tail-flick reflex (Calejesan et al., 2000). As in humans, the PAG in rats sends projections to the rostral ventral medulla (RVM). The ON-cells in the rat PAG increase their firing rates just before a tail-flick response to radiation heat (Fields et al., 2000). Thus, the ACC can indirectly communicate with the RVM. The descending facilitation mediated by the ACC can be blocked by intra-RVM microinjection of an antagonist of AMPA and kainate receptors (Calejesan et al., 2000), further indicating the central role played by the PAG in the descending facilitation of noxious stimuli.

The amygdala also likely contributes to descending facilitation of pain processing. The primate amygdala sends projections to the PAG and receives substantial input from temporal visual-association areas (Aggleton et al., 1980). There are also robust anatomical connections between the sACC and amygdala (Anand et al., 2005; Mobascher et al., 2009; Johansen-Berg et al., 2008). Visual information with negative valence could heighten activity in the amygdala, and thereby indirectly influence the activation of PAG. Animal studies suggest that activation in the pain facilitation pathway appears to depend on an intact amygdala. Lesions of the central amygdala in rats eliminate shock-induced hyperalgesia as measured by a decrease in vocalization thresholds to shock (Crown et al., 2000). In the present study, the bilateral amygdala showed significant activation during presentation of sad pictures, both alone and concurrent with pain stimulation. Thus, it is possible that activation in both the amygdala and the PAG could reflect the influence of sadness on pain processing. The anatomical projection from occipital lobe to the amygdala, and from amygdala to PAG provide a pathway by which emotional information processed in the occipital lobe and amygdala could modulate nociceptive signals, possibly enabling the processing of salient stimuli.

2.4.4 Conclusion

In conclusion, sadness enhanced subjective pain perception, which was accompanied by increased activation within posterior insular/secondary somatosensory cortices (pIn/SII). Moreover, brain regions, including sACC and amygdala, together with the PAG, showed increased activation when painful stimuli were administered to study participants experiencing a sad emotional state. Based on these results, we suggest that increased activation in the pIn/SII could be part of a top-down facilitation of pain processing via neural circuits that include the ACC, amygdala, occipital lobe and PAG. These findings may be relevant to the comorbidity of pain and depression, potentially providing clues to why pain-free persons with pre-existing major depression are at increased risk for developing symptoms of chronic pain conditions (Breslau et al., 2003).

Chapter 3

Functional Connectivity of Brain Networks for Pain Processing and for Interaction of Pain and Sadness

3.1 Introduction

Pain perception can be dramatically affected by one's emotional state. For example, negative emotions, such as unpleasant or depressive mood, can enhance pain intensity and decrease pain tolerance (Meagher et al., 2001; Tang et al., 2008). However, the neural networks underlying interaction of pain and emotional state are not well understood. Functional imaging techniques, such as positron emission tomography (PET) and functional magnetic resonance imaging (fMRI), have been used to investigate human brain activation during either pain processing or emotional experience (see reviews in Apkarian et al., 2005 and Dalgleish, 2004). These neuroimaging studies consistently identify a set of brain regions that are active during pain processing, including primary/secondary somatosensory, insular, anterior cingulate and prefrontal cortices, and the thalamus. Brain regions associated with emotional experience include the anterior cingulate and prefrontal cortices, and the amygdala. Of note, the prefrontal, insular and cingulate cortices, are activated by either pain stimuli or self-generated emotions (Apkarian, 2005; Ressler and Mayberg, 2007; Damasio et al., 2000). In addition, some studies suggest that these brain regions may be involved in the interaction of pain and emotional processing. For example, when painful thermal stimuli are administered to the right arm of major depressive patients, the prefrontal and insular cortical regions show increased activation, compared to healthy subjects (Bär et al., 2007). In another study, participants were more sensitive to painful stimuli when they viewed pictures of sad faces than neutral or happy faces. In these individuals, the anterior

cingulate cortex and amygdala showed increases in activation during increased pain sensitivity (Yoshino et al., 2010).

In Chapter 2, we reported that subjective perception of pain intensity increases when individuals experience a sad mood as a consequence of viewing sad pictures, and that this behavior is accompanied by increased activation in the posterior insular/secondary somatosensory cortex (pIn/SII). In addition, we found increased activation in some emotion-related brain regions such as the subgenual cingulate cortex and the amygdala/hippocampal complex. These observations led us to wonder how discrete brain regions work together in a network to increase the perception of pain during sadness. To answer this question, it was important to identify the functional connectivity among brain regions that are active during the processing of either pain or emotion. We therefore included the insular cortex, cingulate cortex, somatosensory cortex, and amygdala in our investigation of the network that could underlie the altered pain perception during emotional states.

Traditional task-driven fMRI studies detect increased regional cerebral blood flow (rCBF) in response to specific experimental tasks. For example, in the fMRI study of Chapter 2, we designed three trials to investigate the brain activation patterns associated with painful and sad stimuli. In recent years, researchers have become increasingly interested in investigating the brain activity during rest. The resting-state fMRI detects the spontaneous blood-oxygen-level-dependent (BOLD) signal which is usually minimized by averaging in the traditional task-driven fMRI studies. It is assumed that if brain regions participate in a particular common function, their spontaneous BOLD signals during rest should correlate with one another (see reviews in Fox and Raichle, 2007).

The aim of this study was to use resting-state fMRI to examine the functional connectivity within neural networks implicated in the interaction of pain and sadness. We used brain regions identified in Chapter 2 as the seed regions to explore the intrinsic activation patterns in the brain network associated with pain at rest. These regions, the insular cortex, anterior cingulate cortex, somatosensory cortex, and amygdala, were also used as candidates in a path analysis to identify functional connectivity maps of brain networks. We predicted that these four candidate brain regions would be functionally correlated at rest, and that their functional connectivity would be altered when painful conditions were accompanied by and emotion-inducing stimuli.

3.2 Methods

3.2.1 Subjects

Sixteen healthy, right-handed women ages 18 – 33 years (mean 21.9) participated in the study after providing written informed consent approved by Michigan State University's institutional review board.

3.2.2 Image Acquisition

Images were acquired on a GE 3T Signa® HDx MR scanner (GE Healthcare, Waukesha, WI) with an 8-channel head coil. A high-order shimming procedure was conducted to improve magnetic field homogeneity (Kim et al., 2002). During the 7-minute resting-state scan, subjects were instructed to relax, stay awake, and to keep their eyes closed. $T2^*$-weighted echo planar images were collected continuously with the following parameters: 36 interleaved 3-mm axial slices, TR = 2.5 s, TE = 27.7 ms, flip angel = 80°, FOV = 22 cm, matrix size = 64 × 64. The first four time points were discarded during data analysis to ensure that analyzed images were collected after the magnet had reached a steady state. To aid in spatially locating resting-state

fMRI data, high-resolution T1-weighted inversion recovery fast spoiled gradient recalled echo (IR FSPGR) images were acquired with the following parameters: 180 sagittal 1-mm slices, TE = 3.8 ms, TR = 8.6 ms, flip angle = 8°, FOV =25.6 mm and matrix size = 256 x 256.

3.2.3 fMRI Data Preprocessing and Analysis

All images were analyzed using the Analysis of Functional NeuroImages (AFNI) software package (Cox, 1996). Using the last functional image as a reference, images for each subject were corrected for head movements in three translational and three rotational directions. Images were then smoothed with a 4-mm FWHM Gaussian kernel to reduce spatial noise. The effects of head movements, baseline, and system drifting were removed from the original signal through multiple linear regression analysis. The cleaned echo planar imaging (EPI) signals in each time series were then resampled to a voxel size of 3× 3 × 3 mm and converted to the Talairach and Tournoux stereotaxic coordinates (Talairach and Tournoux, 1988) for further analysis.

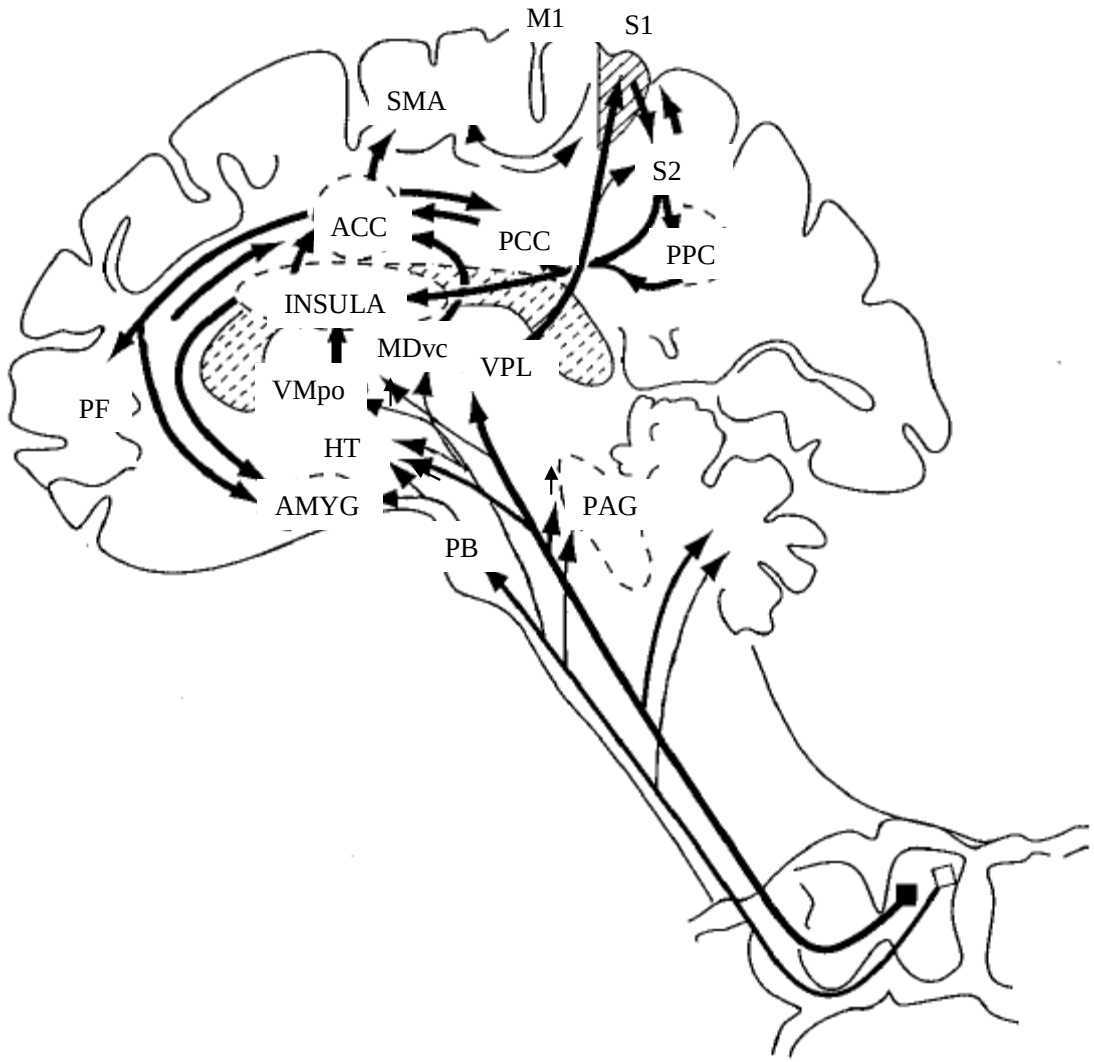

Figure 3.1 Schematic of ascending pathways, subcoritical structures and cortical structures involved in processing pain (Price, 2000). It is as same as Figure 1.3 in Chapter 1.

Based upon the known anatomical connections of subcortical and cortical pain processing regions (Figure 3.1, Price, 2000) and our findings from Chapter 2, a hypothetical model for pain processing was constructed. The following areas were included in the model, because they were observed to be significantly active during pain processing: (1) left primary somatosensory cortex (SI), (2) left posterior insula/secondary somatosensory cortex (pIn/SII), (3) left anterior cingulate

gyrus/BA 24 (ACC), (4) left posterior cingulate gyrus (PCC), (5) left thalamus (Tha) and (6) left periaqueductal gyrus (PAG).

In addition, a hypothetical model for the interaction of sadness and pain was constructed based upon the significant activation observed in the brain regions when pain perception was altered by sadness. The model included all of the brain areas in the pain processing model as well as: (1) bilateral medial prefrontal cortex (mPFC), (2) right inferior frontal gyrus (IFG), (3) right anterior insula (aIn), (4) bilateral amygdala/hippocampal complex (AMY/Hip), (5) left subgenual cingulate gyrus/BA 25 (sACC), (6) left parietal lobule/BA7 (PPC) and (7) bilateral occipital/fusiform gyri (OCP). The ROIs of posterior cingulate gyrus and parietal lobule/BA7 were generated by using atlases in the AFNI software. All other ROIs were adopted from the imaging results of Chapter 2 (See Talairach coordinates of the centers of these ROIs in Table 3.1).

ROIs	Central coordinates of ROIs (Right+/Left-, Anterior+/Posterior-, Superior+/Inferior-)	size (mm^3)
SI	(-44, -25, 47)	479
pIn/SII	(-45, -28, 18)	3155
ACC	(-10, 7, 39)	162
PCC	(-5, -50, 18)	6998
Tha	(-17, -18, 8)	149
PAG	(-5, -28, -8)	171
mPFC	(0, 48, 26)	550
IFG	(46, 15, 19)	1979
aIn	(34, 21, 14)	1948
AMY/Hip	(-26, -24, -10)	2555
sACC	(-6, 25, -8)	94
PPC	(-27, -58, 49)	15255
OCP	(-35, -79, -4)	22191

Table 3.1 Regions of Interest (ROIs)

3.2.4 Simple Correlation analysis and group ICA analysis

Simple correlation analysis used pre-defined seed regions (see below) to detect spatial patterns of spontaneous fluctuations in the pain network during the resting state. Correlation

coefficients were calculated between a given seed region and each voxel in the entire brain (Fox et al., 2005; Greicius et al., 2003). A separate independent component analysis (ICA) was used to analyze the resting-state fMRI data without pre-defined seed regions. ICA assumes that the BOLD signal is composed of linearly-additive independent components. Statistically, these components are maximally independent from one another and each component is associated with a spatial brain activity map. The group-level independent maps can be generated using group independent component analysis (gICA) algorithm (Calhoun et al., 2004).

See regions for the correlation analysis were the posterior insular/secondary somatosensory cortex (pIn/SII), anterior cingulate cortex (ACC) and medial prefrontal cortex (mPFC) (see Table 3.1). These three seed regions were important in both pain and emotion networks. In Chapter 2, we observed that the pIn/SII responds to painful shocks and has significantly increased BOLD signals when sad pictures were presented concomitant with painful shock. The ACC was activated by either pain or sad stimuli. The mPFC was activated by the presentation of sad pictures. To obtain a correlation map, averaged BOLD signals of a seed region during the resting-state scan were first extracted. The corrections between the average time course at a seed region and the time courses of all voxels in the brain were then performed. In group analyses, to normalize the distribution, the R values were first converted to Z values through Fisher's Z transformation. T tests were then performed on the Z values against random chance. A statistical threshold of $P < 0.001$ (uncorrected for the whole brain) was used to determine which brain areas were significantly correlated with the seed region across subjects.

We also used group ICA (Calhoun, 2001) to examine spatial patterns during rest. In this analysis, the fMRI dataset for each subject was pre-processed to remove head movement and global system trend described earlier (e.g., time-shifting of slices, motion correction, smoothing

and normalizing BOLD signals). We then applied principle component analysis (PCA) on individual cleaned datasets to represent most of the variance of the fMRI within a lower dimensionality (McKeown et al., 1998). The dataset for each subject had fewer than 25 sources of variance; therefore, the software package of *3dpc* in AFNI (Cox, 1996) was used to perform PCA with a dimensionality reduction of 25. Because the results were insensitive to the reduction parameter, the dimension of 25 is likely to be a good choice for decreasing computational load in. Preprocessed datasets for all sixteen subjects were concatenated into one dataset and the dimensionality of the aggregated data was then reduced to 20 by using *3dpc*. Because there were fewer than 20 ROIs, we chose 20 to estimate the number of sources present from the dataset to provide a tradeoff between preserving much of information in the dataset and making the calculation and interpretation less intensive. After the dimensionality reduction, the software package 3dICA.R in AFNI was used to run the ICA analysis (http://afni.nimh.nih.gov/sscc/gangc/ica.html). The analysis produced representative time courses of 20 independent components and mixing coefficients associated with these time courses. For each component, the mixing coefficient of an individual voxel showed the weight of corresponding time course component in the original BOLD signal. The group maps of 20 independent components generated from ICA were thresholded by using a Z-threshold criterion ($P < 0.001$, $Z = 2.36$); ICA components were treated as random variables, and a one-sample t-test was performed with the null hypothesis of zero magnitude.

3.2.5 Functional Connectivity Models

Simple correlation analyses demonstrate how one seed region functionally connects to other brain regions at rest. If we want to know correlations among multiple brain regions, the simultaneous functional connectivity among them can be revealed using path analysis. Path

analysis is a causal modeling method to explore correlations within a defined network. However, path coefficients generated from path analysis are not correlation coefficients. Theoretically, path coefficients are standardized versions of linear regression weights which are used to determine the relationship among variables in a mulitivariate system.

Model construction: Two hypothetical models were constructed to investigate brain networks for pain processing and the interaction of pain and sadness (see Figures 3.2 and 3.3). The hypothetical model in Figure 3.3 was simplified to include only ROIs significantly correlated with others (see Table 3.3, the inter-regional Pearson's correlations). For example, the brain activation pattern during rest (Figure 3.5, 3.6 and 3.7 B) suggested strong correlations between the anterior and posterior portions of cingulate cortex, as well as between the anterior insular cortex and anterior cingulate cortex. Thus, the ROIs of ACC, PCC and aIn, and the anatomical connections of these ROIs (Figure 3.1) were included in the hypothetical model. Uncertain directionality of effect between two regions in the hypothetical model was taken care by: (1) trying alternative models with different directionalities; (2) including reciprocal effects; or (3) including all possible paths.

Model analysis: Path analysis was used to explore correlations within the defined networks during both resting and task-driven states. For each subject's dataset, masks of ROIs were created. Within each mask, preprocessing steps were performed across all brain voxels as detailed in section 3.2.3 to remove head movement and system drift. Preprocessed BOLD signals were normalized by dividing the value of each voxel by the mean value of the whole brain. The normalized time series of each mask were then averaged and extracted. The extracted time series were used as inputs for path analysis using the program Amos 17.0 (SPSS Inc.).

Path analysis was applied as a confirmatory test to explore the correlations among ROIs within the hypothetical models. All variables representing BOLD signals of ROIs were observable (endogenous) variables; the analysis did not involve any latent (exogenous) variables. The analysis estimated parameters of path coefficients and the goodness of fit which was used to reject, modify or accept the model. Modification of the model was made one path at a time until the overall goodness of fit was acceptable for the whole model. To achieve an acceptable goodness of fit, a measure of discrepancy is minimized between the observed interregional correlation matrix and the correlation matrix predicted by the model. The measures of this discrepancy are asymptotically distributed as Chi Square. If observed discrepancy has a small probability under this distribution, we can fairly sure that the model adequately fits the observed data. If a small change in a path leads to a large change in other connections, this path would be rejected because of co-linearity.

Model interpretation: Path analysis was based on the hypothesis that brain regions involved in a functional brain network should have strongly inter-correlated activity patterns. For example, if the path coefficient connecting region A to region B indicates that region A increases by one standard deviation from its mean, then region B would be expected to change by the amount of the path coefficient standard deviation from its mean, while all other relevant regional connections were held constant. A positive path coefficient would indicate increased activation in region A, leading to proportionately increased activity in region B.

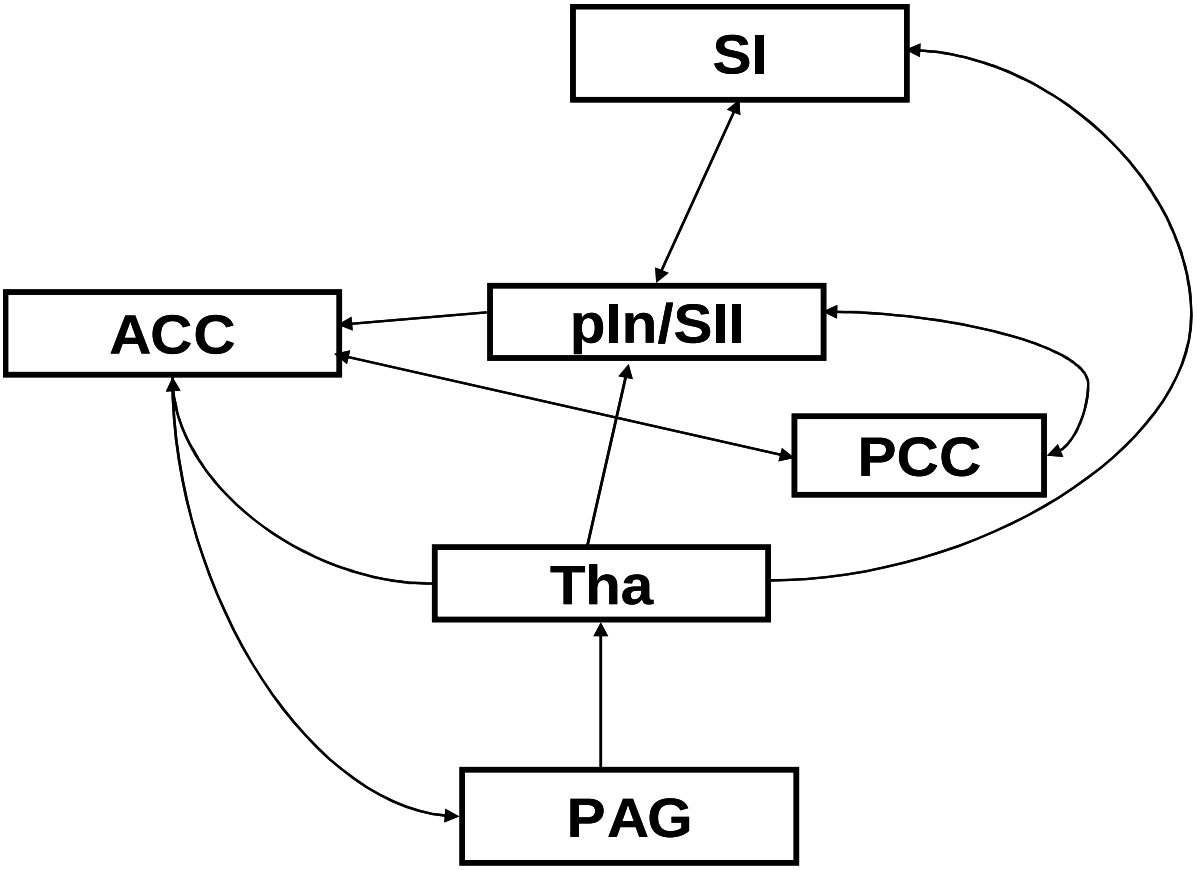

Figure 3.2 A hypothetical model used to investigate the functional connectivity in the supraspinal network involved in pain processing. SI, primary somatosensory cortex; pIn/SII, posterior insular/secondary somatosensory cortex; PCC, posterior cingulate cortex (BA 30); ACC, anterior cingulate cortex (BA 24); Tha, ventral lateral posterior nucleus of thalamus; PAG, periaqueductal gyrus.

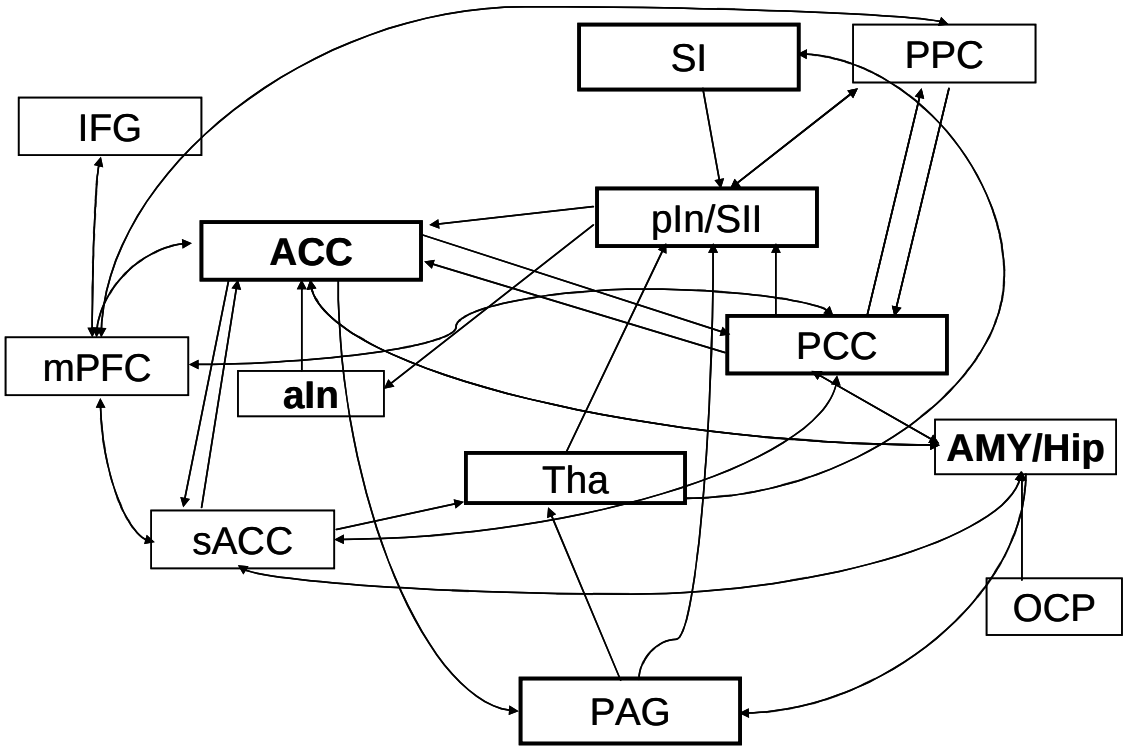

Figure 3.3 A hypothetical model used to investigate the interaction of pain and emotion. This model combines the brain regions involved in both pain and emotional processing. SI, pIn/SII, PPC, Tha, and PAG are brain regions mainly associated with pain processing. IFG, mPFC, and OCP are involved in processing emotional information. The ACC, aIn and AMY/Hip ROIs (bold) are the probable key nodes modulating the pain experience by emotional states.

3.3 Results

3.3.1 Resting-state Maps

During the resting state, the spontaneous BOLD signals of the seed region placed at the posterior insular/secondary somatosensory cortex (pIn/SII) were significantly correlated with signals in the following bilateral brain regions: an area in the inferior frontal junction which included the anterior insular cortex; anterior cingulate cortex (BA24); primary sensory cortex extending to the parietal lobule; and the thalamus (Figure 3.4). Another seed region was placed in the anterior cingulate cortex (ACC), an area which may be important in integrating emotion and pain. This ACC seed region was significantly correlated with the anterior insular cortex and

the thalamus (Figure 3.5). There was also a strong correlation between regions in the anterior and posterior portions of the brain. A seed region placed in the medial prefrontal cortex (mPFC) was positively correlated with anterior regions (anterior insular and anterior cingulate cortices) and a posterior region (posterior cingulate cortex) (Figure 3.6).

Independent Components Analysis (ICA) was also used to confirm functional connectivity without a priori definition of seed regions. Two of the 20 component maps obtained in this analysis were potentially relevant to pain and emotional networks (Figure 3.7). Each independent map represented the weight of a component in the normalized time series during the resting state. The 10^{th} component map (IC 10) included large areas within the somatomotor cortex, extending to the posterior insular cortex. This suggests strong positive correlations between the somatomotor system and the insular cortex in human brain. The 17^{th} component map (IC 17) indicated high levels of activity during rest in bilateral cingulate cortex and medial prefrontal cortex. This spatial pattern suggests strong positive correlations between the anterior portion of the cortex (including medial prefrontal and anterior cingulate cortices) and the posterior portion (including posterior cingulate cortex), consistent with the well-known activation pattern at rest in humans (Greicius et al., 2003).

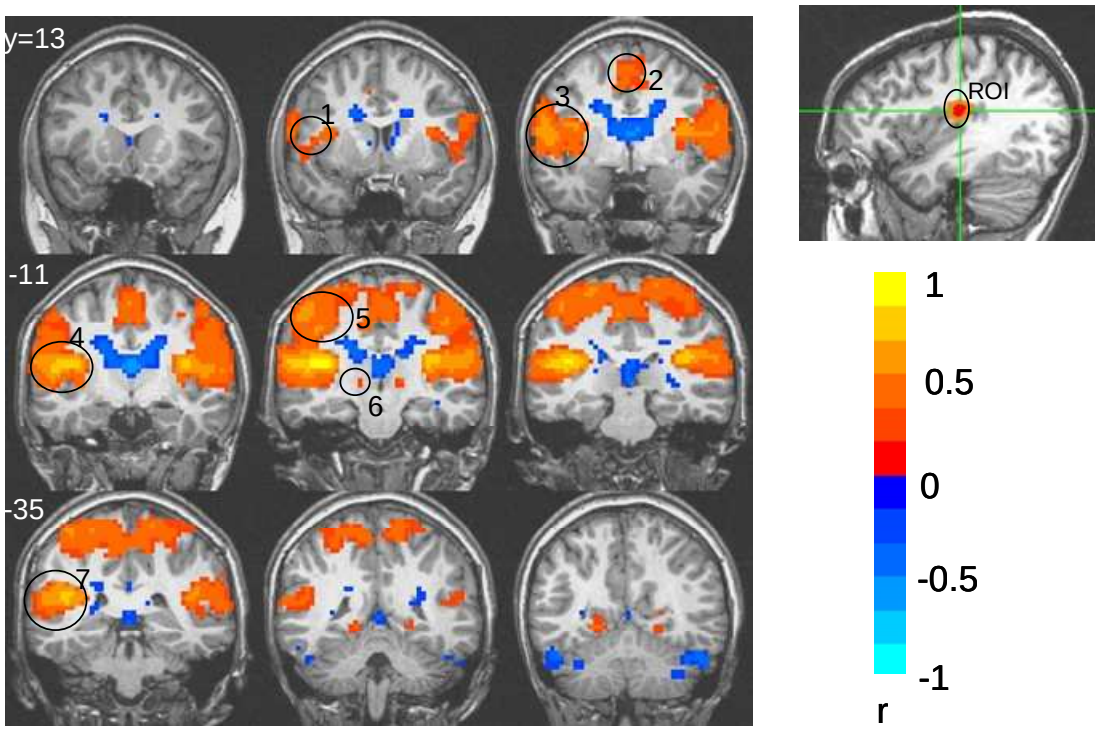

Figure 3.4 Coronal views in standard Talairach stereotactic space of whole-brain interregional functional connectivity during the resting state at a group-level correlation analysis. A pre-defined seed ROI was placed in the posterior insular/secondary somatosensory cortex, $P < 0.001$, correlation coefficient $r > 0.2$. Positive correlations of spontaneous fluctuations between the brain voxels and the ROI voxels are shown in yellow, orange and red. These regions included: 1, inferior frontal junction/anterior insular cortex; 2, anterior cingulate gyrus (BA 24); 3, inferior frontal and superior temporal gyri, anterior/middle insular cortex; 4, posterior insular/secondary somatosensory cortices; 5. primary somatosensory cortex/parietal lobule; 6. thalamus; 7. secondary somatosensory cortex/parietal lobule.

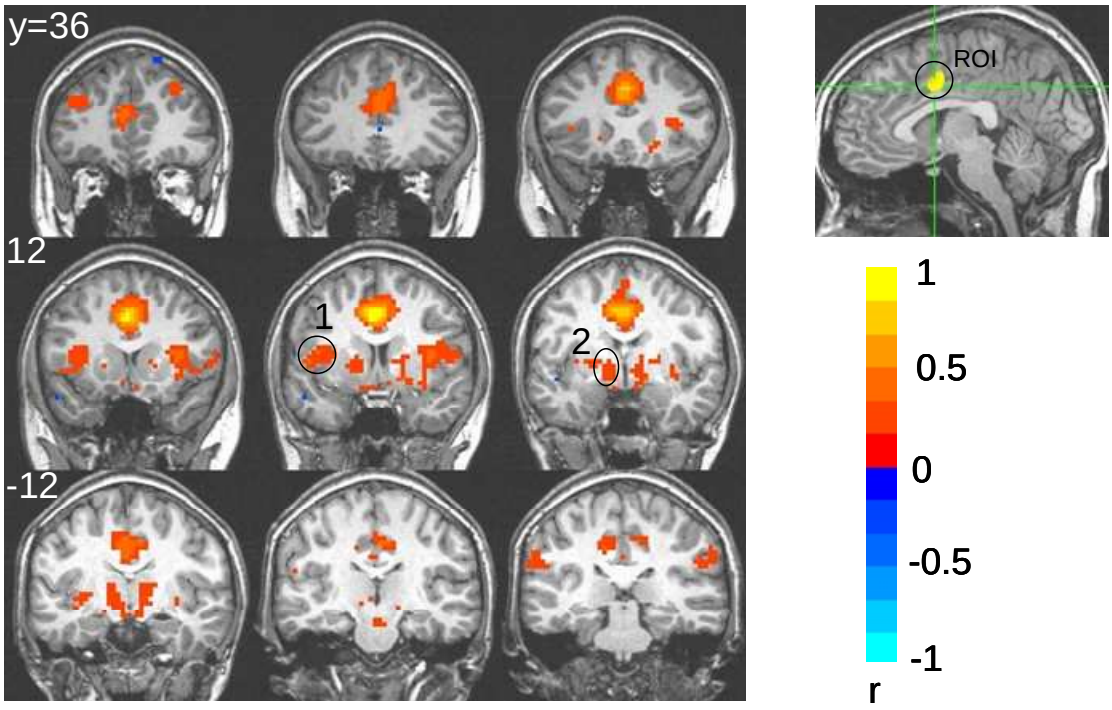

Figure 3.5 Coronal views in standard Talairach stereotactic space of whole-brain inter-regional functional connectivity during the resting state at a group-level correlation analysis. A pre-defined seed ROI was placed in the anterior cingulate cortex, $P < 0.001$, correlation coefficient $r > 0.2$. Positive correlations of spontaneous fluctuations between the brain voxels and the ROI voxels are shown in yellow, orange and red. These regions included: 1. insular cortex; 2. thalamus.

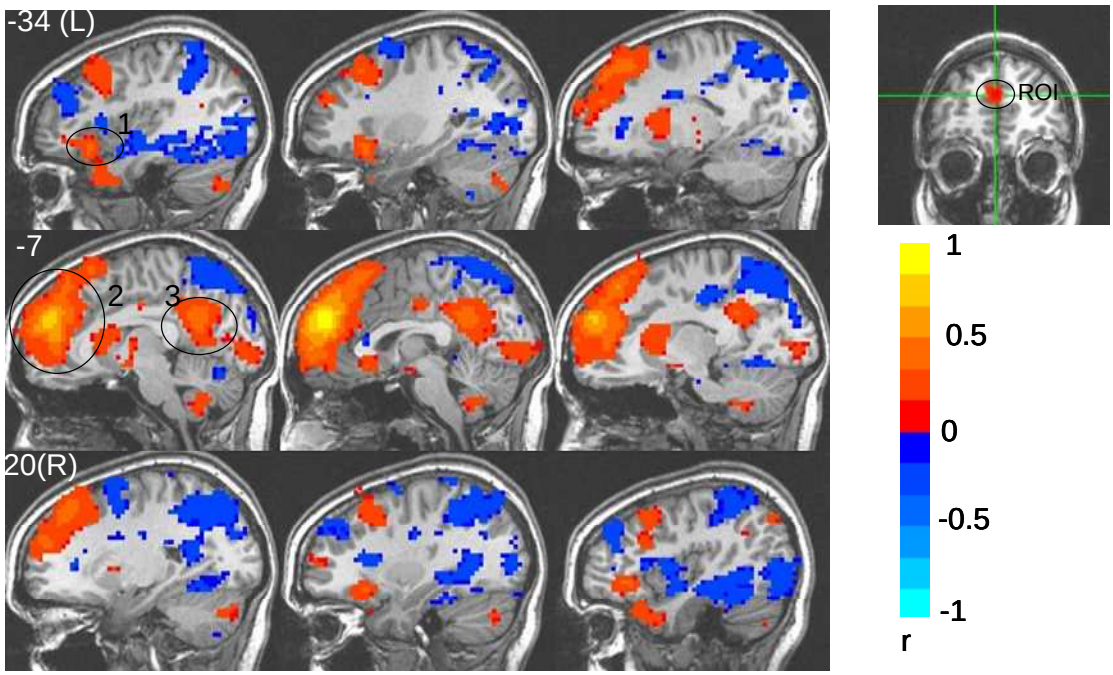

Figure 3.6 Sagittal views in standard Talairach stereotactic space of whole-brain interegional functional connectivity during the resting state at a group-level correlation analysis. A pre-defined seed ROI was placed in the medial prefrontal cortex, $P < 0.001$, correlation coefficient $r > 0.2$. Positive correlations of spontaneous fluctuations between the brain voxels and the ROI voxels are shown in yellow, orange and red. These regions included: 1. anterior insular cortex; 2. prefrontal and anterior cingulate cortices; 3. posterior cingulate cortex.

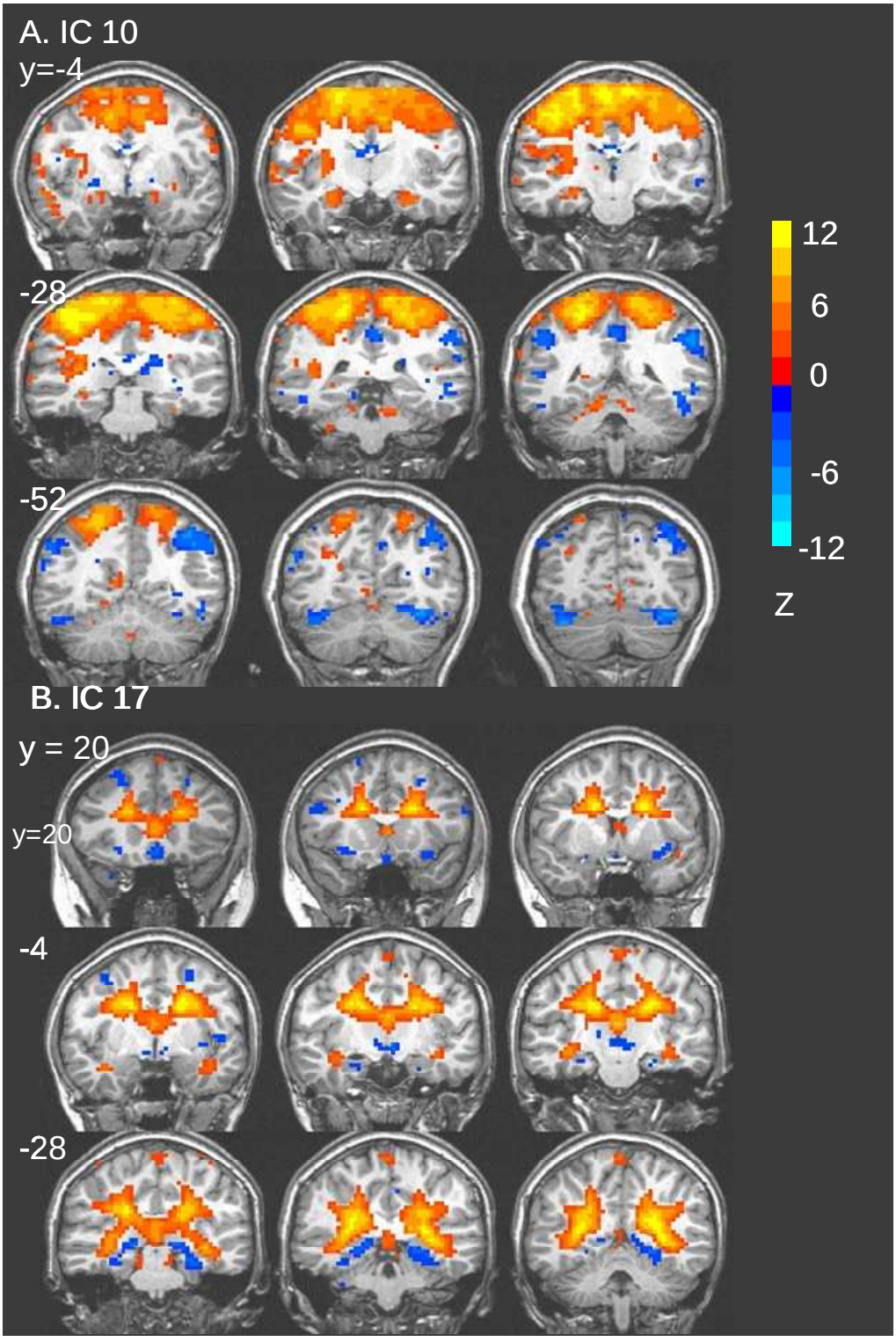

Figure 3.7 A. The 10th independent component map and B. the 17th independent component map (P<0.001, z = 2.06). The temporal patterns of regions in yellow/orange have positive component weights.

3.3.2 Connectivity Model of Pain Network

Pearson correlation coefficiewnts among the regions of interest (ROIs) in the hypothetical model (Figure 3.2) were calculated for both the resting state and during painful stimulation. The six ROIs in the model of Figure 3.2 were significantly correlated with one another (Table 3.2 and Table 3.3). Next, the path analysis calculated the causal relationships among these ROIs during painful stimuliation. The model illustrated in Figure 3.2 was modified to reach acceptable goodness-of-fit (Figure 3.8: $\chi^2(11) = 35.45$, $p < 0.001$; Figure 3.9: $\chi^2(11) = 54.71$, $p < 0.001$). The paths included in the final result all had regression weights that were significantly greater than zero at a p level of 0.001. The pain network during the resting state is depicted in Figure 3.8 with eight statistically significant paths: PAG→Tha; Tha → SI; Tha → ACC; Tha → pIn/SII; SI→ pIn/SII; pIn/SII→ ACC; ACC → PCC; PCC→ ACC. During painful stimulation, the level of functional connectivity increased in four of the paths: Tha →SI; Tha → pIn/SII; SI → pIn/SII; and pIn/SII →ACC (See Figure 3.9, bold arrows). Interestingly, the path coefficient between PAG and Tha changes from a postive value to a strongly negative value, suggesting that the PAG has an inhibitory effect on the pain-perception network.

3.3.3 Connectivity Model for Interaction of Pain and Sadness

Path analysis was also used to analyze the hypothetical model depicted in Figure 3.3 during the interaction of pain and sadness. The model was modified to reach acceptable goodness-of-fitness (Figure 3.10: χ^2 (35) = 126, $p < 0.001$). The final model presented in Figure 3.10 contains three sub-networks, one each for pain, emotion, and the interaction of the two. The significant paths during painful stimulation (Figure 3.9) were also preserved in the emotion/pain model (Figure 3.10): i.e., (1) Tha → SI → pIn/SII →ACC and (2) Tha → pIn/SII. Moreover, the ACC node integrated efferent and afferent information from other subdivisions of cingulate

cortex, and the insular cortex, PAG, and amygdala to form several functional circuits: i.e., (1) pIn/SII → aIn → ACC → PCC, (2) ACC → sACC → Tha →pIn/SII, (3) ACC → AMY/Hip, and (4) ACC → PAG →pIn/SII. These functional circuits reveal that the ACC is in a key functional postion to influence activity in brain regions that process pain perception. Recall from Chapter 2 that the pIn/SII shows increased activation when painful stimuli are adminsterd when a subject is in a sad mood, resulting in increased pain perception (Figure 2.8 in Chapter 2). In the path analysis described here, this pIn/SII ROI receives positive inputs from SI, Tha and PAG, as well as negative input from PPC. Through the node of PPC, there is a combination of positive and negative path coefficients: (1) AMY/Hip → PCC →PPC; (2) ACC → PCC → PPC; and, (3) sACC → PCC → PPC. Thus, the combined effect of these paths has positive influence in the path of PPC → pIn/SII. It suggests the increased activation in AMY/Hip, ACC and sACC leads to the increased activation. Similarly, the positive feedback loop from the pIn/SII → aIn → ACC → PCC → pIn/SII results in an increased activation in the pIn/SII. Finally, the subpath PAG → pIn/SII, which also integrates the inputs from ACC and AMY/Hip, resulted in additional positive influences on pIn/SII.

	ACC	PAG	PCC	pIn/SII	SI	Tha
ACC	1					
PAG	.220**	1				
PCC	.411**	.203**	1			
pIn/SII	.540**	0.057	.573**	1		
SI	.545**	0.115	.543**	.657**	1	
Tha	.499**	.250**	.509**	.335**	.368**	1

Table 3.2 Input data for analyzing the functional connectivity of the pain processing network (Figure 3.2) during rest. Pearson correlations between the ROIs (** $p < 0.01$)

	ACC	PAG	PCC	pIn/SII	SI	Tha
ACC	1					
PAG	-.520**	1				
PCC	.151**	-.248**	1			
pIn/SII	.752**	-.787**	.382**	1		
SI	.783**	-.712**	.305**	.91**	1	
Tha	.564**	-.747**	.172**	.776**	.717**	1

Table 3.3 Input data for analyzing the functional connectivity of the pain processing network (Figure 3.2) during painful stimulation. Pearson correlations between the ROIs (** $p < 0.01$)

	ACC	sACC	aIn	AMY/Hip	pIn/SII	SI	Tha
ACC	1						
sACC	.661**	1					
aIn	.453**	.347**	1				
AMY/Hip	.579**	.592**	.319**	1			
pIn/SII	.761**	.515**	.402**	.791**	1		
SI	.658**	.534**	0.245	.522**	.704**	1	
Tha	.704**	.730**	.286**	.822**	.754**	.673**	1
PAG	.755**	.558**	.458**	.615**	.788**	.520**	.567**
PCC	.775**	.676**	.341**	.615**	.660**	.542**	.730**
PPC	-.492**	-.305**	-.277**	-.441**	-.658**	-.470**	-.420**

Table 3.4 (A) Input data for analyzing functional connectivity of Figure 3.3 when painful stimuli were administered during sad mood. Pearson correlations between the ROIs (** $p < 0.01$)

	PAG	PCC	PPC
ACC			
sACC			
aIn			
AMY/Hip			
pIn/SII			
SI			
Tha			
PAG	1		
PCC	.665**	1	
PPC	-.552**	-0.253	1

Table 3.4 (B) Input data for analyzing functional connectivity of Figure 3.3 when painful stimuli were administered during sad mood. Pearson correlations between the ROIs (** $p < 0.01$)

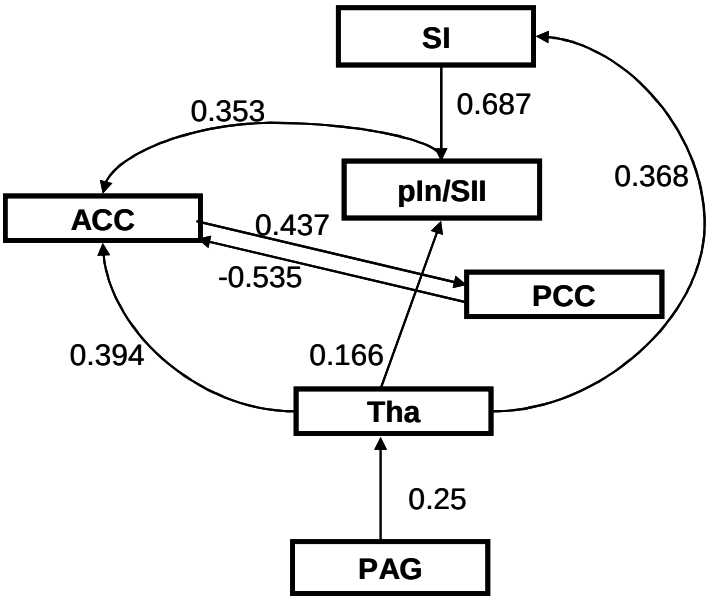

Figure 3.8 Functional connectivity for the pain network during rest. Standardized path coefficients, computed from data in Table 3.2, represent the combined effect of all connections included in the path analysis. The final model is modified based on the hypothetical model in Figure 3.2.

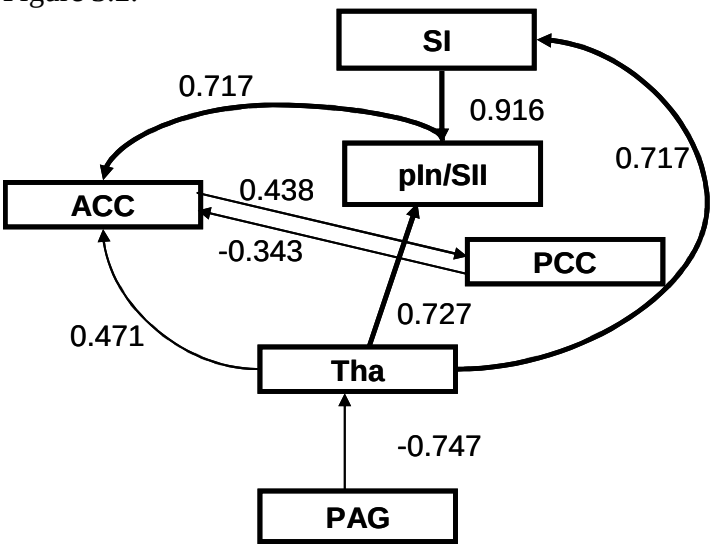

Figure 3.9 Functional connectivity for the pain network during acute painful stimulation. Standardized path coefficients, computed from data in Table 3.3, represent the combined effect of all connections included in the path analysis. Bold arrows indicate increased path coefficients of functional connectivity during painful stimulation compared to resting state.

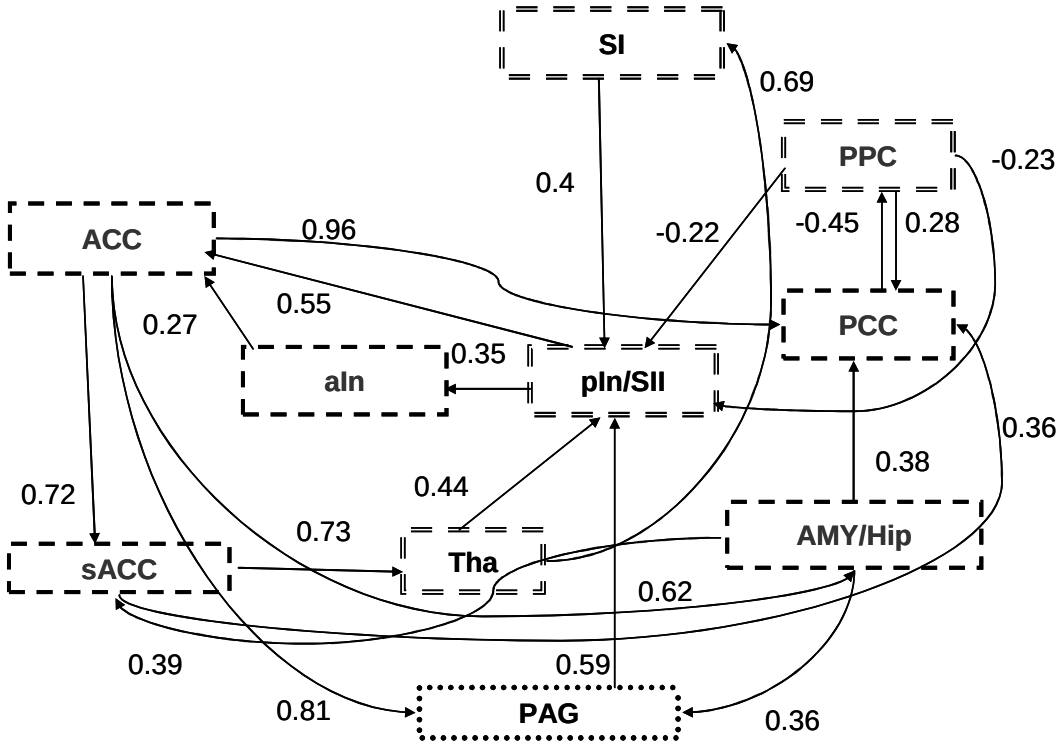

Figure 3.10 Functional connectivity for interaction between painful and sad conditions. Standardized path coefficients, computed from data in Table 3.4, represent the combined effect of all connections included in the path analysis. The ROIs primarily associated with the processing of pain perception, including SI, pIn/SII, PPC and Tha, are indicated by the dashed double line boxes. The ROIs primarily associated with the processing of sad pictures, such as ACC, sACC, aIn, PCC and AMY/Hip, are indicated by the dashed line boxes. PAG is a node that receives inputs from emotional brain regions and is in a position to directly influence activation in the somotosensory cortex. This final model includes statistically significant paths and is modified based on the hypothetical model in Figure 3.3.

3.4 Discussion

To our knowledge, this is the first study to demonstrate functional connectivity among brain regions within the pain matrix in which activity is modulated by sadness. The functional connectivity of these brain regions during the resting and task-driven states provides insights into understanding the altered pain experience influence by sadness.

3.4.1 Functional Network for Pain Perception

We set out to determine if correlations between the posterior insular/secondary somatosensory cortex (pIn/SII) and other brain regions could be used to better understand the brain activation pattern associated with pain processing, and, in the process, constructed a hypothetical model of functional connectivity. The result of the study described in Chapter 2 is that the posterior insular/secondary somatosensory cortex is significantly more active in response to electrical pain shock than during a control condition. This is consistent with the discovery that the SII, neighboring areas BA7b, and the posterior insula contain nociceptive neurons (Robinson and Burton, 1980). These brain regions have consistently been found to encode the intensity of nociceptive stimulation in both PET and fMRI neuroimaging studies (Peyron et al., 2002; Frot et al., 2007). In the resting-state fMRI study described in this chapter, a correlation analysis revealed that in both hemispheres the primary components of the acute pain processing network (i.e., the anterior cingulate cortex (BA 24), SI, insular cortex and thalamus; see reviews in Apkarain 2005) were positively correlated with our pre-defined seed region, the pIn/SII. An independent component analysis conducted without the pre-defined seed region confirmed the same pattern. Because the correlation patterns found during the resting state were also found during task performance, these analyses demonstrate that, even in absence of external stimuli, brain regions within the pain matrix maintain a level of functional connectivity. Comparing the pattern of BOLD activity during rest with those during stimulus presentation, it is then possible to quantitatively describe how external stimuli modulate the functional networks (Fox and Raichle, 2007; Dhond et al., 2008).

We used the resting state activation pattern to construct a hypothetical neural network for pain processing, so that we could employ path analysis to identify functional connections for pain processing during both rest (Figure 3.8) and in response to acute pain (Figure 3.9). During

rest, significant functional connectivity was observed in a circuit beginning with the thalamus and continuing to SI, SII, and the posterior insular and anterior cingulate cortices. The anatomical connections of this functional pathway have been characterized in great detail in several animal species, including humans (Price, 1999). Compared with the resting state, we observed that path coefficients in this pathway increased during acute painful stimuli, seen especially in the large path coefficient increases from thalamus to SI and to pIn/SII. The strong positive interaction most likely means that increased activity in the thalamus directly leads to increased activity in SI and pIn/SII.

We also observed increased functional connectivity from the posterior insular/secondary somatosensory cortex to the anterior cingulate cortex during the response to pain. The ACC is known to be an important region for processing the affective dimension of pain (Rainville, 1997). The functional connection from insula to ACC suggests that the sensory dimension of pain may be integrated with emotional and cognitive factors in the proposed network. This interpretation is consistent with the elctrophysiological properties of nociceptive neurons in the ACC which appear to monitor the overall state of the body with whole-body receptive fields (Vogt and Sikes, 2000).

3.4.2 Functional Network for Interaction of Pain and Sadness

We hypothesized that the pain network would directly interact with brain regions associated with emotional processing. Previous reports have indicated that the ACC, amygdala, and anterior insular cortex play important roles in processing both pain and emotion (Vogt, 2005; Rainville, 1997; Neugebauer et al., 2004; Craig, 2003). In this study, intrinsic connections between the ACC and several brain regions, including the insular cortex, thalamus, and amygdala were observed during rest. Using pre-established knowledge of the anatomical connnections among

those areas, as well as those with the PAG and prefrontal lobe, we created a model of functional connectivity (Figure 3.10). In this proposed model, brain regions that process pain perception primarily interact with subdivisions of cingulate cortex and the amygdala-hippocampal complex. It is possible to decduce how these regions interact to produce a response to pain that is influenced by emotional state.

The Periaqueductal Gray (PAG)

The model includes a direct functional connection from the ACC to the PAG. This is likely to be the substrate through which the ACC can modulate activity in the PAG to either facilitate or inhibit pain perception. The model also includes a direct connection from the amygdala to the PAG. Studies have shown that the amygdala is activated when a person views unpleasant pictures (Phan et al., 2002). In addition, individuals who have sustained sclerotic damage to the amygdala do not show enhanced responses to emotional visual stimuli in visual cortex in fMRI experiments (Vuilleumier et al., 2004). The pathway from the amygdala to the PAG, then, may provide another substrate for the emotional context of the pain stimulus to subsequently affect the PAG's pain-gating function. Finally, the direct pathway from the PAG to the pIn/SII in the model suggests that increased activity in the PAG can lead to increased activation in the pIn/SII. It is possible that the PAG node integrates information from the ACC and amygdala, and intensifies activation in the ascending pain pathway.

The Anterior and Posterior Cingulate Cortices

In our model shown in Figure 3.10, the amygdala and anterior cingulate cortex (BA24) are functionally connected to the subgenual (sACC). The sACC is also functionally connected to brain areas of the pain matrix through the thalamus. The sACC is known to be involved in sadness and depression (Mayberg et al., 1999; Liotti et al., 2000). The model suggests that

information about the emotional context of pain may be integrated in the sACC. The sACC also projects to the posterior cingulate cortex (PCC), consistent with our resting-state results showing connections from the ACC, sACC and amygdala to the PCC, and may also integrate emotional context with noxious information in PCC. A previous study from our laboratory showed that the PCC is often activated by acute pain stimuli (Symonds et al., 2006). The bilateral connection between the PCC and the parietal lobule/BA7 (PPC) suggests that information may be relayed from the PCC to the pIn/SII, where it may influence activity in this primary node of the pain matrix.

The Anterior Insular Cortex

In our model the anterior insular cortex (aIn) receives input from the pIn/SII, and projects to the ACC. The aIn is thought to be involved in processing introspective feelings, including sensory coding, body state assessment and autonomic regulation (Craig, 2009). Therefore, like the sACC, it may also integrate information about pain with its emotional context.

The Prefrontal Cortex

The model in Figure 3.10 does not include prefrontal regions even though they were originally proposed in the hypothetical model seen in Figure 3.3. This is because the inclusion of prefrontal regions did not contribute to the validation of the functional connectivity model. It is possible that there were few cognitive factors involved in the emotional modulation of pain experience in the current study and/or that emotional modulation of pain processing is mainly dependent upon activation in the cingulate cortex and amygdala.

3.4.3 Conclusion

The study described in Chapter 2 demonstrated that sadness can increase pain perception, and that this is accompanied by significantly increased brain activation in the posterior

insular/secondary somatosensory cortices. The study described in this chapter reveals the intrinsic functional connectivity among the main brain regions associated with pain perception at rest. Specifically, the resting state connections between the thalamus and somatosensory cortices show increased path coeffcients in response to pain stimuli. In addition, the results of a path analysis revealed the direct interaction of pain and sadness in regions that process pain and emotional information. Emotional context appears to influence pain perception through functional connectivity among somatosensory, insular, posterior parietal and cingulate cortices, amygdala and periaqueductal gray. Finally, the total effect of emotional context on pain matrix areas through the projections to the posterior insular/ secondary somatosensory cortices is likely to be communicated directly through the periaqueductal gray. These outcomes of path analysis provide specific explanations for the interaction of pain perception and sadness and can now be explicitly tested empirically.

Chapter 4

General Discussion

Emotion and pain are both complicated physiological and psychological constructs, and have received extensive attention in neuropsychological research. Both are considered to be multidimensional, comprising valence and sensory components. Clinical and laboratory studies indicate that negative emotion, particularly sadness, can either increase pain perception or decrease pain tolerance (Meagher et al., 2001; Tang et al., 2008). Depression and chronic pain are often comorbid, providing a clinical impetus to understand the interaction between emotion and pain at the neural level (Breslau et al., 2003).

A number of brain regions that respond to either pain or emotion have been identified in recent years by neuroimaging studies (see reviews in Peyron et al., 2000; Dalgleish, 2004). Some of these studies suggest that because the anterior cingulate cortex (ACC) is activated by both pain and negative affect (Rainville et al., 2002; Vogt, 2005), it may be an important component in the modulation of pain perception during different emotional states. However, it is not clear by which neural circuits the ACC could be involved in the interaction between pain and sadness.

The aim of this dissertation is to test the hypothesis that sadness can influence subjective pain perception, and to explore the functional connectivity of brain networks that are involved in processing both pain perception and sadness. Specifically, the experiments described in Chapters 2 and 3: (1) identify human brain activation during perception of acute pain and how that activity is modified during sadness; and, (2) construct the functional connectivity of neural networks associated with pain processing as well as the interaction between pain and sadness.

4.1 Brain Regions Encoding both Pain and Emotions

Cortical and subcortical regions that process pain perception have been intensively investigated in both healthy subjects and patients with clinical pain conditions. Across a variety of experimental manipulations, researchers find that pain is not encoded in a singular "pain center" of the brain, but is instead located within a network of somatosensory, limbic and associative brain areas that receive parallel input from multiple nociceptive pathways (Peyron et al., 2000; Apkarian et al., 2005). The main components in this brain network for pain processing include primary and secondary somatosensory (SI/SII), insular, anterior cingulate (ACC) and prefrontal cortices and thalamus. Increased regional blood flow changes to noxious stimuli are consistently observed in SI/SII, insular and ACC cortices. The SI/SII and insular cortices are thought to be related to the sensory-discriminative aspects of pain perception such as the intensity or location of a painful stimulus (Coghill et al., 1999; Bushnell et al., 1999). The ACC is observed to be activated in the majority of PET or fMRI studies, but does not seem to be involved in encoding either stimulus intensity or location, and instead has been implicated in affective aspects of pain processing (Rainville et al., 1997; Tölle et al., 1999). For example, the ACC is particularly active when a painful stimulus is perceived as more distressing, regardless of its intensity (Rainville, et al., 1997). Consistent with current neuroimaging, in this study we also find significantly increased BOLD activity in response to acute painful electrical shocks in the contralateral primary somatosensory (SI), bilateral posterior insular/secondary somatosensory (pIn/SII), contralateral anterior cingulate (BA 32), and in the thalamus.

The neuroanatomy of emotion in the human brain has also been the focus of recent neuroimaging studies. The prefrontal cortex, amygdala, and anterior cingulate cortex appear to be key brain regions involved in the emotional experience (Dalgleish, 2004). In a meta-analysis of emotion activation studies in PET and fMRI, Phan et al. (2002) observe: (1) the medial

prefrontal cortex generally is engaged in the representation of elementary emotional states such as happiness, sadness, disgust and the mixture of these emotions; (2) the amygdala plays a crucial role in both the perception of emotional cues and the production and emotional responses, with some evidence suggesting that it is specifically associated with fear-related emotions; (3) the subgenual anterior cingulate (BA 25) cortex is significantly associated with sadness; (4) the anterior cingulate and insular cortices are involved in emotions either with cognitive demand or induced by emotional recall/imagery; and, (5) both the occipital cortex and the amygdala are activated by emotions induced by visual stimuli.

In this study, subjective sadness was successfully induced by visual stimuli selected from the International Affective Picture System (IAPS). Our results, consistent with observations of Phan et al. (2002), show that watching sad pictures significantly activates the brain regions located in the medial frontal cortex (BA9), the right inferior frontal cortex (BA 45/44), the bilateral amygdala/hippocampus, and the bilateral occipital/fusiform gyri.

Not surprising, when we simultaneously present painful and emotional stimuli, significant activation in brain networks for both pain and emotions was found. In addition, significant activation was observed in the periaqueductal gray (PAG). This midbrain region was activate most likely reflects the pain modulation in the ascending pathway. As the PAG also receives direct inputs from emotion-related brain regions such as the ACC and the amygdala, top-down influences of emotion from the ACC and amygdala could be exerted on the PAG, thereby modulating transmission of pain from PAG to the thalamus or to the pIn/SII.

4.2 Secondary Somatosensory and Posterior Insular Cortices

In Chapter 2, we report that in healthy right-handed female participants, pain perception is altered by subjective emotion. Participants rated their pain perception significantly higher when

they received pain stimuli while concurrently watching sad pictures, compared to receiving painful stimulation while watching neutral pictures. Interestingly, we also found that activation in the contralateral posterior insular/secondary somatosensory cortex, a part of the brain network for pain processing, was significantly greater when painful shocks were accompanied by sad pictures than when painful stimuli were presented with emotionally neutral pictures.

The border of secondary somatosensory and insular cortices has not so far been clearly delineated anatomically on MRI slices. Thus, the results reported in our fMRI study do not separate the two regions, and instead consider them to be one functional region. The pIn/SII is most likely associated with the sensory-discriminative aspects of pain processing, as these regions contain nociceptive neurons. Many previous PET/fMRI studies have found reliable pain-related activity in this brain region (see review in Apkarian et al., 2005). For example, the pIn/SII is functionally implicated in the discrimination of intensity of thermal stimuli (Craig et al., 2000; Peyron et al., 1999). With electrodes implanted within SII and posterior insula in patients referred for presurgical evaluation of epilepsy, Frot et al., (2007) reported that increasing thermal intensities of CO2 laser stimulation enhanced evoked potentials in both insular and secondary somatosensory cortices.

When pain is accompanied by sadness, we also observe that increased activation in other brain regions such as dorsal anterior cingulate cortex (ACC), subgenual anterior cingulate cortex (sACC), amygdala/hippocampal complex (AMY/Hip) and periaqueductal gray (PAG). Several studies have shown that the activation of anterior cingulate cortex and amygdala/hippocampal complex is associated with emotional processing. For example, subgenual cingulate cortex has reduced metabolic during rest in patients with clinical depression (Mayberg et al., 1994). The dorsal anterior cingulate cortex is involved in the affective dimension of pain processing

(Rainville et al., 1997). The amygdala is known to process emotional stimuli, including facial expression (Phan et al., 2004). Interestingly, in the functional connectivity analysis described in Chapter 3 we observed that the pIn/SII is functionally connected with these emotion-related brain regions through one or multiple nodes.

When pain perception is increased by sadness, the connections between the pIn/SII and brain regions that process emotions may lead to increased activity in the pIn/SII. The pIn/SII receives projections from the ventroposterior lateral nuclei of thalamus and the PAG in the nociceptive pathways, and this is one of the first cortical relay stations in the central processing of painful stimuli (Treede et al., 2000). The active area of thalamus and the PAG during pain also interact with brain regions that process emotions. For example, our functional connectivity model shows that the thalamus receives positive functional inputs from subgenual anterior cingulate cortex (sACC) and amygdala. The PAG also receives direct input from the anterior cingulate cortex and amygdala. These functional connections suggest that the altered activation in the pIn/SII could be due to activity in the thalamus and PAG nodes in the pain ascending pathway, which themselves receive functional inputs from cortical regions associated with emotions, including the sACC, ACC, and amygdala.

We also find that the pIn/SII receives positive functional inputs from two other nodes: the posterior cingulate cortex (PCC), and the parietal lobule/BA 7 (PPC). The parietal lobule/BA 7 contains nociceptive neurons and activation in the pIn/SII as a result of painful stimulation can extend into this brain region (Peryon et al., 2000). A previous fMRI study in our laboratory shows that the posterior cingulate cortex is also activated by acute painful stimulation (Symonds et al., 2006). In our model presented in Chapter 3, the posterior cingulate cortex receives functional input from the sACC, ACC and amygdala. Thus, the posterior cingulate cortex is

possibly involved in integrating emotional contexts and noxious information. The effect of the path from the posterior cingulate cortex (PCC) to the parietal lobule/BA 7 (PPC) would be to increase activation in the pIn/SII.

4.3 Functional Connectivity Analysis of Pain-Emotion Interaction

To our knowledge, this is the first study demonstrating altered functional connectivity among brain when pain perception is increased by a change in mood. Functional connectivity analysis provides information not available using traditional fMRI contrast analysis methods. For example, fMRI contrast analysis methods cannot distinguish between excitatory and inhibitory activity, but instead rely upon regional changes in the oxygenation of hemoglobin due to increased synaptic activity (Logothetis et al., 2001). On the other hand, functional connectivity analysis is a promising strategy for determining whether rCBF changes are due to excitation or inhibition. This analysis investigates statistical correlation of dynamic flow changes between interconnected regions. Positive or negative path coefficients help to explain the activation of excitation or inhibitation in a downstream brain region.

In Chapter 3, resting state fMRI reveals intrinsic correlations among brain regions that are functionally connected. Based on the observed brain region activation in the task-driven fMRI described in our experiments in Chapter 2, we place ‘seed regions’ in the posterior insular/secondary somatosensory and dorsal anterior cingulate cortices to investigate the interregional correlation patterns in the brain networks for pain and emotions, respectively, during the resting state. The resulting resting-state map of simple correlation analysis indicates that brain regions, including somatosensory, insular, anterior cingulate, and parietal cortices, are intrinsically correlated. Without predefined seed regions, we also used the independent component analysis (ICA) to determine the activation pattern of the pain network at rest. The

correlation map of ICA confirms the intrinsic correlations among somatosensory, insular, cingulate and parietal cortices. These brain regions may therefore have similar functionality in response to external stimuli.

Once the resting state maps was created, path analysis then showed that these regions are, in fact, *functionally* connected with one another. The following functional paths was observed during the rest: (1) projections from the thalamus to the primary somatosensory, dorsal anterior cingulate and posterior insular/secondary somatosensory cortices; (2) a feedback loop starting with primary somatosensory cortex, and going from there to posterior insular/secondary somatosensory cortices, dorsal anterior cingulate cortex, posterior cingulate cortex, and finally back to posterior insular/secondary somatosensory cortices; (3) bi-directional connections between the dorsal anterior cingulate cortex and posterior cingulate cortex; and (4) a projection from the preaqueductal gray to the thalamus. Interestingly, the path coeffcients of some paths increased when painful electrical shocks are administered. Specifically, the path projecting from the thalamus to the primary somatosensory cortex, continuing to the posterior insular/ secondary somatosensory cortices (pIn/SII), and reaching the dorsal anterior cingulate cortex is significantly increased. Similarly, the direct connection from the thalamus to the pIn/SII is also significantly increased. These functional paths outline important relays and connections related to pain processing. In the pain processing network, a higher positive path coefficient in the path from the thalamus to the pIn/SII most likely means that increased activity in the thalamus directly leads to increased activity in the pIn/SII.

In Chapter 3, we presented a model to explain how brain regions that are parts of the pain matrix could directly interact with brain region associated with emotional processing. The functional connectivity results described in Chapter 3 reveal that the dorsal anterior cingulate

cortex receives inputs from brain regions associated with sad emotions, including the amygdala, subgenual cingulate cortex, and anterior insular cortex. Information about sad emotions can then be relayed to pain processing areas via connections within the cingulate cortex, as well as connections between the cingulate cortex and the thalamus, periaqueductal gray, parietal cortex, and finally to the posterior insular/secondary somatosensory cortices (pIn/SII). Thus the functional connections among these sadness- and pain-processing regions can lead to modulated activity in the pIn/SII during sadness. This model and the functional connectivity among the pain and emotional networks explains the observation in the Chapter 2 that increased pain perception during sadness is accompanied by the increased brain activation in the pIn/SII.

4.4 Conclusions

In this study, we identified brain regions associated with either pain or sadness and confirmed results from previous neuroimaging studies. We then demonstrated that sadness can increase pain perception and that this behavioral result is accompanied by significantly increased brain activation in the secondary somatosensory and posterior insular cortices. Finally, we employed resting-state fMRI and functional connectivity analyses to reveal for the first time the neural underpinnings of altered pain perception during sadness.

The connectivity analyses in this study reveal the intrinsic functional connectivity at rest among brain regions associated with pain perception. The functional connections between the thalamus and somatosensory cortex are significantly increased during painful stimulation. In addition, the results of path analysis reveal how sadness can influence pain perception via connectivity among somatosensory, insular, parietal and cingulate cortices, amygdala and periaqueductal gray. The combined effect of activity in emotion-processing areas can then influence the posterior insular/ secondary somatosensory cortices directly through the

periaqueductal gray. Thus, path analysis can provide a neural explanation for how pain perception can be altered by sadness.

4.5 Limitations

There are some limitations in studies described in this dissertation. First, we only recruited female subjects, so that the results from the study in Chapter 2 cannot be generalized to all men. Second, large clusters covering the occipital/fusiform gyri and cerebellum were observed during trials when sad pictures were presented. These large clusters cannot be easily separated into independent small clusters at the alpha value we used. To obtain meaningful activation in other brain regions such as posterior insular/secondary somatosensory cortices, we have to sacrifice the analysis of these large clusters. Finally, path analysis is only used in a confirmatory way. It would have been most useful if we already had a clear hypothesis to test. Our construction of the hypothetical model mostly depended upon known anatomical connections.

4.6 Future Directions

In Chapter 2, we designed a successful fMRI experimental paradigm for investigating how pain perception can be altered by sadness. We intend to extend this paradigm to investigate the relationship between stress and pain, fear and pain, and finally, the relationship between negative emotions and pain in chronic pain patients.

Using the resting-state fMRI paradigm described in Chapter 3, we can further compare the spontaneous brain activation patterns in the pain and emotional networks among different groups, such as chronic pain patients, depression patients and healthy control participants. One possibility is that intrinsic functional connectivity of functional brain networks are altered in different clinical conditions.

Finally, the functional connectivity models developed and described in Chapter 3 can be applied to develop the novel therapies that target the brain circuitry in the cortex rather than the periphery or spinal cord pathways. The models may be modified independently under each type of chronic pain and the changes of functional connectivity may be used to predict the efficiency of therapies.

APPENDICES

APPENDIX A

Programming scripts in AFNI for processing the imaging data of Chapter 2

```
#convert DICOM files from the MRI scanner into AFNI format
to3d -session Sec1 -prefix run01 -epan -time:zt 38 60 3000 seq+z './11548/3/SIM*'
to3d -session Sec1 -prefix run02 -epan -time:zt 38 60 3000 seq+z './11548/4/SIM*'
to3d -session Sec1 -prefix run03 -epan -time:zt 38 60 3000 seq+z './11548/5/SIM*'
to3d -session anatomy -prefix SPGR './11548/6/SIM*'

#!/usr/bin/env tcsh

echo "auto-generated by afni_proc.py, Fri Oct  3 11:39:49 2008"
echo "(version 1.28, Jan 28, 2008)"

# execute via : tcsh -x altpain.pre.GAMblur8 |& tee output.altpain.pre.GAMblur8
# ------------------------------------------------
# script setup
# the user may specify a single subject to run with

if ( $#argv > 0 ) then
    set subj = $argv[1]
else
    set subj = AM5023
endif

# assign output directory name
set output_dir = $subj.results

# verify that the results directory does not yet exist
if ( -d $output_dir ) then
   echo output dir "$subj.results" already exists
    exit
endif

# set list of runs
set runs = (`count -digits 2 1 3`)

# create results directory
mkdir $output_dir

# create stimuli directory, and copy stim files
mkdir $output_dir/stimuli
cp ../../1DFiles/stim.1D $output_dir/stimuli
```

```
# ------------------------------------------------------

# apply 3dTcat to copy input dsets to results dir, while removing the first 0 TRs
3dTcat -prefix $output_dir/pb00.$subj.r01.tcat run01+orig'[0..$]'
3dTcat -prefix $output_dir/pb00.$subj.r02.tcat run02+orig'[0..$]'
3dTcat -prefix $output_dir/pb00.$subj.r03.tcat run03+orig'[0..$]'

# and enter the results directory
cd $output_dir

# ------------------------------------------------------
# run 3dToutcount and 3dTshift for each run
foreach run ( $runs )
   3dToutcount -automask pb00.$subj.r$run.tcat+orig > outcount_r$run.1D
   3dTshift -tzero 0 -quintic -prefix pb01.$subj.r$run.tshift      \
            pb00.$subj.r$run.tcat+orig
end

# ------------------------------------------------------
# align each dset to the base volume
foreach run ( $runs )
   3dvolreg -verbose -zpad 1 -base pb01.$subj.r03.tshift+orig'[59]'  \
            -1Dfile dfile.r$run.1D -prefix pb02.$subj.r$run.volreg   \
            -cubic                                          \
            pb01.$subj.r$run.tshift+orig
end

# make a single file of registration parameters
cat dfile.r??.1D > dfile.rall.1D


# ------------------------------------------------------
# blur each volume
foreach run ( $runs )
   3dmerge -1blur_fwhm 8.0 -doall -prefix pb03.$subj.r$run.blur   \
           pb02.$subj.r$run.volreg+orig
end

# ------------------------------------------------------
# create 'full_mask' dataset (union mask)
foreach run ( $runs )
   3dAutomask -dilate 1 -prefix rm.mask_r$run pb03.$subj.r$run.blur+orig
end

# get mean and compare it to 0 for taking 'union'
3dMean -datum short -prefix rm.mean rm.mask*.HEAD
```

```
3dcalc -a rm.mean+orig -expr 'ispositive(a-0)' -prefix full_mask.$subj

# ----------------------------------------------------
# scale each voxel time series to have a mean of 100
# (subject to maximum value of 200)
foreach run ( $runs )
   3dTstat -prefix rm.mean_r$run pb03.$subj.r$run.blur+orig

   3dcalc -a pb03.$subj.r$run.blur+orig -b rm.mean_r$run+orig  \
          -c full_mask.$subj+orig                              \
          -expr 'c * min(200, a/b*100)'                        \
          -prefix pb04.$subj.r$run.scale
end

# ----------------------------------------------------
# run the regression analysis
# create -stim_times files
make_stim_times.py -prefix stim_times -tr 3.0 -nruns 1 -nt 60        \
                -files stimuli/stim.1D
foreach run ( $runs )
3dDeconvolve -input pb04.$subj.r$run.scale+orig.HEAD                 \
   -polort 2                                                         \
   -mask full_mask.$subj+orig                                        \
   -num_stimts 7                                                     \
   -stim_times 1 stimuli/stim_times.01.1D 'GAM'                      \
   -stim_label 1 stim                                                \
   -stim_file 2 dfile.rall.1D'[0]' -stim_base 2 -stim_label 2 roll   \
   -stim_file 3 dfile.rall.1D'[1]' -stim_base 3 -stim_label 3 pitch  \
   -stim_file 4 dfile.rall.1D'[2]' -stim_base 4 -stim_label 4 yaw    \
   -stim_file 5 dfile.rall.1D'[3]' -stim_base 5 -stim_label 5 dS     \
   -stim_file 6 dfile.rall.1D'[4]' -stim_base 6 -stim_label 6 dL     \
   -stim_file 7 dfile.rall.1D'[5]' -stim_base 7 -stim_label 7 dP     \
   -fout -tout -x1D X.xmat.1D -xjpeg X.jpg                           \
   -fitts fitts.$subj.r$run                                          \
   -bucket stats.$subj.r$run
end

# if 3dDeconvolve fails, terminate the script
if ( $status != 0 ) then
   echo '---------------------------------------'
   echo '** 3dDeconvolve error, failing...'
   echo '   (consider the file 3dDeconvolve.err)'
   exit
endif

# create an all_runs dataset to match the fitts, errts, etc.
```

```
3dTcat -prefix all_runs.$subj pb04.$subj.r??.scale+orig.HEAD

# create ideal files for each stim type
1dcat X.xmat.1D'[9]' > ideal_stim.1D

# -----------------------------------------------------
# remove temporary rm.* files
\rm -f rm.*

#return to parent folder
cd ../
#Copy and paste functional runs
 into 'func.tlrc' folder

#Register functional runs into talairaching view
set subj =  AM5023
cd ../{$subj}.results/
cp stats.{$subj}* ../func.tlrc/
cd ../../anatomy/
cp SPGR* ../Sec1/func.tlrc/
adwarp -apar SPGR+tlrc -dpar stats.{$subj}.r01+orig
adwarp -apar SPGR+tlrc -dpar stats.{$subj}.r02+orig
adwarp -apar SPGR+tlrc -dpar stats.{$subj}.r03+orig

#! now the data analysis for single subject's dataset is done. It is ready for group analysis!
#ANOVA
#this script analyzes pain intensity by subject as a random factor
#COMMENT: this script analyzes pain intensity by subject as a random factor
#MAKE SURE YOU HAVE blevels SET TO THE CORRECT NUMBER OF SUBJECTS AND
THAT YOU
#HAVE THE CORRECT RUN NAME AND PATH FOR EACH SUBJECT
#USE THE WARP AND BLURRED SUBJECT DATA AS INPUT
#YOU SHOULD HAVE 2XTHE NUMBER OF SUBJECTS LINES, EACH DESIGNATED
BY -dset
#sad session with 3 runs: pain only, sad picture only and sad+pain

3dANOVA2 -type 3 -alevels 3 -blevels 15 \
-dset 1 1 ../../AM5023/Sec1/func.tlrc/stats.AM5023.r01+tlrc"[1]" \
-dset 2 1 ../../AM5023/Sec1/func.tlrc/stats.AM5023.r02+tlrc"[1]" \
-dset 3 1 ../../AM5023/Sec1/func.tlrc/stats.AM5023.r03+tlrc"[1]" \
-dset 1 2 ../../Altered_Pain_Control_Subjects/EG5037/Sec1/func.tlrc/stats.EG5037.r01+tlrc"[1]"
\
-dset 2 2 ../../EG5037/Sec1/func.tlrc/stats.EG5037.r02+tlrc"[1]" \
-dset 3 2 ../../EG5037/Sec1/func.tlrc/stats.EG5037.r03+tlrc"[1]" \
-dset 1 3 ../../HG5044/Sec1/func.tlrc/stats.HG5044.r01+tlrc"[1]" \
-dset 2 3 ../../HG5044/Sec1/func.tlrc/stats.HG5044.r02+tlrc"[1]" \
```

```
-dset 3 3 ../../HG5044/Sec1/func.tlrc/stats.HG5044.r03+tlrc"[1]" \
-dset 1 4 ../../LM5057/Sec1/func.tlrc/stats.LM5057.r01+tlrc"[1]" \
-dset 2 4 ../../LM5057/Sec1/func.tlrc/stats.LM5057.r02+tlrc"[1]" \
-dset 3 4 ../../LM5057/Sec1/func.tlrc/stats.LM5057.r03+tlrc"[1]" \
-dset 1 5 ../../NM5022/Sec2/func.tlrc/stats.NM5022.r01+tlrc"[1]" \
-dset 2 5 ../../NM5022/Sec2/func.tlrc/stats.NM5022.r02+tlrc"[1]" \
-dset 3 5 ../../NM5022/Sec2/func.tlrc/stats.NM5022.r03+tlrc"[1]" \
-dset 1 6 ../../EP5047/Sec2/func.tlrc/stats.EP5047.r01+tlrc"[1]" \
-dset 2 6 ../../EP5047/Sec2/func.tlrc/stats.EP5047.r02+tlrc"[1]" \
-dset 3 6 ../../EP5047/Sec2/func.tlrc/stats.EP5047.r03+tlrc"[1]" \
-dset 1 7 ../../KM5039/Sec2/func.tlrc/stats.KM5039.r01+tlrc"[1]" \
-dset 2 7 ../../KM5039/Sec2/func.tlrc/stats.KM5039.r02+tlrc"[1]" \
-dset 3 7 ../../KM5039/Sec2/func.tlrc/stats.KM5039.r03+tlrc"[1]" \
-dset 1 8 ../../LY5043/Sec2/func.tlrc/stats.LY5043.r01+tlrc"[1]" \
-dset 2 8 ../../LY5043/Sec2/func.tlrc/stats.LY5043.r02+tlrc"[1]" \
-dset 3 8 ../../LY5043/Sec2/func.tlrc/stats.LY5043.r03+tlrc"[1]" \
-dset 1 9 ../../KM5053/Sec1/func.tlrc/stats.KM5053.r01+tlrc"[1]" \
-dset 2 9 ../../KM5053/Sec1/func.tlrc/stats.KM5053.r02+tlrc"[1]" \
-dset 3 9 ../../KM5053/Sec1/func.tlrc/stats.KM5053.r03+tlrc"[1]" \
-dset 1 10 ../../PN5045/Sec1/func.tlrc/stats.PN5045.r01+tlrc"[1]" \
-dset 2 10 ../../PN5045/Sec1/func.tlrc/stats.PN5045.r02+tlrc"[1]" \
-dset 3 10 ../../PN5045/Sec1/func.tlrc/stats.PN5045.r03+tlrc"[1]" \
-dset 1 11 ../../TW5058/Sec1/func.tlrc/stats.TW5058.r01+tlrc"[1]" \
-dset 2 11 ../../TW5058/Sec1/func.tlrc/stats.TW5058.r02+tlrc"[1]" \
-dset 3 11 ../../TW5058/Sec1/func.tlrc/stats.TW5058.r03+tlrc"[1]" \
-dset 1 12 ../../AK5046/Sec1/func.tlrc/stats.AK5046.r01+tlrc"[1]" \
-dset 2 12 ../../AK5046/Sec1/func.tlrc/stats.AK5046.r02+tlrc"[1]" \
-dset 3 12 ../../AK5046/Sec1/func.tlrc/stats.AK5046.r03+tlrc"[1]" \
-dset 1 13 ../../DP5031/Sec2/func.tlrc/stats.DP5031.r01+tlrc"[1]" \
-dset 2 13 ../../DP5031/Sec2/func.tlrc/stats.DP5031.r02+tlrc"[1]" \
-dset 3 13 ../../DP5031/Sec2/func.tlrc/stats.DP5031.r03+tlrc"[1]" \
-dset 1 14 ../../KJ5033/Sec2/func.tlrc/stats.KJ5033.r01+tlrc"[1]" \
-dset 2 14 ../../KJ5033/Sec2/func.tlrc/stats.KJ5033.r02+tlrc"[1]" \
-dset 3 14 ../../KJ5033/Sec2/func.tlrc/stats.KJ5033.r03+tlrc"[1]" \
-dset 1 15 ../../RT5026/Sec2/func.tlrc/stats.RT5026.r01+tlrc"[1]" \
-dset 2 15 ../../RT5026/Sec2/func.tlrc/stats.RT5026.r02+tlrc"[1]" \
-dset 3 15 ../../RT5026/Sec2/func.tlrc/stats.RT5026.r03+tlrc"[1]" \
#-dset 1 16 ../../TC5035/Sec2/func.tlrc/stats.TC5035.r01+tlrc"[1]" \
#-dset 2 16 ../../TC5035/Sec2/func.tlrc/stats.TC5035.r02+tlrc"[1]" \
#-dset 3 16 ../../TC5035/Sec2/func.tlrc/stats.TC5035.r03+tlrc"[1]" \
-fa stimuli \
-amean 1 neut \
-amean 2 sad_pics \
-amean 3 sad_pain \
-adiff 1 2 neut_v_pics \
-adiff 3 1 pain_v_neut \
```

```
-adiff 3 2 pain_v_pics \
-acontr -1 -1 1 sadpain_VS_neut_picsonly \
-acontr -1 -1 2 sadpain_v_neut_plus_sadpain_v_piconly \
-bucket anova.15Ss.avgNeut.MTLRC

#The steps for ROI analysis to make masks and get z-scores
#1. convert T score to z core from ANOVA results
3dmerge -doall -1zscore -prefix 15Ss.avgNeut.Zscore
anova.15Ss.avgNeut.MTLRC+tlrc'[3,5,7,9,11,13,15,17,19]'

3dbucket -prefix  anova.15Ss.avgNeut.Zscore \
anova.15S.avgNeut.MTLRC+tlrc'[0]' anova.15S.avgNeut.MTLRC+tlrc'[1]' \
anova.15S.avgNeut.MTLRC+tlrc'[2]' 15Ss.avgNeut.Zscore+tlrc'[0]' \
anova.15S.avgNeut.MTLRC+tlrc'[4]' 15Ss.avgNeut.Zscore+tlrc'[1]' \
anova.15S.avgNeut.MTLRC+tlrc'[6]' 15Ss.avgNeut.Zscore+tlrc'[2]' \
anova.15S.avgNeut.MTLRC+tlrc'[8]' 15Ss.avgNeut.Zscore+tlrc'[3]' \
anova.15S.avgNeut.MTLRC+tlrc'[10]' 15Ss.avgNeut.Zscore+tlrc'[4]' \
anova.15S.avgNeut.MTLRC+tlrc'[12]' 15Ss.avgNeut.Zscore+tlrc'[5]' \
anova.15S.avgNeut.MTLRC+tlrc'[14]' 15Ss.avgNeut.Zscore+tlrc'[6]' \
anova.15S.avgNeut.MTLRC+tlrc'[16]' 15Ss.avgNeut.Zscore+tlrc'[7]'

#2. get clusters either from GUI of AFNI (save masks and cluster information as step 7) or from
the script as the below, and save masks
3dmerge -1thtoin -1noneg -1thresh 4.13 -1clust_order 1.7 128 -prefix
Mask8_9_4.13_.002_Vol200_rmm4 -1dindex 8 -1tindex 9
anova.alt.pain.11UsableSs.041107+tlrc

#3. for each mask, test the false positive of selected p value (optional)
AlphaSim \
-mask Mask8_9_3.58_Vol200_rmm4+tlrc \
-iter 1000 -rmm 4 -pthr .005 -fwhm 3 \
-out SadPicsOnly.Mask.MonteCarlo.005.12_13

#4. use -3dclust to get the ranges of x,y,z; manual select coordinates and make masks for each
cluster (RAI-DICOM order), use excel to sort data and get rid of unnecessary coordinates

3dmaskdump -mask  NeutPain_1.0E4_mask+tlrc -o NeutPain_1.0E4 -noijk -xyz -nozero
anova.14Ss.avgNeut.Zscore+tlrc'[3]'

#5. assembles a 3D dataset from an ASCII list of coordinates
3dUndump -prefix  LSII_NeutPain -master  14Ss.avgNeut.Zscore+tlrc -datum float -xyz LSII.txt

#6. find peaks of clusters
(optional)
3dExtrema -output SadPicsOlny_peaks -mask_file Mask8_9_3.58_Vol200_rmm4+tlrc -maxima
-interior -slice -average anova.alt.pain.11UsableSs.041107+tlrc'[8]'
```

#7. get the summary of cluster (mean, coordinate, peak value)
3dclust -1Dformat -1noneg -1thresh 2.97 1.7 128 anova.14Ss.avgNeut.Zscore+tlrc'[7]' >
SadPain_Zscore2.97_cluster_rmm1.5_p003.1D

#optional
3dROIstats -mask Mask2_3SPic_t4.51_.002_Vol170_rmm1.8+tlrc -minmax -sigma -nzmean
'anova.alt.Sadpain.9Ss.Zscore.181007+tlrc[3]' > Spics.ave.1D

APPENDIX B

Programming scripts in AFNI for processing the imaging data of Chapter 3

```
#To process the resting-state fMRI data
#prepare dataset of each subject for simple correlation and ICA group analysis
# register 2-D images to 3-D AFNI data format
#!/bin/csh -f

to3d -session Afni_analy -prefix RestEyeClose -epan -time:zt 36 164 2500 alt+z
'./RestEyeClose/*'
to3d -session Afni_analy -prefix T1Volume './T1Volume/MRDC.*'

#pre-processing dataset of each subject
3dTshift -prefix ts_RestEyeClose+orig RestEyeClose+orig
3dvolreg -dfile mot_tempRestEyeClose -base 'ts_RestEyeClose+orig[163]' -prefix
reg_RestEyeClose ts_RestEyeClose+orig
3dmerge -1blur_fwhm 4 -doall -prefix reg_RestEyeClose_blur reg_RestEyeClose+orig
3dcalc -prefix RestEyeClose_mask800 -a 'ts_RestEyeClose+orig[163]' -expr 'astep(a,800)'
3dDeconvolve -input reg_RestEyeClose_blur+orig -polort 2 -num_stimts 6 \
      -stim_file 1 'mot_tempRestEyeClose[1]' -stim_label 1 roll \
      -stim_file 2 'mot_tempRestEyeClose[2]' -stim_label 2 pitch \
      -stim_file 3 'mot_tempRestEyeClose[3]' -stim_label 3 yaw \
      -stim_file 4 'mot_tempRestEyeClose[4]' -stim_label 4 IS \
      -stim_file 5 'mot_tempRestEyeClose[5]' -stim_label 5 RL \
      -stim_file 6 'mot_tempRestEyeClose[6]' -stim_label 6 AP \
      -mask RestEyeClose_mask800+orig -fout -tout \
      -cbucket cbucket_coef_RestEyeClose -x1D x1Dmatrix_RestEyeClose \
      -bucket deconv_reg_RestEyeClose

#make clean data for simple correlation analysis
3dSynthesize -cbucket cbucket_coef_RestEyeClose+orig -matrix x1Dmatrix_RestEyeClose -
select all -prefix EffectsOfNoInterest_RestEyeClose
3dcalc -a reg_RestEyeClose_blur+orig -b EffectsOfNoInterest_RestEyeClose+orig -expr 'a-b' -
prefix CleanData_RestEyeClose
adwarp -apar T1Volume+tlrc -dpar 'CleanData_RestEyeClose+orig' -dxyz 3 -prefix
CleanData_RestEyeClose_dxyz3_man
adwarp -apar T1Volume+tlrc -dpar 'RestEyeClose_mask800+orig' -dxyz 3 -prefix
RestEyeClose_mask800_dxyz3_man
3dmaskave -quiet -mask RestEyeClose_mask800_dxyz3_man+tlrc
CleanData_RestEyeClose_dxyz3_man+tlrc > CleanData_RestEyeClose_dxyz3_man_global.1D

##Simple Correlation analysis
#For each defined ROI of each subject, calculate correlation coefficients (use PPA_left as an
example)
```

```
adwarp -apar T1Volume+tlrc -dpar ROI_PPA_Left+orig -dxyz 3 -prefix
ROI_PPA_Left_dxyz3_man
3dcalc -a ROI_PPA_Left_dxyz3_man+tlrc -b RestEyeClose_mask800_dxyz3_man+tlrc -expr
'a*b' -prefix ROI_PPA_Left_dxyz3_man_mask800

3dmaskave -quiet -mask ROI_PPA_Left_dxyz3_man_mask800+tlrc
CleanData_RestEyeClose_dxyz3_man+tlrc >
Seed_CleanData_RestEyeClose_dxyz3_man_PPA_Left.1D

3dDeconvolve -input CleanData_RestEyeClose_dxyz3_man+tlrc -polort 0 -num_stimts 2 \
      -stim_file 1 CleanData_RestEyeClose_dxyz3_man_global.1D -stim_label 1
RegressorOfNoInterest \
      -stim_file 2 Seed_CleanData_RestEyeClose_dxyz3_man_PPA_Left.1D -stim_label 2
CorrCoef -tout -rout -fitts fit_RestEyeClose_PPA_Left -bucket
Corr_RestEyeClose_PPA_Left_3dDeconvolve


## For the group of 16 subjects
set subject = (RS_001 RS_002 RS_003 RS_005 RS_008 RS_009 RS_010 RS_014 RS_015
RS_020 RS_021 RS_022 RS_023 RS_027 RS_028 RS_026)
set ROIs = (SI_Left SII_Left ACC_Left PInsula_Left PInsula_Right MedialFro RInfFro
Hippo_Right Hippo_Left LPAG LBrainstem)

foreach sub($subject)
echo $sub
cd ../{$sub}/Afni_analy/Corr_Analysis/

#take square root of the output from 3dDeconvole to get R
#convert correlation coefficient R to Gaussian

foreach ROI($ROIs)
echo $ROI
gunzip Corr_RestEyeClose_{$ROI}_3dDeconvolve+tlrc.BRIK.gz
3dcalc -a Corr_RestEyeClose_{$ROI}_3dDeconvolve+tlrc'[7]' -b
Corr_RestEyeClose_{$ROI}_3dDeconvolve+tlrc'[5]' -expr 'ispositive(b)*sqrt(a)-
isnegative(b)*sqrt(a)' -prefix Corr_RestEyeClose_{$ROI}_R
3dcalc -a Corr_RestEyeClose_{$ROI}_R+tlrc -expr 'log((1+a)/(1-a))/2' -prefix
corr_{$sub}_{$ROI}_Z
mv corr_{$sub}_{$ROI}_Z* ../../../Corr_Group_Ana/
end
cd ../../../Corr_Group_Ana/
end

#get Z scores or regressor coefficients of all subjects
#covert z-score to t value only indicates r is with some significance level different from 0, does
not necessarily mean a high correlation
```

```
foreach ROI($ROIs)
3dttest -prefix Grp_{$ROI}_Result -base1 0 \
-set2 \
corr_RS_001_{$ROI}_Z+tlrc \
corr_RS_002_{$ROI}_Z+tlrc \
corr_RS_003_{$ROI}_Z+tlrc \
corr_RS_005_{$ROI}_Z+tlrc \
corr_RS_008_{$ROI}_Z+tlrc \
corr_RS_009_{$ROI}_Z+tlrc \
corr_RS_010_{$ROI}_Z+tlrc \
corr_RS_014_{$ROI}_Z+tlrc
end

foreach ROI($ROIs)
3dcalc -a Grp_{$ROI}_Result+tlrc'[0]' -expr '(exp(2*a)-1)/(exp(2*a)+1)' -prefix
Rvalue_Grp_{$ROI}
end

##ICA analysis
#Step 1 preprocess data, reduce functional data dimension to 25 using PCA
#use time-shift, motion corrected, smoothed and normalized data
set subject = (RS_001 RS_002 RS_003 RS_005 RS_008 RS_009 RS_010 RS_014 RS_015
RS_020 RS_021 RS_022 RS_023 RS_026 RS_027 RS_028)

foreach sub($subject)
echo $sub
cd ../{$sub}/Afni_analy/ICA/

#clean data reduce the correlation
3dDeconvolve -input reg_RestEyeClose_blur+orig -polort 2 -num_stimts 6 \
      -stim_file 1 'mot_tempRestEyeClose[1]' -stim_label 1 roll \
      -stim_file 2 'mot_tempRestEyeClose[2]' -stim_label 2 pitch \
      -stim_file 3 'mot_tempRestEyeClose[3]' -stim_label 3 yaw \
      -stim_file 4 'mot_tempRestEyeClose[4]' -stim_label 4 IS \
      -stim_file 5 'mot_tempRestEyeClose[5]' -stim_label 5 RL \
      -stim_file 6 'mot_tempRestEyeClose[6]' -stim_label 6 AP \
      -mask RestEyeClose_mask800+orig -fout -tout \
      -cbucket cbucket_coef_RestEyeClose -x1D x1Dmatrix_RestEyeClose \
      -bucket deconv_reg_RestEyeClose

3dSynthesize -cbucket cbucket_coef_RestEyeClose+orig -matrix x1Dmatrix_RestEyeClose -
select all -prefix EffectsOfNoInterest_RestEyeClose

3dcalc -a reg_RestEyeClose_blur+orig -b EffectsOfNoInterest_RestEyeClose+orig -expr 'a-b' -
prefix CleanData_RestEyeClose
```

```
adwarp -apar T1Volume+tlrc -dpar 'CleanData_RestEyeClose+orig' -dxyz 3 -prefix CleanData

gunzip CleanData+tlrc.BRIK.gz

adwarp -apar T1Volume+tlrc -dpar 'RestEyeClose_mask800+orig' -dxyz 3 -prefix mask800

gunzip mask800+tlrc.BRIK.gz

# reduce time points for each subject from 164 to 25 using PCA

3dpc -vmean -vnorm -pcsave 25 -float -mask mask800+tlrc -prefix PreICA_TP25_{$sub}
CleanData+tlrc

mv  PreICA_TP25_{$sub}* ../../../ICA_Group_Ana/
cd ../../../ICA_Group_Ana/

end

#step 2 concatenate data from all subjects
#copy  mask800+tlrc* from RS_008 to current group analysis folder
3dTcat -session . -prefix Group_PreICA_concat_before_dimreduce PreICA_TP25_RS_001+tlrc
PreICA_TP25_RS_002+tlrc PreICA_TP25_RS_003+tlrc PreICA_TP25_RS_005+tlrc
PreICA_TP25_RS_008+tlrc PreICA_TP25_RS_009+tlrc PreICA_TP25_RS_010+tlrc
PreICA_TP25_RS_014+tlrc PreICA_TP25_RS_015+tlrc PreICA_TP25_RS_010+tlrc
PreICA_TP25_RS_021+tlrc PreICA_TP25_RS_022+tlrc PreICA_TP25_RS_023+tlrc
PreICA_TP25_RS_026+tlrc PreICA_TP25_RS_027+tlrc PreICA_TP25_RS_028+tlrc


##reduce dimension of aggregated data to 20 (number of sources selected)
3dpc -mask mask800+tlrc -reduce 20 Group_PreICA_concat_redim_RestEyeClose -prefix
PreICA_RestEyeClose Group_PreICA_concat_before_dimreduce+tlrc
3drename Group_PreICA_concat_redim_RestEyeClose ICAInput_RestEyeClose

# find the components
# .gz file can not be processed, needs to be unziped
gunzip ICAInput_RestEyeClose+tlrc.BRIK.gz
3dICA.R RestEyeClose_ICAOutput


##to run 3dICA.R, a par.txt file is needed to be saved in the same folder
## par.txt
Input:ICAInput_RestEyeClose+tlrc
CompOutput: RestEyeClose_ICAOutput
MixOutput:Temp
NoComp:20
```

Func:logcosh
Type:parallel

##Preprocess dataset for the path analysis
#step 1: define ROIs (saved in \remote\symonds\synapse3\FromeDavidZhu\mask)
one portion of ROIs are drew according to anatomical definition manually
#in each subjects Corr_analysis folder, run 1deval to covert averaged time series of each ROI into percent signal changes. (extROI.s)
#extract timeseries from masks. The masks are obtained from group analysis of altered pain study (use the ROI of Left ACC as the example)

set subject = (RS_001 RS_002 RS_003 RS_005 RS_008 RS_009 RS_010 RS_014 RS_015 RS_020 RS_021 RS_022 RS_023 RS_026 RS_027 RS_028)

foreach sub($subject)
cd ../{$sub}/Afni_analy/Corr_Analysis/
1deval -expr 'step(a/b)*min(200,(a/b)*100)+step(-a/b)*max(-200,(a/b)*100)' -a Seed_CleanData_RestEyeClose_dxyz3_man_ACC_Left.1D -b CleanData_RestEyeClose_dxyz3_man_global.1D > {$sub}.per_clean_LACC24.1D

mv {$sub}.per_clean*.1D ../../../SEM
cd ../../../SEM/
end

#the other portions of ROIs were drew manually (extROI2.csh)
Use the ROI of Left subgenual ACC(25) as the example
set subject = (RS_001 RS_002 RS_003 RS_005 RS_008 RS_009 RS_010 RS_014 RS_015 RS_020 RS_021 RS_022 RS_023 RS_026 RS_027 RS_028)
foreach sub($subject)
cd ../masks/
cp ROI*_dxyz3_man* ../{$sub}/Afni_analy/Corr_Analysis/
cd ../SEM/
end

foreach sub($subject)
cd ../{$sub}/Afni_analy/Corr_Analysis/

#Left subgenual ACC(25)
rm ROI_LACC25_dxyz3_man_mask800*
rm Seed_CleanData_RestEyeClose_dxyz3_man_LACC25.1D
3dcalc -a ROI_LACC25_dxyz3_man+tlrc -b RestEyeClose_mask800_dxyz3_man+tlrc -expr 'a*b' -prefix ROI_LACC25_dxyz3_man_mask800

```
3dmaskave -quiet -mask ROI_LACC25_dxyz3_man_mask800+tlrc
CleanData_RestEyeClose_dxyz3_man+tlrc >
Seed_CleanData_RestEyeClose_dxyz3_man_LACC25.1D
1deval -expr 'step(a/b)*min(200,(a/b)*100)+step(-a/b)*max(-200,(a/b)*100)' -a
Seed_CleanData_RestEyeClose_dxyz3_man_LACC25.1D -b
CleanData_RestEyeClose_dxyz3_man_global.1D > {$sub}.per_clean_LACC25.1D

mv {$sub}.per_clean*.1D ../../../SEM/
cd ../../../SEM/
end


# to perform path analysis, extract time series from ROIs
#extract timeseries from masks. The masks are the same as those used in resting state fMRI
#For pain network, ROIs are left left SI, left SII, right SII, R & L posterior Insula, L superior
temporal lobe, L ACC(BA24), L PAG, L VLPthalamus, L PCC and L hypothalamus (0 voxels
survives in hypothalamus, so get rid of this ROI)
#use the subjects saved in the folder of Control sec1 as the example (Neutral Pain runs (r01)

set subject = (AM5023 EG5037 HG5044 LM5057)
foreach sub($subject)

cp ../mask/ROI_LSI_mask* ../../../New_Altered_Pain/Altered_Pain_Control_Subjects/{$sub}/Se
c1/{$sub}.results/
cp ../mask/ROI_LPIn_mask* ../../../New_Altered_Pain/Altered_Pain_Control_Subjects/{$sub}/S
ec1/{$sub}.results/
cp ../mask/ROI_PAG_mask* ../../../New_Altered_Pain/Altered_Pain_Control_Subjects/{$sub}/S
ec1/{$sub}.results/
cp ../mask/ROI_LVPLTha_mask* ../../../New_Altered_Pain/Altered_Pain_Control_Subjects/{$s
ub}/Sec1/{$sub}.results/
cp ../mask/ROI_LPCC_mask* ../../../New_Altered_Pain/Altered_Pain_Control_Subjects/{$sub}/
Sec1/{$sub}.results/

cd ../../../New_Altered_Pain/Altered_Pain_Control_Subjects/{$sub}/Sec1/{$sub}.results/

rm roi*
rm *timeseries*


# register motion correced and blurd funcitonal run into tlrc
#get percent signal changes and extract time series

3dmaskave -quiet -mask full_mask.{$sub}+orig pb03.{$sub}.r01.blur+orig >
r01.blur.orig.global.1D

#right SII
```

```
3dfractionize -prefix roi_neut_0001_mask_{$sub} -template pb03.{$sub}.r01.blur+orig -warp
SPGR+tlrc -input  Grp_15Ss_neut_0001_mask+tlrc -preserve -clip 0.5

3dmaskave -quiet -mask roi_neut_0001_mask_{$sub}+orig -mrange 1 1
pb03.{$sub}.r01.blur+orig > {$sub}_Npain1_RSII_timeseries.1D

1deval -expr 'step(a/b)*min(200,(a/b)*100)+step(-a/b)*max(-200,(a/b)*100)' -a
{$sub}_Npain1_RSII_timeseries.1D -b r01.blur.orig.global.1D > {$sub}_pain_RSII.1D

#right posterior insula
3dmaskave -quiet -mask roi_neut_0001_mask_{$sub}+orig -mrange 3 3
pb03.{$sub}.r01.blur+orig > {$sub}_Npain3_RPInsula_timeseries.1D

1deval -expr 'step(a/b)*min(200,(a/b)*100)+step(-a/b)*max(-200,(a/b)*100)' -a
{$sub}_Npain3_RPInsula_timeseries.1D -b r01.blur.orig.global.1D > {$sub}_pain_RPIn.1D

#left SII
3dfractionize -prefix roi_neut_001_mask_{$sub} -template pb03.{$sub}.r01.blur+orig -warp
SPGR+tlrc -input  Grp_15Ss_neut_001_ACC_mask+tlrc -preserve -clip 0.5

3dmaskave -quiet -mask roi_neut_001_mask_{$sub}+orig -mrange 2 2
pb03.{$sub}.r01.blur+orig > {$sub}_Npain2_LSII_timeseries.1D

1deval -expr 'step(a/b)*min(200,(a/b)*100)+step(-a/b)*max(-200,(a/b)*100)' -a
{$sub}_Npain2_LSII_timeseries.1D -b r01.blur.orig.global.1D > {$sub}_pain_LSII.1D

#left ACC
3dmaskave -quiet -mask roi_neut_001_mask_{$sub}+orig -mrange 5 5
pb03.{$sub}.r01.blur+orig > {$sub}_Npain5_LACC_timeseries.1D

1deval -expr 'step(a/b)*min(200,(a/b)*100)+step(-a/b)*max(-200,(a/b)*100)' -a
{$sub}_Npain5_LACC_timeseries.1D -b r01.blur.orig.global.1D > {$sub}_pain_LACC.1D

#left superial tempral gyrus
3dmaskave -quiet -mask roi_neut_001_mask_{$sub}+orig -mrange 4 4
pb03.{$sub}.r01.blur+orig > {$sub}_Npain4_LSTC_timeseries.1D

1deval -expr 'step(a/b)*min(200,(a/b)*100)+step(-a/b)*max(-200,(a/b)*100)' -a
{$sub}_Npain4_LSTC_timeseries.1D -b r01.blur.orig.global.1D > {$sub}_pain_LSTG.1D

#left SI
3dfractionize -prefix roi_LSI_mask -template pb03.{$sub}.r01.blur+orig -warp SPGR+tlrc -
input ROI_LSI_mask+tlrc -clip 0.5

3dmaskave -quiet -mask roi_LSI_mask+orig pb03.{$sub}.r01.blur+orig >
{$sub}_LSI_timeseries.1D
```

```
1deval -expr 'step(a/b)*min(200,(a/b)*100)+step(-a/b)*max(-200,(a/b)*100)' -a
{$sub}_LSI_timeseries.1D -b r01.blur.orig.global.1D > {$sub}_pain_LSI.1D

#left posterior insula
3dfractionize -prefix roi_LPIn_mask -template pb03.{$sub}.r01.blur+orig -warp SPGR+tlrc -
input ROI_LPIn_mask+tlrc -clip 0.5

3dmaskave -quiet -mask roi_LPIn_mask+orig pb03.{$sub}.r01.blur+orig >
{$sub}_LPIn_timeseries.1D

1deval -expr 'step(a/b)*min(200,(a/b)*100)+step(-a/b)*max(-200,(a/b)*100)' -a
{$sub}_LPIn_timeseries.1D -b r01.blur.orig.global.1D > {$sub}_pain_LPIn.1D

#PAG
3dfractionize -prefix roi_PAG_mask -template pb03.{$sub}.r01.blur+orig -warp SPGR+tlrc -
input ROI_PAG_mask+tlrc -clip 0.5

3dmaskave -quiet -mask roi_PAG_mask+orig pb03.{$sub}.r01.blur+orig >
{$sub}_PAG_timeseries.1D

1deval -expr 'step(a/b)*min(200,(a/b)*100)+step(-a/b)*max(-200,(a/b)*100)' -a
{$sub}_PAG_timeseries.1D -b r01.blur.orig.global.1D > {$sub}_pain_PAG.1D

#left VPL thalamus
3dfractionize -prefix roi_LTha_mask -template pb03.{$sub}.r01.blur+orig -warp SPGR+tlrc -
input ROI_LVPLTha_mask+tlrc -clip 0.5

3dmaskave -quiet -mask roi_LTha_mask+orig pb03.{$sub}.r01.blur+orig >
{$sub}_LTha_timeseries.1D

1deval -expr 'step(a/b)*min(200,(a/b)*100)+step(-a/b)*max(-200,(a/b)*100)' -a
{$sub}_LTha_timeseries.1D -b r01.blur.orig.global.1D > {$sub}_pain_LTha.1D

#left posterior cingulate cortex
3dfractionize -prefix roi_LPCC_mask -template pb03.{$sub}.r01.blur+orig -warp SPGR+tlrc -
input ROI_LPCC_mask+tlrc -clip 0.5

3dmaskave -quiet -mask roi_LPCC_mask+orig pb03.{$sub}.r01.blur+orig >
{$sub}_LPCC_timeseries.1D

1deval -expr 'step(a/b)*min(200,(a/b)*100)+step(-a/b)*max(-200,(a/b)*100)' -a
{$sub}_LPCC_timeseries.1D -b r01.blur.orig.global.1D > {$sub}_pain_LPCC.1D


mv {$sub}_pain*.1D ../../../../SEM/Pain
```

```
cd ../../../../SEM/Pain

end


# combine all 1D files into one
set subject =(NM5022 EP5047 KM5039 LY5043 KM5053 PN5045 TW5058 AK5046 DP5031
KJ5033 RT5026)
foreach sub($subject)
1dMarry {$sub}_pain*.1D > {$sub}.pain.10ROIs.1D
end


# calculate mean of each ROIs across 15 Ss
set ROIs = (LACC LPCC LPIn LSI LSII LSTG LTha PAG RPIn RSII)
foreach roi($ROIs)
3dMean -prefix ts_mean_{$roi}  *_pain_{$roi}.1D
end


#finally, put all the exacted time series into the software of AMOS in SPSS and perform the path
analysis.
```

REFERENCES

REFERENCES

Aggleton, J. P., M. J. Burton, et al. (1980). "Cortical and subcortical afferents to the amygdala of the rhesus monkey (Macaca mulatta)." Brain Res 190(2): 347-68.

Albe-Fessard, D., K. J. Berkley, et al. (1985). "Diencephalic mechanisms of pain sensation." Brain Res 356(3): 217-96.

Anand, A., Y. Li, et al. (2005). "Activity and connectivity of brain mood regulating circuit in depression: a functional magnetic resonance study." Biol Psychiatry 57(10): 1079-88.

Apkarian, A. V., M. C. Bushnell, et al. (2005). "Human brain mechanisms of pain perception and regulation in health and disease." Eur J Pain 9(4): 463-84.

Augustine, J. R. (1996). "Circuitry and functional aspects of the insular lobe in primates including humans." Brain Res Brain Res Rev 22(3): 229-44.

Baliki, M. N., P. Y. Geha, et al. (2008). "Beyond feeling: chronic pain hurts the brain, disrupting the default-mode network dynamics." J Neurosci 28(6): 1398-403.

Bär, K.-J., G. Wagner, et al. (2007). "Increased Prefrontal Activation During Pain Perception in Major Depression." Biological Psychiatry 62(11): 1281-1287.

Barbas, H., S. Saha, et al. (2003). "Serial pathways from primate prefrontal cortex to autonomic areas may influence emotional expression." BMC Neuroscience 4(1): 25.

Bard, P. and D. M. Rioch (1937). "A study of four cats deprived of neocortex and additional portions of the forebrain." Bulletin of the Johns Hopkins Hospital 60: 73-153.

Beauregard, M., J. M. Leroux, et al. (1998). "The functional neuroanatomy of major depression: an fMRI study using an emotional activation paradigm." Neuroreport 9(14): 3253-8.

Beck, A. T., R. A. Steer, et al. (1996). "Beck depression inventory." PsychCorp.

Bernard, J. F., H. Bester, et al. (1996). Chapter 14 Involvement of the spino-parabrachio - amygdaloid and -hypothalamic pathways in the autonomic and affective emotional aspects of pain. Progress in Brain Research, Elsevier. Volume 107: 243-255.

Blair, R. J., J. S. Morris, et al. (1999). "Dissociable neural responses to facial expressions of sadness and anger." Brain 122 (Pt 5): 883-93.

Blanchard, E. B., F. Andrasik, et al. (1985). "Behavioral treatment of 250 chronic headache patients: A clinical replication series." Behavior Therapy 16(3): 308-327.

Breslau, N., R. B. Lipton, et al. (2003). "Comorbidity of migraine and depression: investigating potential etiology and prognosis." Neurology 60(8): 1308-12.

Bushnell, M. C., G. H. Duncan, et al. (1999). "Pain perception: is there a role for primary somatosensory cortex?" Proc Natl Acad Sci U S A 96(14): 7705-9.

Calejesan, A. A., S. J. Kim, et al. (2000). "Descending facilitatory modulation of a behavioral nociceptive response by stimulation in the adult rat anterior cingulate cortex." Eur J Pain 4(1): 83-96.

Calhoun, V. D., T. Adali, et al. (2001). "A method for making group inferences from functional MRI data using independent component analysis." Human Brain Mapping 14(3): 140-151.

Calhoun, V. D., T. AdalI, et al. (2004). "A method for comparing group fMRI data using independent component analysis: application to visual, motor and visuomotor tasks." Magnetic Resonance Imaging 22(9): 1181-1191.

Cannon, W. B. (1931). "Again the James-Lange and the thalamic theories of emotion." Psychological Review 38: 281-295.

Cauda, F., K. Sacco, et al. (2009). "Altered resting state in diabetic neuropathic pain." PLoS One 4(2): e4542.

Cavada, C. and P. S. Goldman-Rakic (1989). "Posterior parietal cortex in rhesus monkey: II. Evidence for segregated corticocortical networks linking sensory and limbic areas with the frontal lobe." J Comp Neurol 287(4): 422-45.

Cheng, Y., C. P. Lin, et al. (2007). "Expertise Modulates the Perception of Pain in Others." Curr Biol.

Coghill, R. C., D. J. Mayer, et al. (1993). "Wide dynamic range but not nociceptive-specific neurons encode multidimensional features of prolonged repetitive heat pain." J Neurophysiol 69(3): 703-16.

Coghill, R. C., C. N. Sang, et al. (1999). "Pain intensity processing within the human brain: a bilateral, distributed mechanism." J Neurophysiol 82(4): 1934-43.

Conti, F., M. Fabri, et al. (1988). "Immunocytochemical evidence for glutamatergic cortico-cortical connections in monkeys." Brain Res 462(1): 148-53.

Cox, R. W. (1996). "AFNI: software for analysis and visualization of functional magnetic resonance neuroimages." Comput Biomed Res 29(3): 162-73.

Craig, A. D. (1995). "Distribution of brainstem projections from spinal lamina I neurons in the cat and the monkey." J Comp Neurol 361(2): 225-48.

Craig, A. D. (2002). "How do you feel? Interoception: the sense of the physiological condition of the body." Nat Rev Neurosci 3(8): 655-666.

Craig, A. D. (2003). "A new view of pain as a homeostatic emotion." Trends Neurosci 26(6): 303-7.

Craig, A. D. (2009). "How do you feel [mdash] now? The anterior insula and human awareness." Nat Rev Neurosci 10(1): 59-70.

Craig, A. D., K. Chen, et al. (2000). "Thermosensory activation of insular cortex." Nat Neurosci 3(2): 184-90.

Critchley, H. D., S. Wiens, et al. (2004). "Neural systems supporting interoceptive awareness." Nat Neurosci 7(2): 189-95.

Crown, E. D., T. E. King, et al. (2000). "Shock-induced hyperalgesia: III. Role of the bed nucleus of the stria terminalis and amygdaloid nuclei." Behav Neurosci 114(3): 561-73.

Dagenais, S., J. Caro, et al. (2008). "A systematic review of low back pain cost of illness studies in the United States and internationally." The Spine Journal 8(1): 8-20.

Dalgleish, T. (2004). "The emotional brain." Nat Rev Neurosci 5(7): 583-9.

Damasio, A. R., T. J. Grabowski, et al. (2000). "Subcortical and cortical brain activity during the feeling of self-generated emotions." Nat Neurosci 3(10): 1049-56.

deCharms, R. C., F. Maeda, et al. (2005). "Control over brain activation and pain learned by using real-time functional MRI." Proceedings of the National Academy of Sciences 102(51): 18626-18631.

DeLeo, J. A. (2006). "Basic Science of Pain." J Bone Joint Surg Am 88(suppl_2): 58-62.

Dennis, S. G. and R. Melzack (1977). "Pain-signalling systems in the dorsal and ventral spinal cord." Pain 4(2): 97-132.

Derogatis, L. R. (1993). "Brief Symptom Inventory (BSI®)." PsychCorp.

Devinsky, O., M. J. Morrell, et al. (1995). "Contributions of anterior cingulate cortex to behaviour." Brain 118 (Pt 1): 279-306.

Dhond, R. P., C. Yeh, et al. (2008). "Acupuncture modulates resting state connectivity in default and sensorimotor brain networks." Pain 136(3): 407-18.

Dong, W. K., L. D. Salonen, et al. (1989). "Nociceptive responses of trigeminal neurons in SII-7b cortex of awake monkeys." Brain Res 484(1-2): 314-24.

Drevets, W. C. (2001). "Neuroimaging and neuropathological studies of depression: implications for the cognitive-emotional features of mood disorders." Curr Opin Neurobiol 11(2): 240-9.

Fields, H. L. (2000). "Pain modulation: expectation, opioid analgesia and virtual pain." Prog Brain Res 122: 245-53.

Finnegan, T. F., S. R. Chen, et al. (2005). "Effect of the {mu} opioid on excitatory and inhibitory synaptic inputs to periaqueductal gray-projecting neurons in the amygdala." J Pharmacol Exp Ther 312(2): 441-8.

Fox, M. D. and M. E. Raichle (2007). "Spontaneous fluctuations in brain activity observed with functional magnetic resonance imaging." Nat Rev Neurosci 8(9): 700-11.

Fox, M. D., A. Z. Snyder, et al. (2005). "The human brain is intrinsically organized into dynamic, anticorrelated functional networks." Proceedings of the National Academy of Sciences of the United States of America 102(27): 9673-9678.

Frot, M., M. Magnin, et al. (2007). "Human SII and posterior insula differently encode thermal laser stimuli." Cereb Cortex 17(3): 610-20.

Gallagher, R. M. (1999). "Treatment planning in pain medicine. Integrating medical, physical, and behavioral therapies." Med Clin North Am 83(3): 823-49, viii.

Greenspan, J. D., R. R. Lee, et al. (1999). "Pain sensitivity alterations as a function of lesion location in the parasylvian cortex." Pain 81(3): 273-282.

Greicius, M. D., B. Krasnow, et al. (2003). "Functional connectivity in the resting brain: a network analysis of the default mode hypothesis." Proc Natl Acad Sci U S A 100(1): 253-8.

Gureje, O., G. E. Simon, et al. (2001). "A cross-national study of the course of persistent pain in primary care." Pain 92(1-2): 195-200.

Hamann, S. B., T. D. Ely, et al. (1999). "Amygdala activity related to enhanced memory for pleasant and aversive stimuli." Nat Neurosci 2(3): 289-93.

Hirshberg, R. M., E. D. Al-Chaer, et al. (1996). "Is there a pathway in the posterior funiculus that signals visceral pain?" Pain 67(2-3): 291-305.

Hofbauer, R. K., P. Rainville, et al. (2001). "Cortical Representation of the Sensory Dimension of Pain." J Neurophysiol 86(1): 402-411.

Hsieh, J. C., S. Stone-Elander, et al. (1999). "Anticipatory coping of pain expressed in the human anterior cingulate cortex: a positron emission tomography study." Neurosci Lett 262(1): 61-4.

Jackson, P. L., E. Brunet, et al. (2006). "Empathy examined through the neural mechanisms involved in imagining how I feel versus how you feel pain." Neuropsychologia 44(5): 752-61.

Johansen-Berg, H., D. A. Gutman, et al. (2008). "Anatomical connectivity of the subgenual cingulate region targeted with deep brain stimulation for treatment-resistant depression." Cereb Cortex 18(6): 1374-83.

Kandel, E., J. Schwartz, et al. (2000). "The perception of pain." Principles of Neural Science.

Katims, J. J. (1997). "Neuroselective current perception threshold quantitative sensory test." Muscle Nerve 20(11): 1468-9.

Kenshalo, D. R., Jr. and O. Isensee (1983). "Responses of primate SI cortical neurons to noxious stimuli." J Neurophysiol 50(6): 1479-96.

Kim, D.-H., E. Adalsteinsson, et al. (2002). "Regularized higher-order in vivo shimming." Magnetic Resonance in Medicine 48(4): 715-722.

Klüver, H. and P. C. Bucy (1937). "Psychic blindness and other symptoms following bilateral temporal lobectomy in rhesus monkeys." American Journal of Physiology 119: 352-353.

Lane, R. D., P. M. Chua, et al. (1999). "Common effects of emotional valence, arousal and attention on neural activation during visual processing of pictures." Neuropsychologia 37(9): 989-97.

Lane, R. D., G. R. Fink, et al. (1997). "Neural activation during selective attention to subjective emotional responses." Neuroreport 8(18): 3969-72.

Lang, P. J., M. M. Bradley, et al. (1998). "Emotional arousal and activation of the visual cortex: an fMRI analysis." Psychophysiology 35(2): 199-210.

Lang, P. J., M. K. Greenwald, et al. (1993). "Looking at pictures: affective, facial, visceral, and behavioral reactions." Psychophysiology 30(3): 261-73.

Larsen, R. J. (1984). "Theory and measurement of affect intensity as an individual difference characteristics." Dissertation Abastracts International 85(2297B (University Microfilms No. 84-22112)).

Leonard, C. M., E. T. Rolls, et al. (1985). "Neurons in the amygdala of the monkey with responses selective for faces." Behavioural Brain Research 15(2): 159-176.

Liotti, M., H. S. Mayberg, et al. (2000). "Differential limbic-cortical correlates of sadness and anxiety in healthy subjects: implications for affective disorders." Biological Psychiatry 48(1): 30-42.

Logothetis, N. K., J. Pauls, et al. (2001). "Neurophysiological investigation of the basis of the fMRI signal." Nature 412(6843): 150-7.

MacLean, P. (1949). "Psychosomatic disease and the visceral brain; recent developments bearing on the Papez theory of emotion." Psychosom Med 11(6): 338-53.

Maihofner, C., B. Herzner, et al. (2006). "Secondary somatosensory cortex is important for the sensory-discriminative dimension of pain: a functional MRI study." Eur J Neurosci 23(5): 1377-83.

Manzoni, T., F. Conti, et al. (1986). "Callosal projections from area SII to SI in monkeys: anatomical organization and comparison with association projections." J Comp Neurol 252(2): 245-63.

Mayberg, H. S., S. K. Brannan, et al. (2000). "Regional metabolic effects of fluoxetine in major depression: serial changes and relationship to clinical response." Biol Psychiatry 48(8): 830-43.

Mayberg, H. S., P. J. Lewis, et al. (1994). "Paralimbic hypoperfusion in unipolar depression." J Nucl Med 35(6): 929-34.

Mayberg, H. S., M. Liotti, et al. (1999). "Reciprocal limbic-cortical function and negative mood: converging PET findings in depression and normal sadness." Am J Psychiatry 156(5): 675-82.

Mayer, D. J., D. D. Price, et al. (1975). "Neurophysiological characterization of the anterolateral spinal cord neurons contributing to pain perception in man." Pain 1(1): 51-8.

McIntosh, A. R., Gonzalez-Lima, F. (1992). "The application of structural modeling to metabolic mapping of functional neural systems." Kluwer Academic Publishers: 219-255.

McKeown, M. J., S. Makeig, et al. (1998). "Analysis of fMRI data by blind separation into independent spatial components." Human Brain Mapping 6(3): 160-188.

Meagher, M. W., R. C. Arnau, et al. (2001). "Pain and emotion: effects of affective picture modulation." Psychosom Med 63(1): 79-90.

Melzack, R. (1989). "Labat lecture. Phantom limbs." Reg Anesth 14(5): 208-11.

Melzack, R. (1990). "Phantom limbs and the concept of a neuromatrix." Trends Neurosci 13(3): 88-92.

Melzack, R. and K. Casey (1968). "Sensory, motivational and central control determinants of chronic pain: A new conceptual model." In Kenshalo, DR. The Skin Senses. Springfield, Illinois: Thomas: 432.

Melzack, R. and P. D. Wall (1965). "Pain Mechanisms: A New Theory." Science 150(3699): 971-979.

Merskey, H. and N. Bogduk (1994). "Classification of chronic pain." Seattle (WA): IASP Press.

Mesulam, M. M. and E. J. Mufson (1982). "Insula of the old world monkey. III: Efferent cortical output and comments on function." J Comp Neurol 212(1): 38-52.

Miller, E. K. and J. D. Cohen (2001). "An integrative theory of prefrontal cortex function." Annu Rev Neurosci 24: 167-202.

Mobascher, A., J. Brinkmeyer, et al. (2009). "Laser-evoked potential P2 single-trial amplitudes covary with the fMRI BOLD response in the medial pain system and interconnected subcortical structures." Neuroimage 45(3): 917-26.

Mollet, G. A. and D. W. Harrison (2006). "Emotion and pain: a functional cerebral systems integration." Neuropsychol Rev 16(3): 99-121.

Morris, J. S., C. D. Frith, et al. (1996). "A differential neural response in the human amygdala to fearful and happy facial expressions." Nature 383(6603): 812-5.

Mufson, E. J., M. M. Mesulam, et al. (1981). "Insular interconnections with the amygdala in the rhesus monkey." Neuroscience 6(7): 1231-48.

Neal, J. W., R. C. Pearson, et al. (1987). "The cortico-cortical connections of area 7b, PF, in the parietal lobe of the monkey." Brain Res 419(1-2): 341-6.

Neugebauer, V., W. Li, et al. (2004). "The amygdala and persistent pain." Neuroscientist 10(3): 221-34.

Ogawa, S., T. M. Lee, et al. (1990). "Brain magnetic resonance imaging with contrast dependent on blood oxygenation." Proc Natl Acad Sci U S A 87(24): 9868-72.

Ogino, Y., H. Nemoto, et al. (2007). "Inner experience of pain: imagination of pain while viewing images showing painful events forms subjective pain representation in human brain." Cereb Cortex 17(5): 1139-46.

Oldfield, R. C. (1971). "The assessment and analysis of handedness: the Edinburgh inventory." Neuropsychologia 9(1): 97-113.

Pandya, D. N., G. W. Van Hoesen, et al. (1981). "Efferent connections of the cingulate gyrus in the rhesus monkey." Exp Brain Res 42(3-4): 319-30.

Papez, J. W. (1995). "A proposed mechanism of emotion. 1937." J Neuropsychiatry Clin Neurosci 7(1): 103-12.

Pessoa, L., S. Padmala, et al. (2005). "Fate of unattended fearful faces in the amygdala is determined by both attentional resources and cognitive modulation." NeuroImage 28(1): 249-255.

Peyron, R., L. Garcia-Larrea, et al. (1999). "Haemodynamic brain responses to acute pain in humans: sensory and attentional networks." Brain 122 (Pt 9): 1765-80.

Peyron, R., B. Laurent, et al. (2000). "Functional imaging of brain responses to pain. A review and meta-analysis (2000)." Neurophysiol Clin 30(5): 263-88.

Phan, K. L., T. Wager, et al. (2002). "Functional neuroanatomy of emotion: a meta-analysis of emotion activation studies in PET and fMRI." Neuroimage 16(2): 331-48.

Phan, K. L., T. D. Wager, et al. (2004). "Functional neuroimaging studies of human emotions." CNS Spectr 9(4): 258-66.

Phillips, M. L., A. W. Young, et al. (1997). "A specific neural substrate for perceiving facial expressions of disgust." Nature 389(6650): 495-498.

Porreca, F., M. H. Ossipov, et al. (2002). "Chronic pain and medullary descending facilitation." Trends Neurosci 25(6): 319-25.

Price, D. D. (1999). "Psychological Mechanisms of Pain and Analgesia." Progress in Pain Research and Management 15.

Price, D. D. (2000). "Psychological and neural mechanisms of the affective dimension of pain." Science 288(5472): 1769-72.

Price, D. D., S. Long, et al. (1992). "Sensory testing of pathophysiological mechanisms of pain in patients with reflex sympathetic dystrophy." Pain 49(2): 163-73.

Raichle, M. E., A. M. MacLeod, et al. (2001). "A default mode of brain function." Proc Natl Acad Sci U S A 98(2): 676-82.

Rainville, P. (2002). "Brain mechanisms of pain affect and pain modulation." Curr Opin Neurobiol 12(2): 195-204.

Rainville, P., G. H. Duncan, et al. (1997). "Pain affect encoded in human anterior cingulate but not somatosensory cortex." Science 277(5328): 968-71.

Rauch, S. L., M. A. Jenike, et al. (1994). "Regional cerebral blood flow measured during symptom provocation in obsessive-compulsive disorder using oxygen 15-labeled carbon dioxide and positron emission tomography." Arch Gen Psychiatry 51(1): 62-70.

Reiman, E. M. (1997). "The application of positron emission tomography to the study of normal and pathologic emotions." J Clin Psychiatry 58 Suppl 16: 4-12.

Reiman, E. M., R. D. Lane, et al. (1997). "Neuroanatomical correlates of externally and internally generated human emotion." Am J Psychiatry 154(7): 918-25.

Ressler, K. J. and H. S. Mayberg (2007). "Targeting abnormal neural circuits in mood and anxiety disorders: from the laboratory to the clinic." Nat Neurosci 10(9): 1116-24.

Reynolds, D. V. (1969). "Surgery in the Rat during Electrical Analgesia Induced by Focal Brain Stimulation." Science 164(3878): 444-445.

Robinson, C. J. and H. Burton (1980). "Somatic submodality distribution within the second somatosensory (SII), 7b, retroinsular, postauditory, and granular insular cortical areas of M. fascicularis." The Journal of Comparative Neurology 192(1): 93-108.

Schweinhardt, P., N. Kalk, et al. (2008). "Investigation into the neural correlates of emotional augmentation of clinical pain." Neuroimage 40(2): 759-66.

Semple, W. E., P. F. Goyer, et al. (2000). "Higher brain blood flow at amygdala and lower frontal cortex blood flow in PTSD patients with comorbid cocaine and alcohol abuse compared with normals." Psychiatry 63(1): 65-74.

Sewards, T. V. and M. A. Sewards (2002). "The medial pain system: Neural representations of the motivational aspect of pain." Brain Research Bulletin 59(3): 163-180.

Singer, T., B. Seymour, et al. (2004). "Empathy for pain involves the affective but not sensory components of pain." Science 303(5661): 1157-62.

Stahl, S. M. (2002). "Does depression hurt?" J Clin Psychiatry 63(4): 273-4.

Sudheimer, K., K. Davis, et al. (2001). "An emotion induction paradigm for neuroimaging: International Affective Picture System (IAPS)." Society of Neuroscience Abstract 27.

Symonds, L. L., N. S. Gordon, et al. (2006). "Right-Lateralized Pain Processing in the Human Cortex: An fMRI Study." J Neurophysiol 95(6): 3823-3830.

Tang, N. K., P. M. Salkovskis, et al. (2008). "Effects of mood on pain responses and pain tolerance: An experimental study in chronic back pain patients." Pain.

Taylor, S. F., I. Liberzon, et al. (1998). "The effect of emotional content on visual recognition memory: a PET activation study." Neuroimage 8(2): 188-97.

Tolle, T. R., T. Kaufmann, et al. (1999). "Region-specific encoding of sensory and affective components of pain in the human brain: a positron emission tomography correlation analysis." Ann Neurol 45(1): 40-7.

Treede, R. D., D. R. Kenshalo, et al. (1999). "The cortical representation of pain." Pain 79(2-3): 105-11.

Valet, M., T. Sprenger, et al. (2004). "Distraction modulates connectivity of the cingulo-frontal cortex and the midbrain during pain--an fMRI analysis." Pain 109(3): 399-408.

Villemure, C., S. Wassimi, et al. (2006). "Unpleasant odors increase pain processing in a patient with neuropathic pain: psychophysical and fMRI investigation." Pain 120(1-2): 213-20.

Vogt, B. A. (2005). "Pain and emotion interaction in subregions of the cingulate gyrus." Nat Rev Neurosci 6(7): 533-44.

Vogt, B. A. and R. W. Sikes (2000). "The medial pain system, cingulate cortex, and parallel processing of nociceptive information." Prog Brain Res 122: 223-35.

Vogt, B. A., R. W. Sikes, et al. (1999). Chapter 16 The medial pain system, cingulate cortex, and parallel processing of nociceptive information. Progress in Brain Research, Elsevier. Volume 122: 223-235.

Vuilleumier, P., M. P. Richardson, et al. (2004). "Distant influences of amygdala lesion on visual cortical activation during emotional face processing." Nat Neurosci 7(11): 1271-8.

Weisenberg, M., T. Raz, et al. (1998). "The influence of film-induced mood on pain perception." Pain 76(3): 365-75.

Weiskrantz, L. (1956). "Behavioral changes associated with ablation of the amygdaloid complex in monkeys." J Comp Physiol Psychol 49(4): 381-91.

Wiech, K., M. Farias, et al. (2008). "An fMRI study measuring analgesia enhanced by religion as a belief system." Pain 139(2): 467-476.

Willis, W. D. (1985). "Nociceptive pathways: anatomy and physiology of nociceptive ascending pathways." Philos Trans R Soc Lond B Biol Sci 308(1136): 253-70.

Willis, W. D. and K. N. Westlund (1997). "Neuroanatomy of the Pain System and of the Pathways That Modulate Pain." Journal of Clinical Neurophysiology 14(1): 2-31.

Willoughby, S. G., B. J. Hailey, et al. (2002). "The effect of laboratory-induced depressed mood state on responses to pain." Behav Med 28(1): 23-31.

Yoshino, A., Y. Okamoto, et al. (2010). "Sadness enhances the experience of pain via neural activation in the anterior cingulate cortex and amygdala: an fMRI study." Neuroimage 50(3): 1194-201.

Young, A. W., J. P. Aggleton, et al. (1995). "Face processing impairments after amygdalotomy." Brain 118 (Pt 1): 15-24.

Zhang, E. T. and A. D. Craig (1997). "Morphology and distribution of spinothalamic lamina I neurons in the monkey." J Neurosci 17(9): 3274-84.

Zubieta, J. K., Y. R. Smith, et al. (2001). "Regional mu opioid receptor regulation of sensory and affective dimensions of pain." Science 293(5528): 311-5.

Zubieta, J.-K., T. A. Ketter, et al. (2003). "Regulation of Human Affective Responses by Anterior Cingulate and Limbic {micro}-Opioid Neurotransmission." Arch Gen Psychiatry 60(11): 1145-1153.